The background of the cover features a large, semi-transparent globe of the Earth showing the continents, set against a blue sky with white clouds. Below the globe is a lush green landscape with a river or lake in the foreground, reflecting the sky and trees. The scene is framed by several overlapping white arcs that create a sense of depth and movement.

**Proceedings  
of CWW 2024**  
*Water and Climate:  
Building Resilient Communities*

**By the CWW Scientific Committee**

## TABLE OF CONTENTS

Day 1	Theme 1: Transboundary Water Governance for Sustainable Development	2
Day 2	Theme 2: Strategic Water Resources Management in Enhancing Community Resilience	27
Day 3	Theme 3: Innovation and Financing Resilient Solutions for Water Security	32
Day 4	Theme 4: Actions for Water and Climate Adaptations and Resilience	49
Day 5	Theme 5: Climate-Smart Communities Planning and Legislation	71
Day 4	POSTER	85

**Theme 1: Transboundary Water Governance for  
Sustainable Development  
Day 1**

## Stochastic Opportunity Cost Assessment of Cooperative GERD Operation

Rameen Abdelhady<sup>1\*</sup>, Loay Seif<sup>2</sup>, Aref Gharib<sup>3</sup>, Hussam Fahmy<sup>4</sup>

<sup>1\*,4</sup> National Water Research Center, MWRI, EGYPT

(E-mail: [rameens@hotmail.com](mailto:rameens@hotmail.com), [hussam.fahmy@yahoo.com](mailto:hussam.fahmy@yahoo.com))

<sup>2,3</sup> Nile Water Sector, MWRI, EGYPT

(E-mail: [arefgharib@yahoo.com](mailto:arefgharib@yahoo.com), [loa2y@yahoo.com](mailto:loa2y@yahoo.com))

### ABSTRACT

Owen Falls Dam Agreements set a model for cooperative dam operation between two Nile Basin riparian countries: Uganda and Egypt. The purpose of the agreement was twofold: to regulate the water outflow and to provide Uganda with hydroelectric energy. This manuscript is inspired by Owen Falls Dam Agreements. Where the non-generated hydroelectric energy, due to adoption of cooperative operation policy, is considered. During the trilateral marathon of GERD negotiation several proposals have been considered, among which is two extreme minimum annual release proposals: 31 BCM by Ethiopia and 47 BCM by Egypt and Sudan. The objective of this research is to assess stochastically the energy generated under the extreme minimum annual release and comparing them to maximum energy generation, where the difference in energy production, considered as opportunity cost for the Ethiopian. The maximum energy scenario is considered as a reference scenario as it reflects Ethiopian interests only without considering the downstream hydrologic conditions and needs. While the minimum annual release scenarios consider the hydrologic conditions and downstream needs from the two sides perspectives. The design of hydro power plant is accurately modelled to calculate all the power plant parameters. Due to GERD hydrologic design (sizing and zoning), results show clearly that GERD generated power is more sensitive to minimum release constraints than head constraints. Probabilistic analysis of the two minimum release scenarios proves that: Ethiopia regains about only one fifth of the lost power generation (if it insists on its proposal for the minimum annual flow). While one third of the normal natural flow will not be guaranteed for Egypt and Sudan.

**Keywords:** Agreement. AHD, Ethiopia, Egypt, GERD, Hydropower generation

### INTRODUCTION:

Egypt relies on the Nile for 98% of its water, all of which comes from upstream Nile basin countries. This dependence makes Egypt especially vulnerable to unplanned and unsustainable activities and projects throughout the Nile basin. In Egypt, a decrease of just 1 billion cubic meters of water would result in 290,000 people losing their incomes in the agricultural sector alone, a loss of 130,000 hectares of cultivated land, an increase of \$150 million in food imports, and a \$430 million loss in agricultural production. Prolonged and increasing water shortages would have incalculable ripple effects on every sector of Egypt's economy and its socio-political stability [1].

Regardless of the downstream impacts, Ethiopia started unilaterally constructing the Grand Ethiopian Renaissance Dam (GERD) across the Blue Nile in 2011, which is tens of kilometres away from the Sudan border. It was announced in June 2024 by Ethiopia's chief negotiator on GERD and ambassador to the US that the entire project is 94% complete, with the last concrete set to be poured by September 2024. The lack of comprehensive impact studies on downstream countries, which are essential for reaching agreements on dam size, filling, and operation, poses a threat to Egypt's water security, national economy, and stability as the most downstream country.

The boundaries of the pool that maximises generated energy is defined by the Full Supply Level (FSL) of 640 m a.m.s.l. corresponding to storage volume 74 BCM, and the Minimum Pool Level (MPL) 625 m a.m.s.l. corresponding to storage volume of 49.3. Each turbine has 270 m<sup>3</sup>/sec flow capacity. The updated turbines data is 11 Francis turbines with 400 MW total installed capacity and 2 Francis turbines with 375 MW installed capacity in the left powerhouse. (Figure 1).

Eldardiry and Hossain [2] demonstrated that current GERD capacity (5150 MW) is more reasonable than previous designs (e.g., 6000 and 6450 MW). They did not use actual flow records at El-Deim station (outlet of the Blue Nile Basin), but they generated a flow series d for 37 years spanning the period from 1981 to 2017, by employing a macroscale hydrological model. An optimization scheme based on the Deterministic Dynamic Programming (DDP) approach was adopted to simulate the likely operation of the GERD. Their approach was developed to determine a safe range of releases that would prevent downstream flooding (very high releases) or drought conditions (low releases). They concluded that the current design with 5150 MW is more feasible for mitigating hydrological constraints in the Upper Blue Nile (UBN) and harnessing the hydropower potential of GERD compared to previous designs (e.g., 6000 and 6450 MW). On average, the current installed capacity of 5150 MW would result in approximately eight turbines remaining idle out of the 13 turbines installed throughout the year.



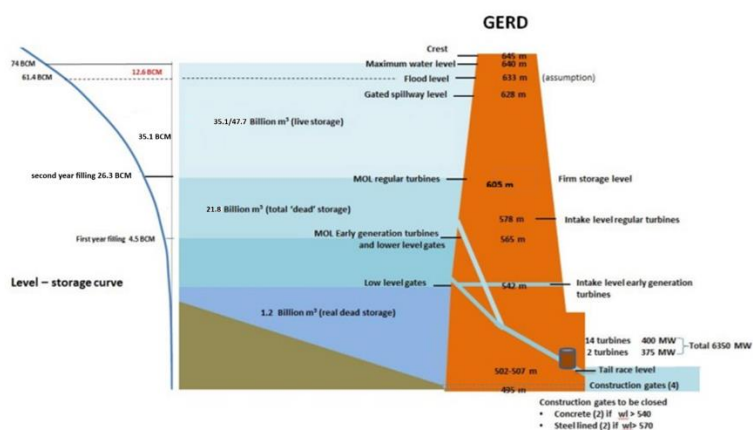


Figure 1: Cross-section of the Grand Ethiopian Renaissance Dam

The objective of this research is to assess stochastically the non-generated energy due deviation from maximum energy generation scenario to minimum annual release scenarios, where the difference in energy production, considered as opportunity cost for the Ethiopian side. Two downstream requirements are tested. The design of hydro power plant is accurately modelled to calculate all the power plant parameters. Turbines' efficiency is assumed to be directly proportional with the site head.

## METHODOLOGY:

Detailed hydropower plant simulation model is developed based on hydrologic reservoir simulation model (with monthly time step). Two GERD operation scenarios constrained by minimum annual release (47 and 31 BCM) are compared to the maximum energy generation as a reference scenario. Power generation under the three scenarios are assessed using hundred El-Deim flow series generated from a 102-year historical record of monthly flows [3]. The results are presented as Cumulative Distribution Function (CDF) of the non-generated energy (opportunity cost) for each constrained scenario (47 BCM and 31 BCM).

## RESULTS:

The difference in energy generation under non-cooperative scenario (maximum energy generation) and under each of the cooperative sub scenarios (47 BCM and 31 BCM) (minimum annual release) are presented as Cumulative Distribution Function (CDF) of the opportunity cost (non-generated energy) in Figure 2 and 3. Comparison between the two scenarios are presented in box plot shown in Figure 4

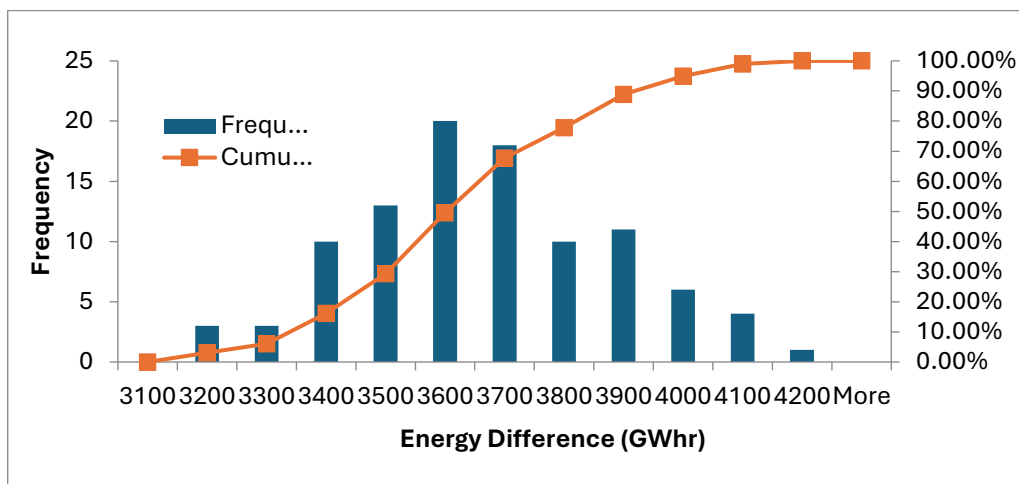


Figure 2: Average Energy Difference Under Minimum Annual Release of 47 BCM

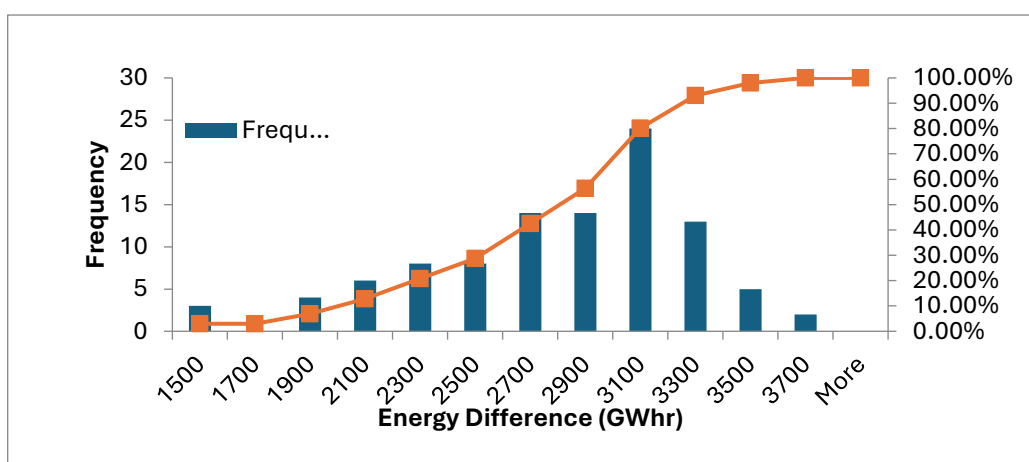


Figure 3: Average Energy Difference Under Minimum Annual Release of 31 BCM

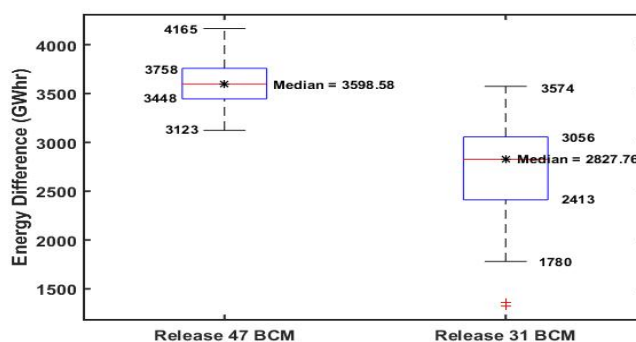


Figure 4: Comparison Between the two Minimum Annual Release Scenarios

**CONCLUSION:**

Adherence to principles of equal rights, shared interests, and international law necessitates to adopt a scientifically based and non-discriminatory approach to conflict resolution. In support of negotiation

to reach an agreement on GERD operation, this paper suggests stochastic system dynamics as scientifically based and non-discriminatory approach. Through a detailed GERD hydropower simulation model, it examines stochastically: the implications of GERD operation deviation from maximum energy generation to consideration of downstream requirements. Presenting the results in probabilistic terms, to negotiators, facilitates reaching a compromise without being fixed on specific values. Due to GERD hydrologic design (sizing and zoning), results show clearly that GERD generated power is more sensitive to minimum release constraints than head constraints that maximize the power generation. Probabilistic analysis of the two minimum release scenarios proves that: Ethiopia regains about one fifth of the lost power generation (if it insists on its proposal for the minimum annual flow). While one third of the normal natural flow will not be guaranteed for Egypt and Sudan.

#### **REFERENCES:**

- [1] Deltares & MWRI: 'United Nations: Egypt's Submission to the UN 2023 Concept Paper Water for Cooperation: Transboundary and International Water Cooperation', 2023, Cross Sectoral Cooperation, including Scientific Cooperation, and Water Across the 2030 Agenda.
- [2] Eldardiry, H. and Hossain, F.: 'Evaluating the hydropower potential of the Grand Ethiopian Renaissance Dam', J. Renew. Sustain. Energy., 2021, 13, (2).
- [3] Deltares: Impacts of GERD on Egypt, 1230569-000-ZWS-002, 2018.



## Reviving the Transboundary River Ichamati for Sustaining the Sundarbans Ecosystem

T. Bhadra\*<sup>1</sup>

<sup>1</sup> Department of Geography, Adamas University, INDIA.  
(E-mail: [tuhinbhadra.au@gmail.com](mailto:tuhinbhadra.au@gmail.com))

### ABSTRACT

The Ichamati River, a vital freshwater source for the Sundarbans mangrove ecosystem straddling the India-Bangladesh border, faces significant challenges due to disconnection from its freshwater source. This study employs hydrological modelling techniques to assess the potential for river basin rejuvenation and restoration of flow connectivity. Using a SWAT model, the runoff volume of the basin is estimated. The hypothetical channel form for the disconnected segment is constructed based on existing and regenerated cross-sections. Furthermore, HEC-RAS modelling is utilized to estimate flow availability under present and restored conditions, revealing a stark disparity between lean periods, where flow dwindles to less than 1 cumec, and monsoon seasons, with flow peaking at 100 cumecs. Environmental flow assessments employing the holistic Building Block method (BBM) demonstrate the necessity for sustained freshwater inflows to the non-tidal part of the river. Following proposed restoration efforts, flow values are projected to increase to approximately 188 cumecs during monsoon and over 30 cumecs in lean months. The study underscores the importance of transboundary collaboration between India and Bangladesh for reviving the degraded channel and ensuring adequate environmental flows to sustain the Sundarbans, a UNESCO World Heritage and Ramsar site shared by both nations. By addressing challenges such as flow regulation and restoration, this collaborative approach presents opportunities for integrated water resources management, fostering ecosystem resilience and supporting the livelihoods of local communities dependent on the Sundarbans' ecological services.

**Keywords:** Ichamati, Sundarbans, Environmental Flows, SWAT, HEC-RAS, River Restoration.

### METHODOLOGY

The river Ichamati begins at Majdia, West Bengal (23°24'15.55"N, 88°42'37.59"E), originating from the Mathabhanga River. It spans 216 km from its source to its mouth at Hasnabad, where it flows into the Bay of Bengal through the Sundarbans. In recent decades, Ichamati has been separated from its parent river and lacks consistent upstream flows [1]. Previous studies on the river Ichamati have

been limited in scope, particularly concerning its flow characteristics and minimum flow requirements, which have not been adequately addressed. Therefore, the current study aims to fill these gaps by estimating both the flow availability within the river channel and the necessary environmental flow to sustain its ecological health.

Data collection involved obtaining cross-sections, discharge, and water level information from the River Research Institute (RRI) and the Bidyadhari Drainage Division of the West Bengal Irrigation and Waterways Department (I&WD). Detailed surveys of disconnected river sections were conducted to evaluate their current conditions. Utilizing a physically-based hydrological model, SWAT, in the ArcGIS environment, synthetic flow data for the river Ichamati were generated. Input parameters included the SRTM 30m DEM, NRSC land use maps, FAO soil data, and IMD gridded rainfall and temperature datasets. The SWAT-CUP's SUFI-2 program facilitated model calibration and validation, ensuring accuracy in flow simulations [2].

The potential of river restoration and reconnection to enhance freshwater availability was evaluated using the HEC-RAS model. Cross-section adjustments based on I&WD guidelines were applied to simulate a hypothetical scenario of river restoration from Majdia to Kalanchi, estimating flow dynamics under current and restored conditions. Assessment of environmental flows was conducted using the holistic Building Block Method, BBM [3], considering three key blocks: hydro-morphological, ecological, and socio-economic. Each block addressed specific needs such as navigation depth, habitat requirements for species like the Ganges Dolphin, and migration patterns of commercially important species like Hilsa. Relationships between flow availability, and water depth across different river stretches were established using outputs from SWAT and HEC-RAS models. The highest flow requirement identified across these blocks was designated as the environmental flow necessary for sustaining the river Ichamati's ecosystem health.

## **RESULTS**

The river Ichamati relies irregularly on discharge from the Mathabhanga-Churni river system, primarily receiving upstream freshwater flow only during peak monsoon months. At Majdia, Ichamati's flow fluctuates from 0 cumec in lean periods to 20 cumecs during typical monsoons (Figure 1). During flood years, peak monsoonal flow can reach up to 100 cumecs, contrasting sharply with dry years where it may dwindle to just 4 cumecs (Figure 1). Research indicates that restoring the river channel would significantly enhance flow availability in Ichamati (Figure 1). Reconnecting Ichamati with Mathabhanga could ensure a minimum flow of 30 cumecs during lean periods and

increase monsoonal flow at Majdia from 20 cumecs to 150 cumecs (Figure 1). Post-reconnection, total monsoonal freshwater flow from the river basin at Taki is projected to reach approximately 275 cumecs in a normal year, 700 cumecs during floods, and 133 cumecs in dry years. This study underscores that river reconnection and rejuvenation could augment Ichamati's flow by at least 30 cumecs during dry seasons.

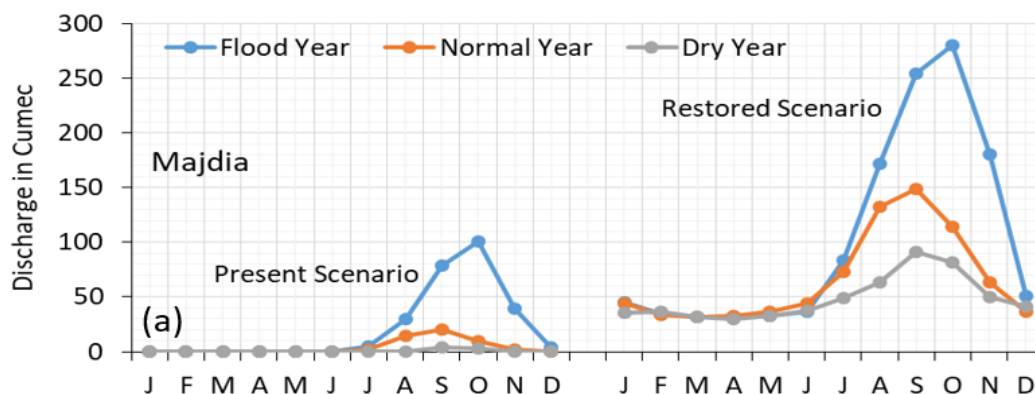


Figure 1: Hydrographs (SWAT and HEC-RAS model output) showing the flow availability in the river Ichamati at Majdia (off-take) in Present and Restored Scenario.

The indicator-based approach has been applied to assess the environmental flows in the BBM. The depth discharge relationships have been established in different reaches of the river to assess the block-wise flow requirement. The study indicates that at least 31 cumecs flows in the river channel are required to maintain 3 metres depth [4] around the year for navigation. Around 187 cumecs flow has to be maintained during the migration period of Hilsa to maintain 7 metres depth [5]. To maintain 5 metres depth [6] for the movement of Gangetic Dolphins 76 cumecs of flows have to be maintained within the channel. Although dolphin movement takes place throughout the year, the required flow for dolphin movement is not available during the lean period. The BBM estimates the environmental flow requirement for the river Ichamati as 31 cumecs during low flow seasons and 187 cumecs during high flow seasons.

## CONCLUSIONS AND RECOMMENDATIONS

Ichamati, a transboundary river crucial for freshwater supply in the eastern Sundarbans, faces water scarcity outside of monsoon season due to its disconnection from the Mathabhanga River. In typical years, it receives about 20 cumecs during monsoons but none during lean periods. Reconnecting it could raise monsoonal flow to 150 cumecs and ensure 31 cumecs during lean periods. This restoration would also enhance flow in other Ichamati reaches. According to the BBM, maintaining navigability (3m depth) requires 31 cumecs, 5m depth for Gangetic Dolphins

needs 76 cumecs, and 7m depth for Hilsa migration demands 187 cumecs. BBM suggests environmental flows of 31 cumecs in lean periods and 187 cumecs in monsoons. To augment the estimated environmental flows, the river needs to be reconnected with its source and the two neighbouring countries should mutually contribute to maintain round-the-year flows for the sustainable supply of fresh water to nurture the Sundarbans ecosystem.

### **ACKNOWLEDGMENT**

The author would like to express his gratitude to River Research Institute and Bidyadhari Drainage Division, I&WD, Govt. of West Bengal for providing cross-sections, water level and discharge data of the river Ichamati.

### **REFERENCES**

- [1] Bhadra, T., Mukhopadhyay, A. and Hazra, S.: 'Identification of River Discontinuity Using Geo-Informatics to Improve Freshwater Flow and Ecosystem Services in Indian Sundarban Delta' In Hazra, S. et al (Eds.), Environment and Earth Observation, Springer Remote Sensing/Photogrammetry, Springer, Cham, 2017, pp.137-152.
- [2] Abbaspour, K.C., Rouholahnejad, E., Vaghefi, S., Srinivasan, R., Yang, H. and Kløve, B.: 'A continental-scale hydrology and water quality model for Europe: Calibration and uncertainty of a high-resolution large-scale SWAT model' Jour. Hydrol., 2015, v.524, pp.733-752.
- [3] King, J. M., Tharme, R. E. and de Villiers, M. S. (Eds.): 'Environmental Flow Assessments for Rivers: Manual for the Building Block Methodology' Water Research Commission Technology Transfer Report No. TT131/00, Pretoria, SA, Water Research Commission, 2008, p.340.
- [4] Hazra, S., Bhadra, T., Ghosh, S. and Barman, B. C.: 'Assessing Environmental Flows for Indian Sundarban: a suggested approach' River Behaviour and Control, 2015, v.35, pp.65-74.
- [5] Mojumdar, C.H.: 'Foreshore fishing in the eastern parts of the Bay of Bengal' Science and Culture, 1939, v.5(4), p.219.
- [6] Behera, S., Areendran, G., Gautam, P. and Sagar, V.: 'For Living Ganga: Working with People and Aquatic Species' WWF-India: New Delhi, 2011, p.84.

## Sensitivity Analysis of the Nile River Basin Hydrologic Model

Mohamed Refaat Elgendy\*<sup>1</sup>, Paulin Coulibaly<sup>2,3</sup> and Sonia Hassini<sup>4</sup>

<sup>1</sup> Dept. of Civil Engineering, McMaster University, CANADA.

(E-mail: [elgendym@mcmaster.ca](mailto:elgendym@mcmaster.ca))

<sup>2</sup> Dept. of Civil Engineering and School of Earth, Environment & Society, McMaster Univ., CANADA.

(E-mail: [couliba@mcmaster.ca](mailto:couliba@mcmaster.ca))

<sup>3</sup> United Nations University Institute for Water, Environment, and Health, CANADA.

<sup>4</sup> Dept. of Civil Engineering, McMaster University, CANADA.

(E-mail: [hassins@mcmaster.ca](mailto:hassins@mcmaster.ca))

### ABSTRACT

The Nile is the longest river in the world, serving millions of people with fresh water, fisheries, and hydroelectric power. Considering its complexity as a shared basin, many hydrologic and water management models were developed and calibrated for the Nile River Basin (NRB). However, there is still a need to identify the critical hydrologic and routing parameters that affect the entire NRB hydrologic model's results and performance. This study aims to perform a sensitivity analysis to recognize and prioritize these critical parameters to be focused on in future models' development, calibration, and validation. Data relevant to these parameters should be collected with as much accuracy, intensity, and wideness as possible. The Raven hydrologic modelling platform is used to develop a semi-distributed hydrologic model for the NRB. The sensitivity analysis included parameters related to catchment land use and land cover (e.g., impermeability, forest coverage and sparseness, and depressions storage), vegetation (e.g., vegetation height and leaf index area), soil (e.g., porosity and field capacity), and routing (e.g., Manning roughness coefficient). The preliminary results indicate that the soil and routing parameters are amongst the most critical ones for the NRB hydrologic modelling. These results help guide future studies to prioritize the hydrologic model's parameters, which improves its performance while reducing the time needed for calibration and validation. Additionally, they assist in predicting the degree of the NRB hydrologic response to future related changes, including climate change and land use land cover change, leading to more effective water management strategies.

**Keywords:** Hydrologic Modelling, Nile River Basin, Raven Modelling Platform, Sensitivity Analysis, Normalized Sensitivity Coefficient.

## METHODOLOGY

This study aims to recognize and rank the significant hydrologic parameters in the NRB by investigating their impacts on the NRB hydrologic model's response. Raven modelling platform [1] is used to develop a semi-distributed hydrologic model for the entire NRB by emulating the Hydrologiska Byråns Vattenbalansavdelning (HBV) conceptual model [2]. To consider spatial variation of the basin characteristics, the sensitivity analysis is performed at three flow stations, i.e., Lake Tana, Malakal, and Akhsas (Figure 1), distributed at critical locations over the NRB major subbasins, i.e., Blue Nile, White Nile, and Main Nile.[3].

The hydrologic model continuously simulates NRB-relevant hydrologic processes, including precipitation, infiltration, baseflow, and evaporation from canopy, soil, and surface water. The sensitivity analysis covers 28 parameters that vary between land use/cover, soil, vegetation, routing, , and lake outlet parameters. Each parameter's minimum and maximum values are determined based on the Raven manual [4] and previous studies, e.g., [5,6]. The analysis was performed in a few steps: First, simulating the hydrologic model using the mean value ( $P_{mean}$ ) for all parameters, and estimating the corresponding Nash Sutcliffe Efficiency ( $NSE_{mean}$ ) based on simulated and observed daily streamflow. Second, running the model for each parameter's minimum ( $P_{min}$ ) and maximum ( $P_{max}$ ) values while keeping other parameter values unchanged, and calculating their corresponding  $NSE_{min}$  and  $NSE_{max}$ , respectively. Third, estimating the Normalized Sensitivity Coefficient (NSC), using Eq. (1) adopted from [7], to quantify the model sensitivity to the studied parameters, which have different units and orders of magnitude [7,8]. Finally, identifying and ranking of the significant parameters with non-zero NSC in descending order of significance.

$$NSC = \left( \frac{NSE_{max} - NSE_{min}}{NSE_{mean}} \times \frac{P_{mean}}{P_{max} - P_{min}} \right)^2 \quad \text{Eq. (1)}$$



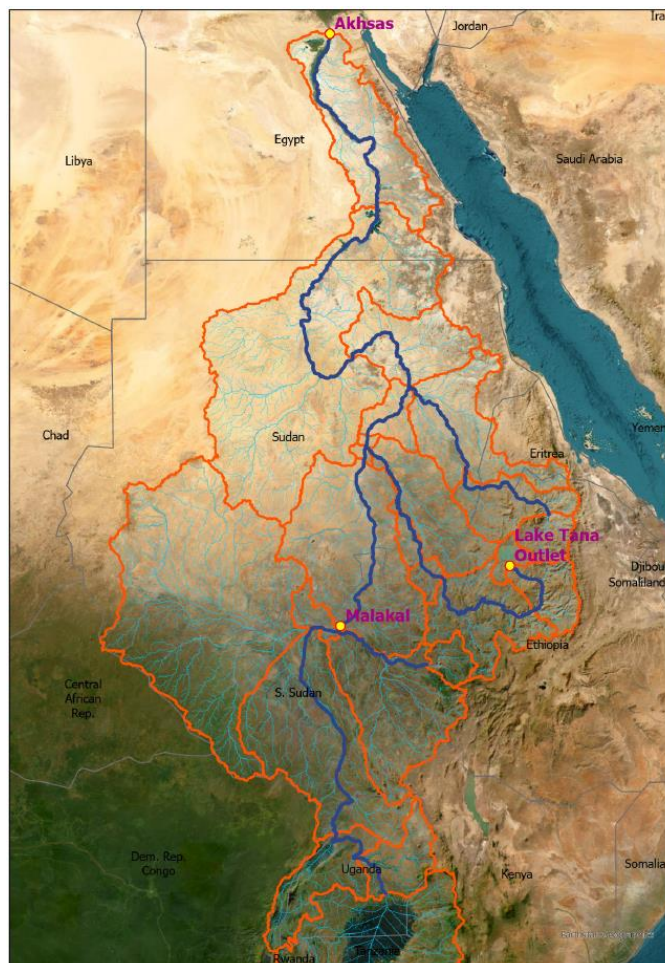


Figure 1. NRB and stations where sensitivity analysis is performed

## RESULTS AND MAIN FINDINGS

The results indicated that, for the NRB, 14 of the investigated 28 parameters are significant in the analysis. However, they are differently ranked at the three studied stations. Generally, the soil parameters were found to be dominant due to their impacts on soil infiltration. Figure (2) provides a similar indication since soil parameters, i.e., soil hygroscopic minimum saturation (i.e., SAT\_WILT), field capacity saturation (i.e., FIELD\_CAPACITY), topsoil thickness (i.e., TOPSOIL) and effective porosity (i.e., POROSITY) are top ranked at all stations. The Manning coefficient representing the in-channel routing parameter comes next in the mean rank over the three stations. However, the lake's initial stage is the most significant parameter at the outlet of Tana's subbasin, which includes Lake Tana near its outlet. Significant parameters included also in-catchment routing (i.e., time of concentration) and land use (e.g., maximum depression storage) parameters. It is worth mentioning that this study's findings are based on the selected stations in the NRB, which may represent NRB behaviour but they may be different for other basins.

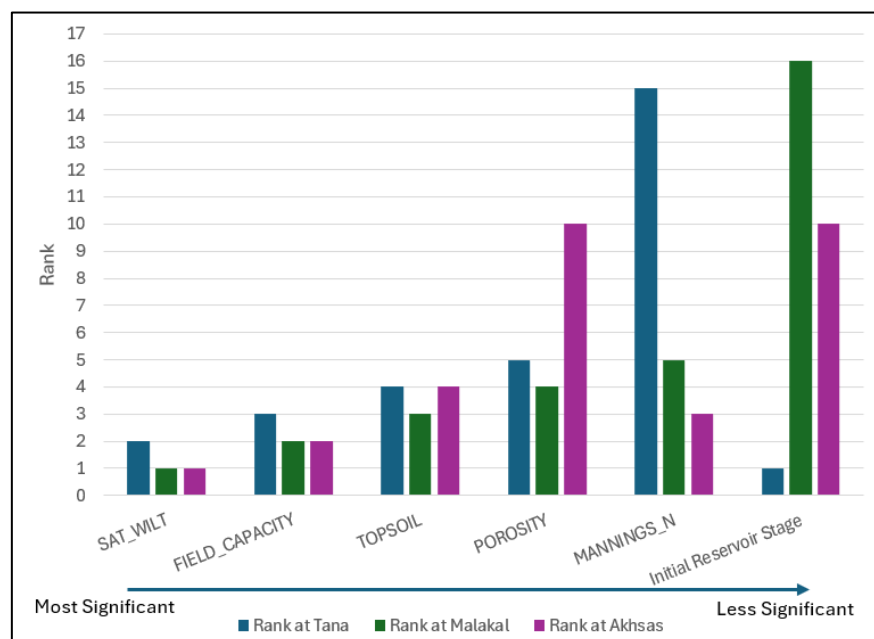


Figure 2. Ranks of the most significant parameters at the studied stations

## CONCLUSIONS AND RECOMMENDATIONS

This study provides a comprehensive sensitivity analysis to investigate the significant hydrologic and routing parameters in the NRB hydrologic model. This analysis was performed using the NSC method at three critical locations in the Blue Nile, White Nile, and Main Nile subbasins to consider the hydrologic characteristics' spatial variation. The results revealed 14 significant out of 28 investigated parameters, with soil (e.g., wilting point and field capacity) and routing (i.e., Manning's coefficient) parameters top-ranked. However, lake parameters (e.g., initial water level) are most significant in subbasins dominated by large lakes. The identified significant parameters should be considered in the model calibration/validation stage. However, refining their ranges before calibration is recommended since conservative ranges were used in this study. In addition, a similar sensitivity analysis is recommended for other subbasins to consider the spatial variation in the NRB characteristics more broadly.

**ACKNOWLEDGMENT** The authors would like to express appreciation for the support of the Natural Science and Engineering Research Council (NSERC) of Canada, grant NSERC Canadian FloodNet [Project Number = NETGP-451456].

## **REFERENCES**

- [1] Craig JR, Brown G, Chlumsky R, Jenkinson RW, Jost G, Lee K, Mai J, Serrer M, Sgro N, Shafii M, Snowdon AP. Flexible watershed simulation with the Raven hydrological modelling framework. *Environmental Modelling & Software*. 2020 Jul 1;129:104728.
- [2] Bergström S. Development and application of a conceptual runoff model for Scandinavian catchments. 1976.
- [3] Sutcliffe JV. The hydrology of the Nile Basin. In *The Nile: Origin, environments, limnology and human use 2009* May 6 (pp. 335-364). Dordrecht: Springer Netherlands.
- [4] Craig, J.R., and the Raven Development Team, Raven user's and developer's manual (Version 3.8), URL: <http://raven.uwaterloo.ca/> (Accessed June, 2024)
- [5] Iio A, Hikosaka K, Anten NP, Nakagawa Y, Ito A. Global dependence of field-observed leaf area index in woody species on climate: a systematic review. *Global Ecology and Biogeography*. 2014 Mar;23(3):274-85.
- [6] Hu Y, Zhang XZ, Mao R, Gong DY, Liu HB, Yang J. Modeled responses of summer climate to realistic land use/cover changes from the 1980s to the 2000s over eastern China. *Journal of Geophysical Research: Atmospheres*. 2015 Jan 16;120(1):167-79.
- [7] Bhatti UN, Bashmal S. Performance evaluation of a standing wave thermoacoustic refrigerator using normalized sensitivity coefficients. *Journal of Thermal Science and Engineering Applications*. 2021 Jun 1;13(3):031013.
- [8] Qureshi BA, Zubair SM. A comprehensive design and rating study of evaporative coolers and condensers. Part I. Performance evaluation. *International journal of refrigeration*. 2006 Jun 1;29(4):645-58.

## Water Operators' Partnerships 'WOPs' and their role in strengthening resilience for a changing climate in MENA

Dahlia Sabri \*<sup>1</sup>, Mai Wardeh<sup>2</sup> and Emrah Engindeniz<sup>3</sup>

<sup>1</sup> MEYAH-Arab International Water Foundation, Cairo, Egypt.

(E-mail: [dsabri@uni-bonn.de](mailto:dsabri@uni-bonn.de))

<sup>2</sup> UN-Habitat, Global Water Operators' Partnership Alliance (GWOPA), Cairo, Egypt.

(E-mail: [mai.wardeh@un.org](mailto:mai.wardeh@un.org))

<sup>3</sup> UN-Habitat, Global Water Operators' Partnership Alliance (GWOPA), Bonn, Germany.

(E-mail: [emrah.engindeniz@un.org](mailto:emrah.engindeniz@un.org))

### ABSTRACT

The climate change crisis underscores the critical role of water service providers as it causes significant harm and challenges the resilience of water utilities facing extreme weather and droughts, and various short- and long-term shocks and pressures. Water management can play a vital role in climate change adaptation and building resilience to changing climate, especially in a water scarce region like MENA. This spans various levels, involving operators and key stakeholders. The Global Water Operators' Partnerships Alliance (GWOPA), established by UN-Habitat in 2009, collaboratively addresses water-related challenges on a global scale. This review paper shows different Water Operators' partnerships (WOPs) case studies from multiple cities and discusses specific approaches and regulatory framework conditions facilitating cross-sectoral collaboration. In addition to SWOT analysis of WOPs challenges, best practices and lessons learned. Relying on WOPs data and drawing on the experiences, it is evident that utilities can strengthen their resilience to the changing climate using the WOPs approach. This paper suggests that collaboration through WOPs is helping water utilities face the climate change implications and is a cost-effective way to share experiences, strengthen long-term capacity, and improve service delivery. The analysis reveals that WOPs have become a widespread and understood form of collaboration within the water sector. It provides a unique opportunity to focus on how alternative water resources might enhance the resilience and sustainability of cities to climate change and decrease the gap between water demand and supply.

**Keywords:** Changing climate, climate resilience in cities, urban water utilities, wastewater treatment plants, WOPs, SWOT.

**Abstract:**

Water scarcity in the MENA region, increased by climate change, population growth, and poor management practices, presents a critical challenge for utilities. The region experiences the highest global water stress, with per capita renewable water resources ten times less than the global average [1]. Over the past 40 years, MENA's water resources have declined by two-thirds and are projected to halve again by 2050 [2]. The World Bank estimates that climate-related water scarcity will cost the MENA region at 6-14% by 2050 due to impacts on agriculture, health, and incomes [2].

This crisis underscores the vital role of water utilities in addressing water scarcity and building climate resilience and has also provided valuable insights that can help water operators adapt to its enduring consequences and enhance their disaster preparedness. Effective water management is crucial for climate change adaptation and building resilience at multiple levels, involving operators and key stakeholders [3].

The Global Water Operators' Partnerships Alliance (GWOPA), established by UN-Habitat in 2009, with a comprehensive global governance framework in place to oversee its operations. As an alliance comprising water operators, water associations, UN Agencies, development partners, labour and civil society organizations, international financial institutions, and the private sector, GWOPA collaboratively addresses water-related challenges on a global scale. GWOPA supports water operators through Water Operator's Partnerships (WOPs). These partnerships are peer support exchanges between two or more water operators on a not-for-profit basis, aimed at strengthening their capacity, enhancing their performance, and enabling them to deliver better services to more people [3, 4]. In the context of global climate change, WOPs facilitate the sharing of best practices for climate adaptation and mitigation, aiding mentee utilities in becoming more climate-resilient and sustainable.

In recent years, WOPs have become increasingly important in the MENA region due to the significant challenges faced by water utilities. These challenges have increased the pressure on the already limited water resources and strained the capacity of water utilities. This study presents different WOPs by examining the methods involved in WOP projects. The paper discusses specific approaches and strategy framework conditions facilitating cross-sectoral collaboration in addition to a SWOT analysis of different WOPs exploring the challenges faced, best practices and lessons learned for future WOPs. The case studies are selected from the MENA region, from different countries in the Arab states including Tunisia, Palestine, Somaliland, Jordan, Egypt and Morocco (Table 1).

Table 1. WOPs case studies in the MENA region.

Case study	Country	Approach/Strategy
WaCCliM Project	Jordan	Development of a climate-friendly, low-emission water sector; introduction of technologies to reduce greenhouse gas emissions; integration of water and energy sectors
ACWUA-WANT Project	MENA	Capacity building, compliance with technical standards, business certifications, energy efficiency regulations, e-learning
Climate Change Adaptation in the Water Sector	MENA	Development and implementation of national adaptation strategies, capacity building; adaptive measures such as reuse of drainage water, solar farming, groundwater recharge.
Managing Water Scarcity	Jordan	Private sector integration, human resources, and leadership development. National water master plan, water resources allocation modelling, water sector reform.
Efficient Use of Nile Water	Egypt	Reducing water losses, improving irrigation infrastructure, enhancing efficiency in water use.
Supporting Yarmouk Water Company	Jordan	Infrastructure rehabilitation, capacity building, asset management, procurement, and tendering improvements.
Strengthening Lebanese Water Sector (Beqaa Valley)	Lebanon	Managed Artificial Recharge, soil moisture sensors, advanced agricultural practices, online water quality monitoring. Capacity building focusing on gender equality.
Reforming Palestinian Water Sector	Palestine	Consolidating service providers, capacity building, asset management, water quality improvement, mobile wastewater treatment plant innovations.
Improving Water Supply and Treatment (Rabat)	Morocco	Alternative disinfection methods, groundwater modeling, training for operation and maintenance
Enhancing Water Management in Gabes	Tunisia	Participatory and inclusive methods, capacity building, assessment studies, pilot projects. Non-revenue water management, urban drainage, community involvement
Enhancing water services delivery for Hargeisa Water Agency	Somaliland	Capacity building, water supply reliability; reducing energy consumption and transition; meter management; services for the urban poor; data-driven tracking; operational and maintenance procedures; leakage control; illegal water use reduction; adaptive management

One example from the established WOP which aims to enhance water management in Gabes, Tunisia. The project contributes to climate resilience through a vital component of building climate resilience by engaging the community and fostering sustainable practices. The WOP engages local citizens and businesses in water conservation efforts by running educational programs that promote awareness of responsible water use. By fostering a culture of sustainability, these initiatives empower individuals to contribute actively to building resilience in water management.

**Error! Reference source not found.** presents the results of SWOT for WOPs in the MENA. The results show that WOPs in the region have employed a variety of shared methods to enhance the water and sanitation resilience to climate change through peer-to-peer partnerships by applying different comprehensive strategies that address key water management challenges. By focusing on capacity building and training, technical and operational development, infrastructure improvement, strategic planning and policy development and community and stakeholder engagement, WOPs foster sustainable water management in the face of climate-induced challenges.



Through cross-sectoral collaboration and partnerships, the beneficiary utilities are better equipped to adapt to and mitigate the impacts of climate change, ultimately enhancing the resilience of both the utility and the community it serves.

*Table 2. SWOT analysis for WOPs case studies in the MENA region.*

<b>Strengths</b>	<b>Weaknesses</b>
<ul style="list-style-type: none"> <li>• Collaborative approach: partnerships leverage local and international expertise.</li> <li>• Capacity building: training programs enhance technical skills and institutional capacities.</li> <li>• Innovative tools and technologies: introduction of advanced tools and online monitoring systems.</li> <li>• Positive outcomes: significant improvements in water supply and service efficiency and better face the climate change implications.</li> </ul>	<ul style="list-style-type: none"> <li>• Financial constraints: limited funding can hinder project implementation and sustainability.</li> <li>• Geographical and infrastructural challenges: difficult terrains and outdated infrastructure can impede progress.</li> <li>• Complex coordination: managing multiple stakeholders across regions can be challenging.</li> </ul>
<b>Opportunities</b>	<b>Threats</b>
<ul style="list-style-type: none"> <li>• Scalability: successful models can be replicated in other regions.</li> <li>• Policy integration: projects can influence national and regional water policies.</li> <li>• Private sector involvement: increased collaboration with private entities can enhance resource allocation and management.</li> </ul>	<ul style="list-style-type: none"> <li>• Climate change: increasing variability and extremity of weather patterns pose ongoing risks.</li> <li>• Political instability: regional conflicts and governance issues can disrupt projects.</li> <li>• Resource scarcity: growing demand and limited water resources require sustainable management.</li> </ul>

In conclusion, WOPs provide a unique opportunity to focus on how alternative water resources might enhance the resilience and sustainability of cities to climate change and decrease the gap between water demand and supply.

WOPs facilitate collaboration between water utilities to tackle the climate crisis. These partnerships are a cost-effective way to share expertise, enhance long-term capacity, and improve service delivery. With climate change causing significant economic, social, and environmental damage—along with increased vulnerability to extreme weather events—WOPs help utilities adapt and strengthen resilience. Lessons learned from current climate challenges can better prepare water operators for future disasters and long-term impacts. However, to ensure the sustainability and effectiveness of WOPs projects, enhanced financial support is critical. Finally, the article highlights entry points for future research on case studies by suggesting that comparative studies of WOPs can offer fresh insights into transnational partnerships, South-South cooperation, and the politics of solidarity in water and sanitation services.

## **REFERENCES**

- [1] Mateo-Sagasta, J.; Al-Hamdi, M.; AbuZeid, K. (Eds.): 'Water reuse in the Middle East and North Africa: a sourcebook', International Water Management Institute (IWMI), 2022, Colombo, Sri Lanka, pp. 292.
- [2] World Bank: 'Beyond Scarcity: Water Security in the Middle East and North Africa', MENA Development Report., 2018, Washington, DC, pp.174.
- [3] Ludwig, F., van Slobbe, E., and Cofino, W.: 'Climate change adaptation and Integrated Water Resource Management in the water sector', J. Hydrol., 2014, 518, pp. 235–242.
- [4] Wright-Contreras, L., Perkins, J., Pascual, M., and Soppe, G.: 'Water operators' partnerships and their supporting role in the improvement of urban water supply in Da Nang', Int. J. Water Resour. Dev., 2020, 36, (1), pp. 1–26.
- [5] UN-Habitat: 'GWOPA Strategy 2020–2024', 2020, pp. 1–56. Available: <https://gwopa.org/wp-content/uploads/2022/05/Strategy-Report-2020-2024.pdf>.

## Mapping Flood Hazards Along the Red Sea Region, Egypt

Ahmed G. Abdelgawad\*<sup>1</sup>, Esam Helal<sup>1</sup>, Mohmaed F. Sobeih<sup>1</sup> and Hamdy Elsayed<sup>1,2</sup>

<sup>1</sup> Civil Engineering Department, Faculty of Engineering, Menoufia University, EGYPT.

(E-mail: [aga.abdelgawad@sh-eng.menofia.edu.eg](mailto:aga.abdelgawad@sh-eng.menofia.edu.eg), [Esamhelal@sh-eng.menofia.edu.eg](mailto:Esamhelal@sh-eng.menofia.edu.eg), [sobeih@yahoo.com](mailto:sobeih@yahoo.com))

<sup>2</sup> Department of Earth Sciences, Faculty of Geosciences, Utrecht University, The Netherlands.

(E-mail: [hamdy.abdelwahed@sh-eng.menofia.edu.eg](mailto:hamdy.abdelwahed@sh-eng.menofia.edu.eg))

### ABSTRACT

Flash floods pose significant threats to communities and ecosystems, particularly in arid regions like the Red Sea region in Egypt, which has experienced severe flash floods in recent years. The area from Safaga to Port Ghalib along the Red Sea coast is vulnerable to recurrent flash floods. To assess flood hazards in this region, we employ a GIS-based morphometric analysis with two sets of parameters. Together with basin area, slope, circularity ratio, drainage intensity, and curve number, the first set includes the shape factor and sinuosity index, while the second set includes the form factor and elongation ratio. Data on land use, soil type maps, and digital elevation models (DEMs) were collected and processed. Watersheds and drainage networks were delineated using GIS techniques. Morphometric parameters and curve numbers for sub-basins were estimated from the digitised soil type and land use maps. These parameters were used to calculate the flood hazard in each sub-basin using a five-level grade, ranging from very low to very high. Results indicate nearly half of the study area faces a very high flood hazard level. Although the overall distribution of hazard degrees for the two parameter sets is similar, basins with morphometric characteristics sensitive to flood risks showed changes in flood hazard. These findings highlight the sensitivity of flood hazards to different morphometric parameters. Furthermore, morphometric analysis can assist in identifying flood-prone areas, protecting local communities, and managing extreme flood events. Identifying these areas could help policy and decision-making to mitigate flood risks and enhance community resilience in arid regions.

**Keywords:** Flood hazard mapping, GIS-based morphometric analysis, Sustainable development goals, The Red Sea region, Water resources management.

## **METHODOLOGY**

Flash floods are sudden, dangerous natural disasters caused by intense precipitation, often occurring in areas with steep hillsides, impermeable soils, and exposed rocks. The Red Sea coast region of Egypt is particularly susceptible due to its topography and erratic rainfall patterns [1], resulting in significant human and economic losses [2]. Understanding these hazards is crucial for risk mitigation and sustainable development. Flood hazard mapping is a common approach for analysing flood risk and studying flood characteristics [3].

The methodology involves the integration of GIS techniques and morphometric analysis to map flood hazards, as shown in Figure (1). The employed method is applied to a study area spanning from Safaga to Port Ghalib. High-resolution DEMs from the US Geological Survey (USGS) were processed using ArcGIS Pro to delineate drainage networks. Soil type and land use data from the soil association map of Egypt were digitised to compute the curve number using the Watershed Modeling System (WMS) software. Key morphometric parameters were calculated, and each parameter's hazard degree was evaluated on a five-point scale, with one indicating very low and five indicating very high. Finally, the overall hazard degree for each basin was determined by summing the individual hazard scores.

This study aims to assess morphometric parameter sets for flood hazards. The two sets include basin area, slope, drainage intensity, circularity ratio, and curve number. The first set also includes shape factor and sinuosity index, while the second parameter set includes form factor and elongation ratio. The form factor represents the shape of the basin, while the elongation ratio depicts the overall morphology of the basin, providing comprehensive coverage of watershed aspects due to their stronger correlation with flood potential [4].

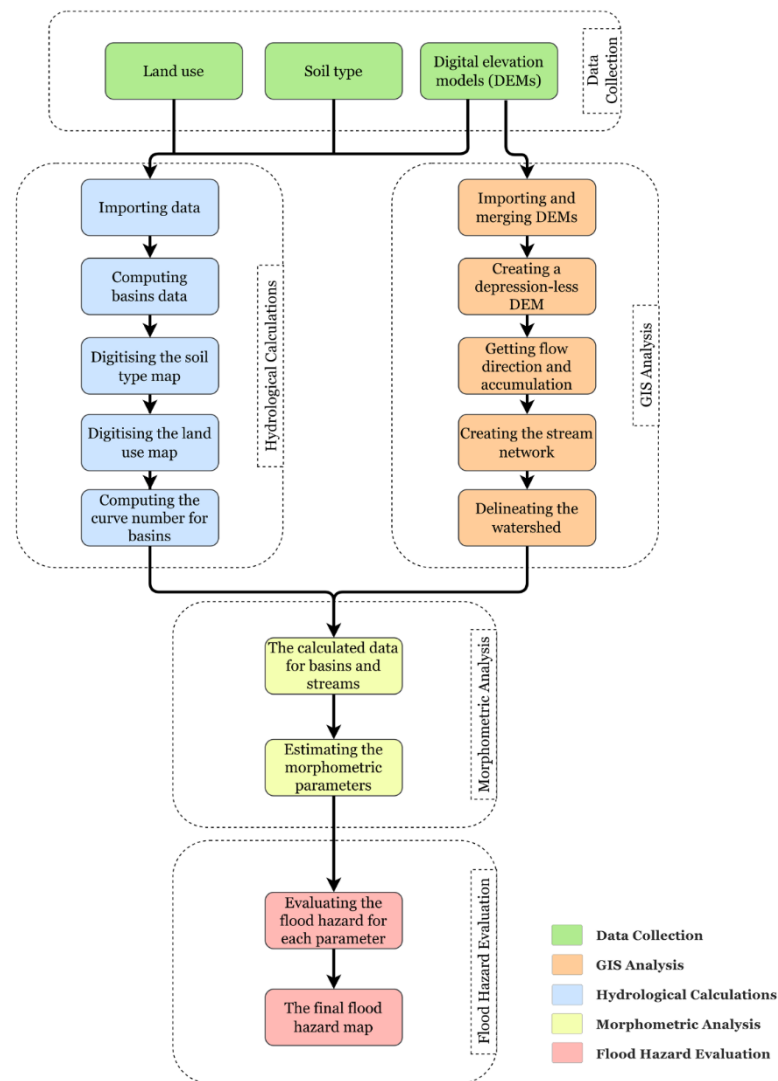
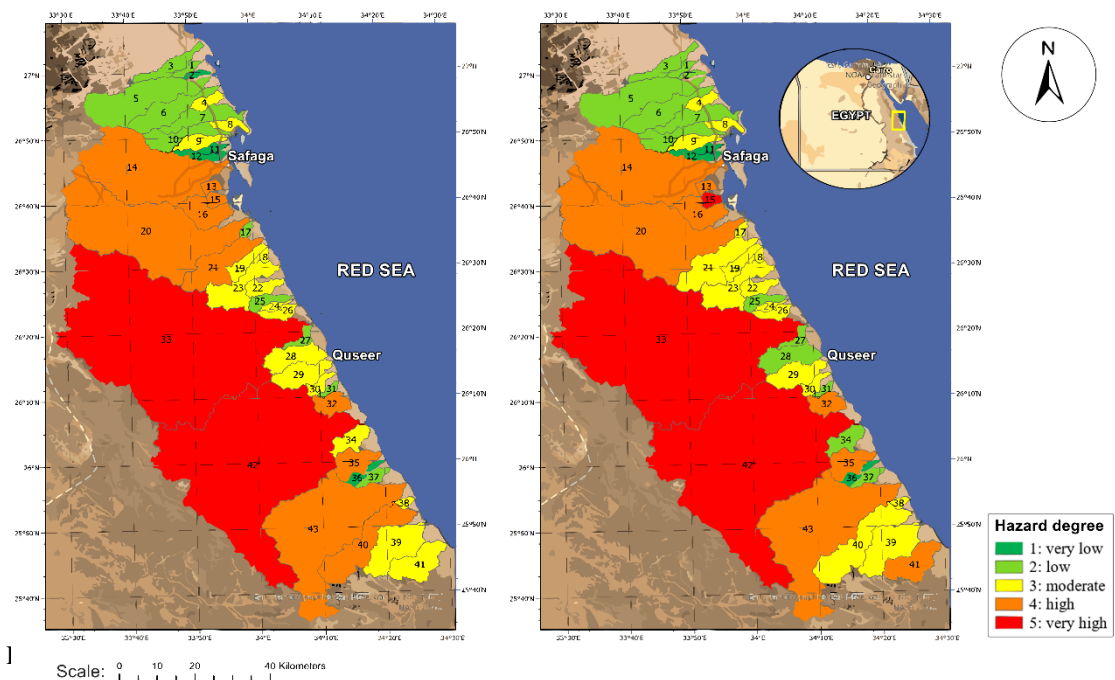


Figure 1. Procedure for GIS-morphometric estimation for flood hazard mapping [5]

## RESULTS

The study area encompasses 43 basins; each basin is evaluated for flood hazards using the two sets of morphometric parameters. The flood hazard maps of both combinations are shown in Figure (2). The two basins, B33 and B42, showed a very high hazard degree in both combinations. This is attributed to their large areas, steep slopes, and numerous first-order streams, increasing their runoff potential and making them highly vulnerable to flooding [5]. The analysis using the first combination revealed that basins with very low and low hazard degrees typically had small areas, low slopes, and higher shape factors. These characteristics contribute to their reduced vulnerability, as they allow for more infiltration and less rapid runoff [6].



The overall distribution of hazard degrees for the second parameter set remained similar to those in the first set, with medium and high hazard degrees being predominant. In the second combination, hazard degrees of 35 remained unchanged, while eight basins exhibited changes in their hazard categories. Basins with higher form factor and elongation ratio values were found to have a higher flood hazard. This is due to their morphology's impact on rapid runoff concentration. Higher form factor values lead to high peak flows of shorter duration, while higher values of elongation ratio indicate a more compacted basin shape, resulting in shorter infiltration times and higher runoff [4]. Comparing both combinations highlights the sensitivity of flood hazards to different morphometric parameters. This assessment allows for improved identification of flood-prone areas.

## **CONCLUSIONS AND RECOMENDATIONS**

This study underscores the advantage of GIS-based morphometric analysis in evaluating flood hazards in the Red Sea region. Analysis of two different morphometric parameter combinations revealed key factors influencing flood potential, particularly in basins B33, B42, and B15 classified with very high hazard degrees in the second combination. These findings can help enhance flood risk planning and management strategies in flood-prone regions



**REFERENCES**

- [1] M. O. Arnous, A. E. El-Rayes, H. El-Nady, and A. M. Helmy, “Flash flooding hazard assessment, modeling, and management in the coastal zone of Ras Ghareb City, Gulf of Suez, Egypt,” *J Coast Conserv*, vol. 26, no. 6, Dec. 2022, doi: 10.1007/s11852-022-00916-w
- [2] A. A. Elnazer, S. A. Salman, and A. S. Asmoay, “Flash flood hazard affected Ras Gharib city, Red Sea, Egypt: a proposed flash flood channel,” *Natural Hazards*, vol. 89, no. 3, pp. 1389–1400, Dec. 2017, doi: 10.1007/s11069-017-3030-0.
- [3] R. B. Mudashiru, N. Sabtu, I. Abustan, and W. Balogun, “Flood hazard mapping methods: A review,” *J Hydrol (Amst)*, vol. 603, p. 126846, Dec. 2021, doi: 10.1016/j.jhydrol.2021.126846.
- [4] S. Soni, “Assessment of morphometric characteristics of Chakrar watershed in Madhya Pradesh India using geospatial technique,” *Appl Water Sci*, vol. 7, no. 5, pp. 2089–2102, 2017, doi: 10.1007/s13201-016-0395-2.
- [5] A. G. Abdelgawad, E. Helal, M. F. Sobeih, and H. Elsayed, “Flood hazard mapping using a GIS-based morphometric analysis approach in arid regions, a case study in the Red Sea Region, Egypt,” *Appl Water Sci*, vol. 14, no. 4, p. 81, 2024, doi: 10.1007/s13201-024-02130-5.
- [6] M. Obeidat, M. Awawdeh, and F. Al-Hantouli, “Morphometric analysis and prioritisation of watersheds for flood risk management in Wadi Easal Basin (WEB), Jordan, using geospatial technologies,” *J Flood Risk Manag*, vol. 14, no. 2, Jun. 2021, doi: 10.1111/jfr3.12711.

**Theme 2: Strategic Water Resources Management in  
Enhancing Community Resilience**  
**Day 2**

## The Water, Energy and Food Nexus: Toward Resilient Built Environments

Zeina ElZein\*<sup>1</sup>

<sup>1</sup> Assistant Professor, Architecture Department, Faculty of Fine Arts, Helwan University, Cairo, Egypt.

(E-mail: [Zeina.ElZein@f-arts.helwan.edu.eg](mailto:Zeina.ElZein@f-arts.helwan.edu.eg), [Zeinabaher@gmail.com](mailto:Zeinabaher@gmail.com) )

### ABSTRACT

Urban areas are facing threats of the availability of core resources. Large percentage of urban dwellers are facing water, energy and food (WEF) insecurity. In recent years, urban resilience has been a research focus. COVID-19 pandemic has impacted the urban infrastructure, service provision, interconnectedness and accessibility to core resources. Urban resilience has been focusing on the ability of cities to face and recover from shocks and crises, yet, nowadays, a holistic approach is needed. This paper explores the need for interdisciplinary approaches to the built environment that integrate WEF resources. The research studies publications over the past years on concepts of the WEF nexus, and urban resilience, to identify the key research focus, gaps and needs for future research. The importance of the study is that it links disciplines in the built environment: architects, urban designers and planners, with technical WEF disciplines to ensure a holistic sustainable development of communities. The study recommends future research to focus on 4 main pillars: economic and funding to Urban Agriculture (UA) that promotes circular economy in vulnerable communities; engagement of stakeholders in terms of interviews, trainings, inclusion of local communities and academic institutions; quantitative assessment of UA, urban water solutions and urban water use, in addition to inclusion of socioeconomic aspects in assessment; promotion of participatory tools, simulation models, feedback tools, control technologies and market models. These recommendations aim to provide a foundation for future research that rely on an interdisciplinary sustainable resilience approach.

**Keywords:** Built Environment, Community Resilience, Sustainable Development, Water-energy-food Nexus, Water Security

### METHODOLOGY

This study explores academic content on the WEF Nexus, urban context and resilience, to identify the gaps and challenges, and provide guidance for needed future research.

A systematic literature review was carried out using the Web of Science Database to identify

literature on the WEF Nexus in an urban context, addressing resilience. The keywords used were: (ALL=(water energy and food nexus)) AND ALL=(urban) AND ALL=(resilience). The search was limited between January 2020 to January 2024. Results were filtered to identify open access, English articles or review articles, using the Science Citation Index Expanded, Social Science Citation Index and Emerging Sources Citation Index. The search was carried out on January 31st, 2024. Documents were manually filtered, eliminating those missing one or two of the keywords in text, to end with 26 documents. Most documents were published in 2023 (10 articles), followed by 2021 (7 articles).

The resulting 26 documents were analyzed based on the focus on the three elements of the nexus, within the urban and resilience context. It was found that articles focusing mainly on one element of the nexus were either focusing on water or food. While the rest of the articles focused on the integration of the WEF nexus. It is worth noting that articles focusing on energy solely, within the search context of urban resilience were not found. Using the word cloud engine, the abstracts of the 26 articles were analyzed to identify the main keywords, and to guide the analysis of the literature. It was found that the words “Urban” and “Water” were the most frequent, followed by “food”, then other words related to “energy”, “resilience” “nexus”, as in Figure (1).



Figure 1. Word cloud representation of the most frequent words found in the bibliography from analyzing the abstracts.

## **RESULTS/FINDINGD**

Nexus-based urban planning supports efficient decision-making for resilient integrated approaches that address all sectors and are based in the city context.

Policies often rely on sector-based decision-making, overlooking the interconnections between the WEF nexus, especially in cities and small plots [1].

Many studies on UA overlook its consumption of resources and its impact on the environment and the importance of waste management, recycling and reuse [2]. It also shows that UA requires technological approaches to ensure it supports sustainable and resilient environmental food systems.

UA offers local food production, but it is limited due to the uncertainty of selling the crops and the large land area requirements [3]. Expanding UA to include adjacent areas to cities would make local food production more feasible. Effective food waste management should focus on the consumer level and on redistribution at the supply level. The economic sector is key in setting regulations that support a circular economy. Supporting the diversity of farmers enhances food security [4].

Quantitative assessment of water needs for green spaces in cities is limited. Urban water management solutions increase the resilience of the WEF systems and support the concept of circular cities [5].

Implementing the WEF nexus in an urban context ensures shared cross-sectoral governance, resilience against disasters, equity of resource distribution and better quality of life [6]. It requires the involvement of stakeholders, participatory approaches and consideration of both urban and rural areas. Municipal decision-making often does not include guidelines on the integration of the nexus. Additionally, urban nexus approaches overlook the socio-ecological aspects due to their complexity. The nexus can support climate change adaptive planned migration through qualitative system modeling to ensure resource accessibility and availability [7]

Modeling platforms can support the optimization of decision-making regarding WEF resources. Active control technologies can also improve the efficiency of urban water management solutions [8].

## **CONCLUSIONS AND RECOMENDATIONS**

Figure (2) summarizes the key recommendations categorized into four sections: funds/economy; stakeholders; assessment and tools for promoting resilient cities through the implementation of the WEF nexus into the urban context.

The study recommends including UA in policies and regulations, providing sufficient funds and incentives for vulnerable communities, identifying their vulnerabilities, engagement of stakeholders, linking urban and rural areas and studying climate migration flows are critical towards resilient community planning.

Future research should focus on quantitative assessment of the used resources in UA systems and green areas to explore its impact on resource consumption in different climatic and geographic contexts.

Simulation models and technologies should be developed to understand WEF nexus dynamics in cities and include socio-economic aspects. Participatory and feedback tools should be developed to facilitate

data analysis and support decision-making. Establishing market models for food and electricity is also recommended.

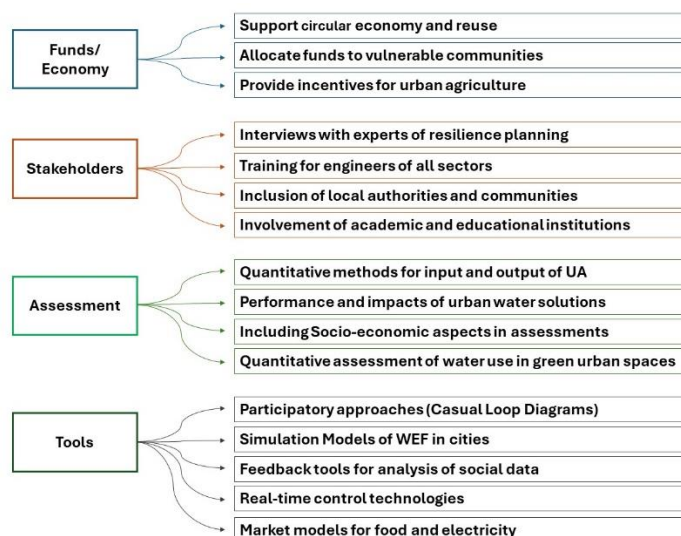


Figure 2. Key recommendations categorized into four sections.

## REFERENCES

- [1] Dargin, J., Berk, A., Mostafavi, A.; ‘Assessment of household-level food-energy-water nexus vulnerability during disasters’. *Sustainable Cities and Society* 2020. 62, 102366.
- [2] Dorr, E., Hawes, J.K., Goldstein, B., Fargue-Lelièvre, A., Fox-Kämper, R., Specht, K., Fedenczak, K., Caputo, S., Cohen, N., Ponizy, L., Schoen, V., Górecki, T., Newell, J.P., Jean-Soro, L., Grard, B.: ‘Food production and resource use of urban farms and gardens: a five-country study. *Agron. Sustain. Dev.* 2023. 43, 18.
- [3] Thompson, J., Ganapathysubramanian, B., Chen, W., Dorneich, M., Gassman, P., Krejci, C., Liebman, M., Nair, A., Passe, U., Schwab, N., Rosentrater, K., Stone, T., Wang, Y., Zhou, Y.: ‘Iowa Urban FEWS: Integrating Social and Biophysical Models for Exploration of Urban Food, Energy, and Water Systems’. *Front. Big Data* 2021. 4, 662186.
- [4] Fox-Kämper, R., Kirby, C.K., Specht, K., Cohen, N., Ilieva, R., Caputo, S., Schoen, V., Hawes, J.K., Ponizy, L., Béchet, B.: ‘The role of urban agriculture in food-energy-water nexus policies: Insights from Europe and the U.S’. *Landscape and Urban Planning* 2023. 239, 104848.
- [5] Pan, L., Zhao, Y., Zhu, T.: ‘Estimating Urban Green Space Irrigation for 286 Cities in China: Implications for Urban Land Use and Water Management’. *Sustainability*. 2023. 15, 8379.
- [6] Gondhalekar, D., Erlbeck, R.: ‘Application of the Nexus Approach as an Integrated Urban Planning Framework: From Theory to Practice and Back Again. *Front. Sustain. Cities* 2021 3, 751682.
- [7] Ghodsvali, M., Dane, G., De Vries, B.: ‘The nexus social-ecological system framework (NexSESF): A conceptual and empirical examination of transdisciplinary food-water-energy nexus’. *Environmental Science & Policy* 2022. 130, 16–24.
- [8] Vinca, A., Parkinson, S., Byers, E., Burek, P., Khan, Z., Krey, V., Diuana, F.A., Wang, Y., Ilyas, A., Köberle, A.C., Staffell, I., Pfenninger, S., Muhammad, A., Rowe, A., Schaeffer, R., Rao, N.D., Wada, Y., Djilali, N., Riahi, K.: ‘The NEXUS Solutions Tool (NEST) v1.0: an open platform for optimizing multi-scale energy–water–land system transformations’. *Geosci. Model Dev.* 2020, 1095–1121.



**Theme 3: Innovation and Financing Resilient Solutions for Water  
Security**  
**Day 3**

## **Agricultural water consumption management, a case study from Turpan, China**

Weiwei Zhu\*<sup>1</sup>, Nana Yan<sup>1</sup>, Bingfang Wu<sup>1</sup> and Zonghan Ma<sup>1</sup>

<sup>1</sup> Key Laboratory of Remote Sensing and Digital Earth, Aerospace Information Research Institute, Chinese Academy of Sciences, P.R. CHINA.

(E-mail: zhuww@aircas.ac.cn, yannn@aircas.ac.cn, wubf@aircas.ac.cn, [mazh@aircas.ac.cn](mailto:mazh@aircas.ac.cn))

### **ABSTRACT**

Evapotranspiration (ET) is the real water loss in the arid and semi-arid regions in the world, signifying the actual water consumption. Reducing agricultural water consumption and improving agricultural water management are crucial for the sustainable development. In this case study from Turpan of China, we introduce a method for calculating the maximum available consumption water in agriculture for human activities. The water consumptions in natural and artificial ecosystems were separated using ET, precipitation and land cover data. Then, we design the scenarios and analyze the target water consumption for agriculture in the context of industrial and domestic development. Furthermore, the maximum allowable cultivated area was proposed. This method can significantly aid in the sustainable management of water resources in Turpan, and has been also implemented in Lebanon as a practical case study under the support by the China-Lebanon joint laboratory on modern agriculture and water management project.

**Keywords:** Evapotranspiration, Available water consumption, Agricultural water consumption management, Remote sensing.

### **METHODOLOGY**

The study area is the Ertanggou watershed in Turpan at Xinjiang Province of China, which covers about 23 percent of cultivated area of Turpan. The headwaters of this watershed predominantly function as water-yielding zones, while the downstream areas are utilized for agricultural water consumption, with a multi-year annual average rainfall of 16mm. The significant escalation of agricultural water consumption in the downstream areas has resulted in severe over-extraction of groundwater, causing the AiDing Lake near the downstream oasis to nearly dry up and vanish, leading to unsustainable agriculture development in the area. ET data from 2008 to 2013 was estimated based on ETWatch model [1]. Meteorological data, industrial and domestic water consumption data were accessed from the Turpan Water Resources Bureau. Land cover and crop map data were monitored using remote sensing data [2].

The concept of maximum available consumption water (ACW) for human activities has been proposed [3], which refers to the amount of water that can be consumed by human activities in all forms for domestic, industrial and agricultural purposes within a regional context without jeopardizing the environment and the sustainable development of ecosystems; the formula is shown as below.

$$ACW = P + InF - ETn - OutF \quad (1)$$

Where, P is annual precipitation. InF and OutF are annual inflow and outflow runoff for a certain region, respectively. ETn is water consumption by natural ecosystems, which is calculated based on machine learning methods using ET, precipitation and meteorological data.

### **RESULTS/FINDINGS**

The average annual precipitation for the whole watershed from 2008 to 2013 was 107.99 million m<sup>3</sup>. The average ETn was 20.82 million m<sup>3</sup>. ACW in the upper areas of Ertangou watershed from 2008 to 2013 was 87.17 million m<sup>3</sup>, accounting for about 81% of the total ET. Because of very low precipitation in the downstream areas, the main water resources for irrigation of farmland and industrial and domestic water consumption in lower reaches are from the flow of the upper reaches through underground qanats. Total average actual water consumption for human activities in the downstream areas during the period of 2008-2013 was 153.7 million m<sup>3</sup>. Thus, the average actual groundwater overdraft in Ertangou from 2008 to 2013 was approximately 66.7 million m<sup>3</sup>. Table 1 shows that the target water consumption for agriculture is 8297 million m<sup>3</sup> in the stage (2008-2013), and 7,816 million m<sup>3</sup> in 2030.

Combined crop type proportion and annual ET information (see Figure 1), the ET intensity of crops was 441 m<sup>3</sup>/mu. Considering the limit of the target water consumption for agriculture during two different stages, the maximum allowable cultivated area for cropland was estimated at 18.81\*10<sup>4</sup> mu in the stage (2008-2013), and 17.72\*10<sup>4</sup> mu in 2030 (see Table 2). However, the redline for protection of cropland area was only 20.8\*10<sup>4</sup> mu, which was also beyond the maximum allowable cultivated area. Therefore, it is necessary to carry out the cropland withdrawal policy in order to ensure sustainable development of agriculture water resources. The table2 also shows the abandon cropland areas in different periods.

Table 1. Target water consumption in downstream of Ertanggou

Year	Target water consumption / million m <sup>3</sup>			
	Total	Domestic	Industrial	Agricultural
2008-2013	8,717	213	207	8,297
2030	8,717	224	677	7,816

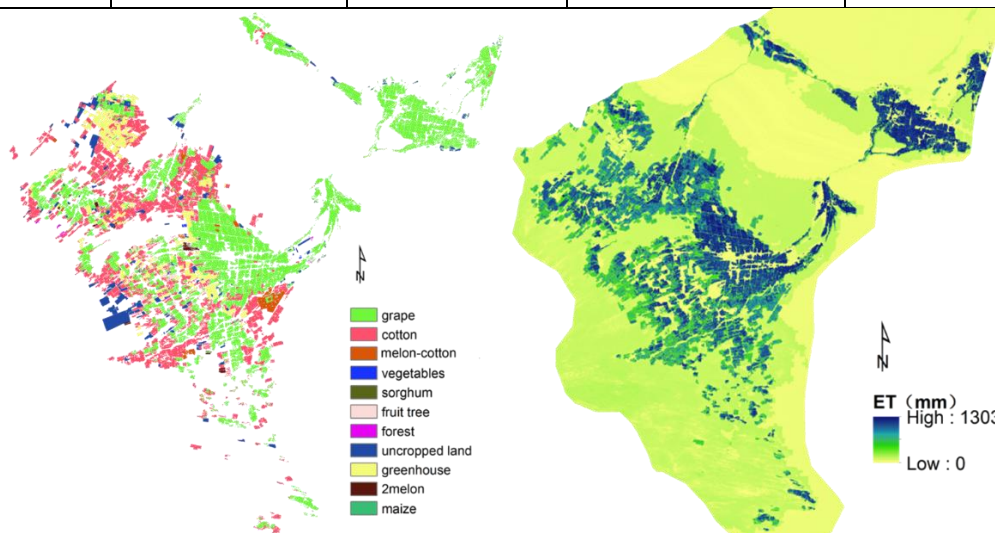


Figure 1. Spatial distribution of Cropland and ET in the downstream areas of Ertanggou

Table 2. Maximum cropped land under the cap of agricultural ACW in the downstream areas of Ertanggou

Year	Current Area (10 <sup>4</sup> mu)	AWC of agricultural (10 <sup>4</sup> m <sup>3</sup> )	ET intensity (m <sup>3</sup> /mu)	Allowable cultivated area (10 <sup>4</sup> mu)	Required abandon cropland area (10 <sup>4</sup> mu)
Stage (2008-2013)	32.51	8,297	441	18.81	13.70
2030	32.51	7,816	441	17.72	14.79

## CONCLUSIONS AND RECOMENDATIONS

This study proposed a method to estimate the maximum available water consumption in agriculture for human activities in Ertanggou watershed. The target water consumption in agriculture and the maximum allowable cultivated area for cropland were analyzed to enhance the knowledge of the current water resource problems in agriculture and feasible solutions. This approach can effectively support the sustainable use of water resources in Turpan, and this case study has been practically applied in Lebanon under the supported by the National Key R&D Program of China, China-Lebanon joint laboratory on modern agriculture and water management Project.

**ACKNOWLEDGMENT** The authors would like to express appreciation for the support of the National Key R&D Program of China [2022YFE0113900].

## **REFERENCES**

- [1] Bingfang, W., Weiwei Z., Nana, Y., et al.: 'Regional actual evapotranspiration estimation with land and meteorological variables derived from multi-source satellite data', *Remote Sens.*, 2020, 12(2), pp.332
- [2] Nana, Y., Bingfang, W., Weiwei Z., et al.: 'Assessment of Agricultural Water Productivity in Arid China', *WATER*, 2020, 12(4), pp.1161
- [3] Bingfang, W., Hongwei, Z., Nana, Y., et al.: 'Approach for Estimating Available Consumable Water for Human Activities in a River Basin'. *Water Resour. Manag.*, 2018, 32, pp.2353–2368

## Efficient Removal of Organic Dyes and Lead Ions Using Thermally Induced Catalytic Decomposition and Adsorption Mechanisms with $\alpha$ -Fe<sub>2</sub>O<sub>3</sub>-CuO Nanocomposites

Abdelmeguid E. Aboubaraka<sup>(1)</sup>, Eman F. Aboelfetoh<sup>(2)</sup> and El-Zeiny M. Ebeid<sup>(2)</sup>

<sup>(1)</sup>R & D Department of El-Gharbia Water and Wastewater Company, Tanta, Egypt

([abdelmeguidbaraka@gmail.com](mailto:abdelmeguidbaraka@gmail.com))

<sup>(2)</sup>Chemistry Department, Faculty of Science, Tanta University, Tanta, Egypt

### ABSTRACT

Wastewater treatment for recycling is vital in conserving water resources, reducing environmental pollution, and fostering sustainability through responsible and efficient water management. The present study provides a new, eco-friendly, and cost-effective approach for the synthesis of  $\alpha$ -Fe<sub>2</sub>O<sub>3</sub>-CuO nanocomposite by a moderate thermal oxidative decomposition of copper hexacyanoferrate complex. The structure and surface morphology of the synthesized nanocomposite were verified using various characterization techniques. In the presence of H<sub>2</sub>O<sub>2</sub>, the nanocomposite  $\alpha$ -Fe<sub>2</sub>O<sub>3</sub>-CuO displayed promising activity as a heterogeneous catalyst to stimulate thermally induced degradation of organic dyes, including direct brown 4 (DV4), methylene blue (MB), and rhodamine b (RhB) without any light irradiation. As a result of the synergistic effect of Fe<sub>2</sub>O<sub>3</sub> and CuO in the nanocomposite, enhanced catalytic activity was achieved compared with Fe<sub>2</sub>O<sub>3</sub> and CuO nanoparticles. The reaction rate increased substantially with the temperature, revealing its key role in the degradation process. The reactive species and mechanism of H<sub>2</sub>O<sub>2</sub> activation on  $\alpha$ -Fe<sub>2</sub>O<sub>3</sub>-CuO were studied. The chemical oxygen demand and total organic carbon results further indicated that all dyes decomposed into simple inorganic materials. The catalyst maintained notable stability for five successive cycles. The ability of  $\alpha$ -Fe<sub>2</sub>O<sub>3</sub>-CuO to remove Pb(II) ions via adsorption was evaluated under various conditions. The adsorption process was governed by the Freundlich equation and follows first-order kinetics. The great performance and stability of this nanocomposite for the elimination of a wide variety of pollutants render it promising for application in the recycling of industrial wastewater.

**Keywords:** Heterogeneous catalysis; Recycling, Synergistic effect, Temperature driven



## METHODOLOGY

Figure 1(a) shows that the  $\alpha$ -Fe<sub>2</sub>O<sub>3</sub>-CuO nanocomposite was synthesized by thermal oxidative decomposition of copper hexacyanoferrate complex. The surface morphology was examined using Scanning Electron Microscopy (SEM), which revealed monoclinic CuO particles and  $\alpha$ -Fe<sub>2</sub>O<sub>3</sub> nanorods as shown in figure 1(a). Transmission Electron Microscopy (TEM) confirmed the nanoscale structure, while X-Ray Diffraction (XRD) patterns indicated a high-density CuO phase and successful composite synthesis. Fourier Transform Infrared (FTIR) spectroscopy showed overlapping Cu–O and Fe–O bands at 530 cm<sup>-1</sup>. Energy-Dispersive X-ray (EDX) analysis determined the elemental composition with a Fe-to-Cu ratio of 1:2. The optical band gap was calculated using the Tauc equation [1], revealing a value of 2.92 eV. The catalytic activity was tested for degrading organic dyes (DV4, MB, RhB) in the presence of H<sub>2</sub>O<sub>2</sub>. Adsorption capacity was evaluated for Pb(II) ions at varying concentrations, nanocomposite doses, and pH levels. Kinetics and isotherm models were applied to understand the adsorption mechanism, including pseudo-first-order kinetics and Freundlich isotherm.

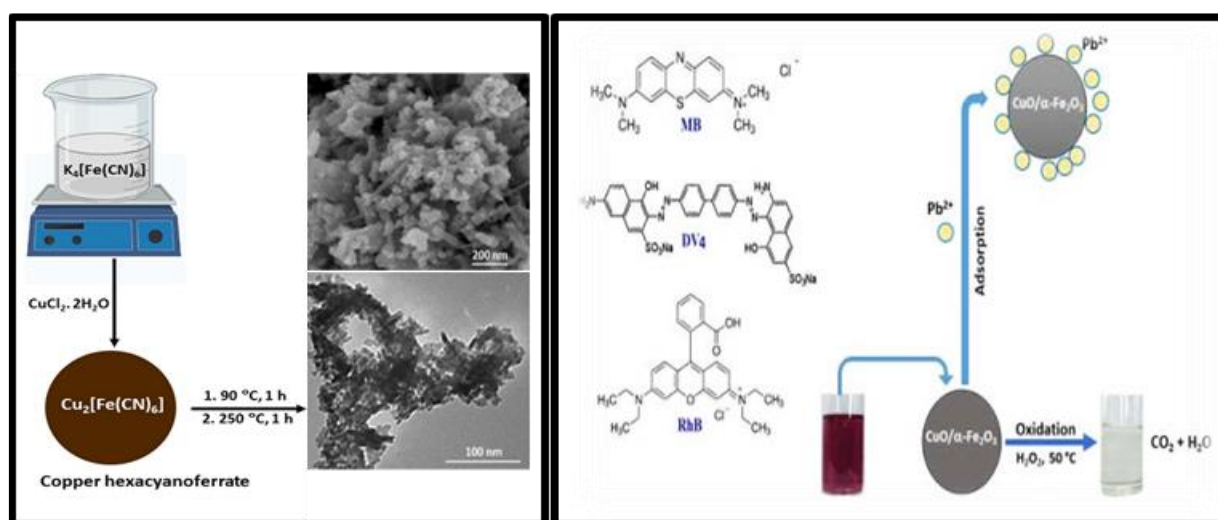


Figure 1: Preparation of the  $\alpha$ -Fe<sub>2</sub>O<sub>3</sub>-CuO nanocomposite and SEM and TEM image of it (a), Graphical abstract shows the Structure of organic dyes; (MB), (DV4), and (RhB) and the nanocomposite effect on different pollutants

## RESULTS/FINDINGS

The  $\alpha$ -Fe<sub>2</sub>O<sub>3</sub>-CuO nanocomposite significantly enhanced the degradation of (DV4) dye due to the synergistic effect between Fe<sub>2</sub>O<sub>3</sub> and CuO components. Optimal degradation was achieved using hydrogen peroxide (H<sub>2</sub>O<sub>2</sub>) within the concentration range of 0.01 to 0.07 M and a catalyst dose of 0.04 g, providing more active sites. Higher doses reduced efficiency due to radical self-quenching and particle aggregation. The lowest DV4 concentration tested ( $1.4 \times 10^{-5}$  M) achieved nearly complete degradation in 15 minutes. Temperature and pH were crucial, with temperatures from 25 to 70 °C significantly enhancing degradation efficiency. The optimal pH for DV4 degradation was pH 6, with variations affecting the catalyst's surface charge and its interaction with dye molecules as shown in figure 2(a).

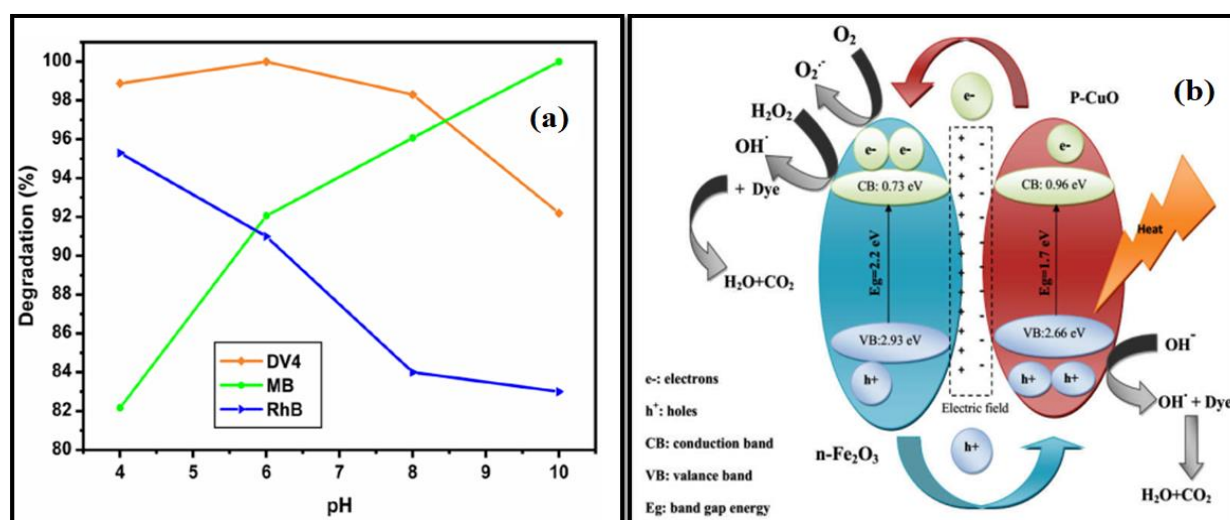


Figure 2: Degradation percentage of 4 (DV4), (MB), and (RhB) (a) at various pH values, the double charge transfer proposed mechanism of dyes degradation by  $\alpha$ -Fe<sub>2</sub>O<sub>3</sub>-CuO nanocomposite

Figure 2(b) shows a type-II heterojunction mechanism was employed [2], promoting charge carrier separation and boosting thermal catalytic activity, with an internal electric field facilitating electron flow from CuO to  $\alpha$ -Fe<sub>2</sub>O<sub>3</sub>. TOC and DOC measurements indicated around 92%, 90%, and 79% degradation of DV4, MB, and RhB, respectively, to CO<sub>2</sub> and H<sub>2</sub>O after 2 hours. The catalyst demonstrated excellent recyclability after five runs.

The nanocomposite also showed efficient adsorption for Pb(II) ions. At room temperature, a 0.01 g dose removed Pb(II) ions from 8 mg/L solution with an equilibrium efficiency of 87.8% after 60 minutes. Increasing the Pb(II) concentration from 4 to 16 mg/L decreased removal efficiency due to saturation of adsorption sites. Higher nanocomposite doses improved removal efficiency by providing more binding sites[3]. Kinetic studies indicated a pseudo-first-order reaction predominated.

Table3 : Adsorption isotherm parameters for the removal of Pb(II) by the  $\alpha$ -Fe<sub>2</sub>O<sub>3</sub>-CuO nanocomposite

Adsorption models	Equations	Parameters	Values
Langmuir	$\frac{C_e}{q_e} = \frac{1}{q_m K_L} + \frac{C_e}{q_m}$	$q_{max}$ (mg/g)	500
		$K_L$ (min <sup>-1</sup> )	0.151
		$R^2$	0.9475
Freundlich	$\ln q_e = \ln K_F + \frac{1}{n} \ln C_e$	$K_F$	74
		$n$	1.17
		$R^2$	0.9995
D-R isotherm	$\ln q_e = -\beta \varepsilon^2 + \ln q_s$ $\varepsilon = RT \ln \left( \frac{1}{C_e} + 1 \right)$ $E = \frac{1}{\sqrt{2\beta}}$	$q_s$	145
		$E$	6.70
		$R^2$	0.9788

The Freundlich isotherm model best fit the experimental data, implying favorable multilayer adsorption on a heterogeneous surface as shown in table 1. The D-R isotherm confirmed physical adsorption (table 1). The nanocomposite maintained 70% efficacy in removing Pb(II) after four cycles.

## CONCLUSIONS AND RECOMENDATIONS

This study showcases an eco-friendly and cost-effective synthesis of an  $\alpha$ -Fe<sub>2</sub>O<sub>3</sub>-CuO nanocomposite, which is confirmed by various analytical techniques and demonstrates high efficiency in degrading organic dyes and removing Pb(II) from water. The degradation process, enhanced by H<sub>2</sub>O<sub>2</sub> and temperature, is characterized by a charge transfer mechanism, leading to significant dye degradation and recyclability of the catalyst. The adsorption kinetics align with a pseudo-first-order model, and the Freundlich isotherm describes the adsorption equilibrium well, highlighting the nanocomposite's potential as a reusable catalyst and adsorbent in wastewater treatment. SO, it is recommended to conduct pilot-scale testing, environmental assessment, regulatory compliance, and explore expanding applications for industrial wastewater treatment using the  $\alpha$ -Fe<sub>2</sub>O<sub>3</sub>-CuO.

## REFERENCES

- [1] Arulkumar, E., S.S. Shree, and S. Thanikaikarasan, Structure, morphology, composition, optical properties of CuO/NiO nanocomposite for electrochemical energy storage devices. Results in Chemistry, 2023. 6: p. 101087.
- [2] Balapure, A., J.R. Dutta, and R. Ganesan, Recent advances in semiconductor heterojunction: a detailed review of fundamentals of the photocatalysis, charge transfer mechanism, and materials. RSC Applied Interfaces, 2023.
- [3] Jung, K.-W., et al., A facile one-pot hydrothermal synthesis of hydroxyapatite/biochar nanocomposites: adsorption behavior and mechanisms for the removal of copper (II) from aqueous media. Chemical Engineering Journal, 2019. 369: p. 529-541.

## Seasonal Assessment of Water Clarity and Algal Blooms in Lake Burullus Using Satellite Imagery

Mostafa Aboelkhear\*<sup>1</sup>, Aya Abd El-Moneim<sup>2</sup>, Dina I.Mohamed<sup>3</sup>, Mohamed Embaby<sup>4</sup>, Eman R.Nofal<sup>5</sup>,  
M.Suhyb Salama<sup>6</sup>

<sup>1, 3</sup> Assistant Researcher, Environmental and climate change institute, National Water Research Centre, El-Kanater El-Khairiya, Egypt.

(E-mail: Mostafaaboelkhear@gmail.com, Eng-Dina2010@hotmail.com)

<sup>2</sup> Researcher, Drainage Research Institute, National Water Research Centre, El-Kanater El-Khairiya, Egypt.

(E-mail: Ayaezz2007@yahoo.com)

<sup>4</sup> Associate Professor, National Water Research Centre, Fum Ismailia Canal, P.O.Box 74, Shoubra El-Kheima 13411, Cairo, Egypt.

(E-mail: m\_moh1979@yahoo.com)

<sup>5</sup> Associate Professor, Institute for Groundwater, National Water Research Center, El-Kanater El-Khairiya, Egypt.

(E-mail: emanragab29@yahoo.com)

<sup>6</sup> Professor, Faculty of Geo-Information Science and Earth Observation, University of Twente, 7500 AE Enschede, The Netherlands.

(E-mail: s.salama@utwente.nl)

### ABSTRACT

Lake Burullus is Egypt's second-largest lagoon and plays a vital role in the region's ecological balance. This study leverages satellite imagery to assess the seasonal variations in water quality parameters, specifically focusing on turbidity and algal growth. Situated along the Mediterranean coast, it lies between the two branches of the Nile River. The study investigates the potential of satellite imagery in evaluating seasonal variations in water clarity and algal blooms within Lake Burullus, Egypt. Utilizing Sentinel-2 data spanning from January 2018 to January 2024, computations were conducted for the Normalized Difference Turbidity Index (NDTI) and Normalized Difference Chlorophyll Index (NDCI). The investigation revealed considerable seasonal variations in Lake Burullus's water quality. Winter displayed clear water with substantial algal growth and minimal sediment resuspension. Summer experienced ongoing algal proliferation and increased turbidity due to heightened temperatures and nutrient levels. Autumn demonstrated significant sediment resuspension and moderate to high turbidity. Spring exhibited diverse conditions with moderate to high turbidity and high chlorophyll-a concentrations, highlighting the complex factors affecting the lake's ecology. These findings suggest a potential correlation with eutrophication (nutrient enrichment) based on the observed seasonal trends in algae and turbidity.

**Keywords:** Lake Burullus, NDTI, NDCI, algal blooms, eutrophication.

## METHODOLOGY

A Python script was developed on the Google Earth Engine (GEE) platform to analyze Sentinel-2 satellite imagery focused on Lake Burullus, Egypt's second-largest lagoon[1]. Level-2A data, sourced reliably within a specified timeframe (e.g., Jan 2018 - Jan 2024), was acquired for a user-defined Area of the lake. Following data filtering and scene masking, monthly calculations of NDTI (Normalized Difference Vegetation Index) and NDCI (Normalized Difference Water Index) were performed to evaluate vegetation health and water quality[2]. Subsequently, the NDTI/NDCI data was exported for further analysis using spreadsheet software, facilitating the exploration of trends and statistical summaries throughout the entire observation period.

## RESULTS/FINDINGD

The probability distribution of positive NDTI values fluctuated from 0% to 25% across individual point, while positive NDCI values consistently registered at 100%, as illustrated in Figure 1.

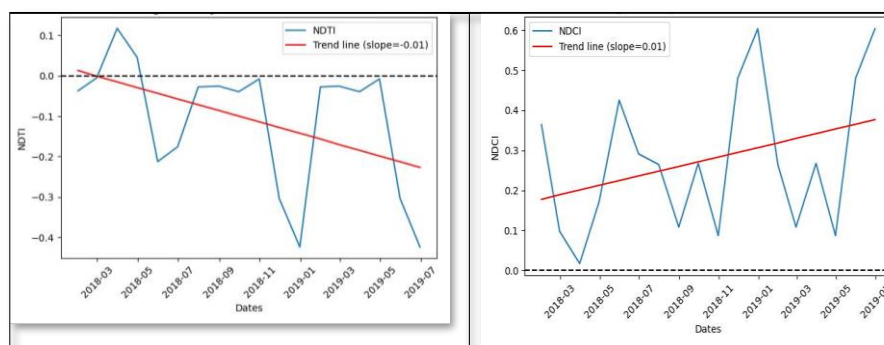


Figure 1. The average monthly values of NDTI and NDCI for autumn at Lake Burullus

By applying the probability distribution of positive NDTI and NDCI values for each season as shown at figure 2. During winter, approximately 80.97% of Lake Burullus exhibited low turbidity (NDTI) and high chlorophyll-a levels, indicating clear water with significant algal growth. In summer, 34.73% maintained these conditions, while 65.27% experienced increased turbidity attributed to rising temperatures and nutrient levels. Autumn witnessed 44.03% with moderate to high turbidity and high chlorophyll-a concentrations, suggesting notable sediment resuspension, with only 1.33% showing low turbidity. Spring showed 73.23% of the lake with moderate to high turbidity and high chlorophyll-a levels, and 8.19% with low turbidity and high chlorophyll-a levels, indicating a variety of influencing factors. The investigation revealed considerable seasonal variations in Lake Burullus's water quality. Winter displayed clear water with substantial algal growth and minimal sediment resuspension. Summer experienced ongoing algal proliferation and increased turbidity due to heightened

temperatures and nutrient levels. Autumn demonstrated significant sediment resuspension and moderate to high turbidity. Spring exhibited diverse conditions with moderate to high turbidity and high chlorophyll-a concentrations, highlighting the complex factors affecting the lake's ecology. These findings suggest a potential correlation with eutrophication (nutrient enrichment) based on the observed seasonal trends in algae and turbidity.

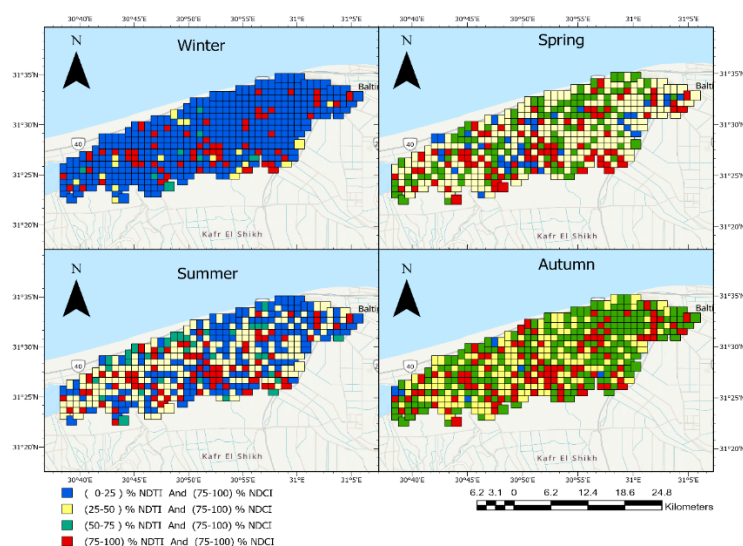


Figure 2. Probability of positive ratios for the Four Season NDTI and NDCI over Burullus Lake.

## CONCLUSIONS AND RECOMENDATIONS

Satellite imagery analysis using NDTI and NDCI revealed seasonal variations in Lake Burullus' health. Winter had the clearest water with high algae levels. Summer saw ongoing algae growth, but also increased turbidity, possibly due to warmer temperatures and more nutrients. Autumn displayed the most significant changes, with substantial sediment resuspension and organic matter entering the lake. Spring was the most diverse, with areas of clear and murky water alongside high algae. This study highlights the lake's dynamic nature. To further understand these changes, we recommend:

- **Stop nutrients at the source:** Upgrade wastewater treatment, educate residents on smart fertilizer use, and plant buffer strips around lakes to capture nutrients before they enter.
- **Manage nutrients within the lake:** Increase oxygen levels to suppress algae growth, apply alum to bind phosphorus, and consider dredging in severe cases.
- **Focus on long-term solutions:** Educate the community and implement



**ACKNOWLEDGMENT** We extend our sincere thanks to Dr. Syuib Salama for his invaluable guidance and support throughout this project. We also acknowledge the Project Earth Observation for Climate Change and the National Water Research Center for their funding and resources.

## **REFERENCES**

- [1] N. A. El-Naggar and A. E. Rifaat, "AQUASEA hydrodynamic and transport model: Salinity and dissolved oxygen simulation in El-Burullus Lake (Nile Delta, Egypt) considering different boundary conditions," *The Egyptian Journal of Aquatic Research*, vol. 48, pp. 107-113, 2022.
- [2] C. Zablan, A. Blanco, Y. Primavera-Tirol, and K. Nadaoka, "Development of Google Earth Engine Application for Spatiotemporal Analysis of Turbidity in Batan Estuary, Aklan Through the Harmonization of Landsat and SENTINEL-2 Imagery," *The International Archives of the Photogrammetry, Remote Sensing and Spatial Information Sciences*, vol. 48, pp. 1965-1971, 2023.

## Design Water Level for Coastal Engineering Applications along the Northern Coast of Egypt

Ahmed A. Romya\*<sup>1</sup>, Asmaa A. Abu Zed<sup>1</sup> and Moheb M. Iskander<sup>1</sup>

<sup>1</sup> Coastal Research Institute (CoRI), National Water Research Center (NWRC), Egypt  
(Asmaa\_bakr90@yahoo.com)

### ABSTRACT

Sea level is an important parameter in coastal engineering applications especially in design of coastal structures. Extreme water sea level is mainly generated coincidentally when large storm surges are combined with the high tide and maximum wave setup. This value which called design water sea level is used to identify the structure level. Also, the minimum water level is used to design the structure toe. The minimum sea level can be identified by using low tide with the maximum negative surge and wave sit-down. This paper aims to determine the distribution of extreme sea levels along the Egyptian Mediterranean coast. Delft3D model D-Flow module is used to simulate hydrodynamics along the Egyptian Mediterranean coast to identify the distribution of astronomical tide and surge heights. The model is calibrated and validated by using the available hourly measured water level data within the study area. Also, storm surge characteristics are defined using the available hourly measured water level data at Rosette, Burullus and Damietta stations. T-TIDE software package which works under the Matlab® environment is used to analyze measured water level data. Along the Egyptian Mediterranean coast, tidal range increases gradually from 0.188 m at the Northwestern coast to 0.448 m along the Sinai coast of Egypt. Based on the measured water level maximum and minimum surge heights reach 0.68 to -0.497, 0.62 to -0.4, and 0.63 to -0.52 m at Rosette, Burullus, and Damietta, respectively.

**Keywords:** Astronomical tide, Delft3d\_FM, Hydrodynamics, Surge distribution, T\_TIDE, Water level.

### METHODOLOGY

Two different approaches were used to obtain the surge characteristics along the Egyptian Mediterranean coast. The first approach is depending on the measured water level data. Three different tidal gauges distributed along the Egyptian Mediterranean coast were used to extract storm surge heights. T\_TIDE software package [1], which works under the Matlab® environment is used to analyze measured water level data to get storm surge elevations.

## METHODOLOGY

Two different approaches were used to obtain the surge characteristics along the Egyptian Mediterranean coast. The first approach is depending on the measured water level data. Three different tidal gauges distributed along the Egyptian Mediterranean coast were used to extract storm surge heights. T\_TIDE software package [1], which works under the Matlab® environment is used to analyze measured water level data to get storm surge elevations.

The second approach depends on numerical modelling. Delft 3D FM, D-Flow module is used to simulate the variation of water level (astronomical tide and storm surge) along the entire Egyptian Mediterranean coast during the period from 2019 to 2023. The model extends offshore to a latitude of 32.5° degrees north and the mesh was established within the spherical WGS84 coordinate system to accurately depict the Earth's surface. The refinement phases in the network refinement approach are based on isobaths. The grid resolution at the offshore boundary is about 8 km to reach 250 m along the near shore area as shown in Figure 3. Field- measured data collected by Coastal Research Institute, bathymetrical online data from EMODnet and a detailed admiralty charts were used to represent the depths.

Delft Dashboard, (<https://publicwiki.deltares.nl/display/DDB/Delft+Dashboard>) is used to generate the astronomical tidal components along the model boundaries from the global tidal model (TPXO 7.2 Global Inverse Tide Model). Finally, meteorological data which includes wind data (speed and direction), air pressure data, and Charnock coefficient are obtained from the ECMWF-ERA5. The model is calibrated and validated using measured water level data obtained from Coastal Research Institute at El-Burullus, Rosetta and Alexandria stations during 2015 and 2017 respectively. Finally, extreme surge height and associated return periods are calculated using the methods discussed in Isaacson and MacKenzie, 1981 [2].

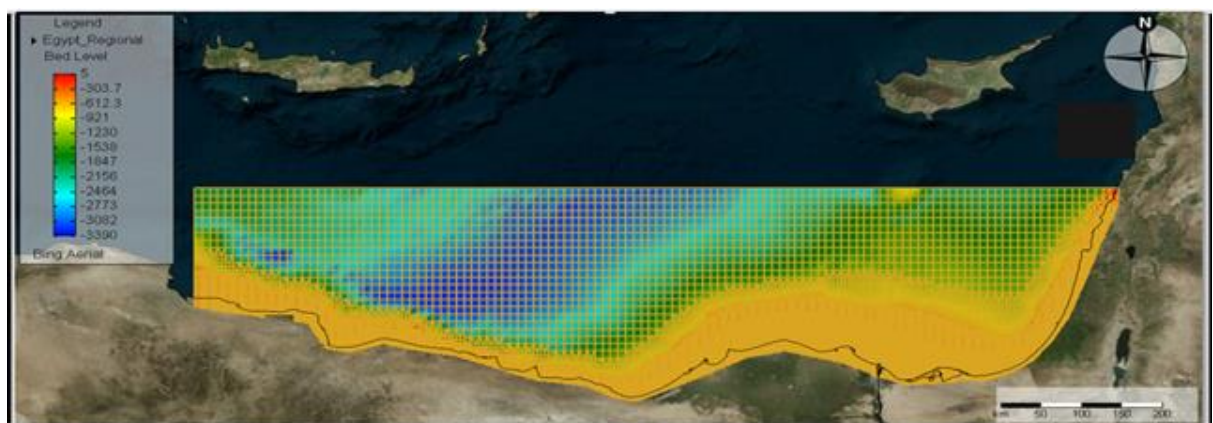


Figure 3 Thematic map showing the layout of the mesh and the bathymetric data used for the flow module

## RESULTS/FINDINGD

Extreme coastal sea levels are generated coincidentally when large storm surges are combined with high water of a spring tide. Extreme tides and storm surges can be accurately predicted, independently, by using observational data as well as statistical and numerical models. First, tidal ranges along the Egyptian Mediterranean Sea are obtained using Delft3D FM numerical Model. The model was calibrated and validated during 2015 and 2017 respectively using measured data. Figure 4 shows the results of the harmonic analysis used during the calibration process. The statistics show that the model has very good results at all stations with an average correlation of 89.3% and RMSE of about 6.2 cm. For the validation process the average RMSE and R% are 7 cm and 85% respectively. Overall, the model validation results provide confidence in the model's ability to simulate the water level variations of the studied coastal system accurately. Tidal range along the Egyptian Mediterranean Coast increases gradually from 0.188 m west of the study area to 0.448 m east of the study area. The maximum positive and negative surges obtained is about 0.68 and -0.5 m, respectively. The maximum expected positive and negative surge heights occurring once in fifty years at the most important stations along the Egyptian Mediterranean coast, Rosetta, Burullus and Damietta are 0.81 to -0.67, 0.9 to -0.57 and 0.77 to -0.68 respectively.

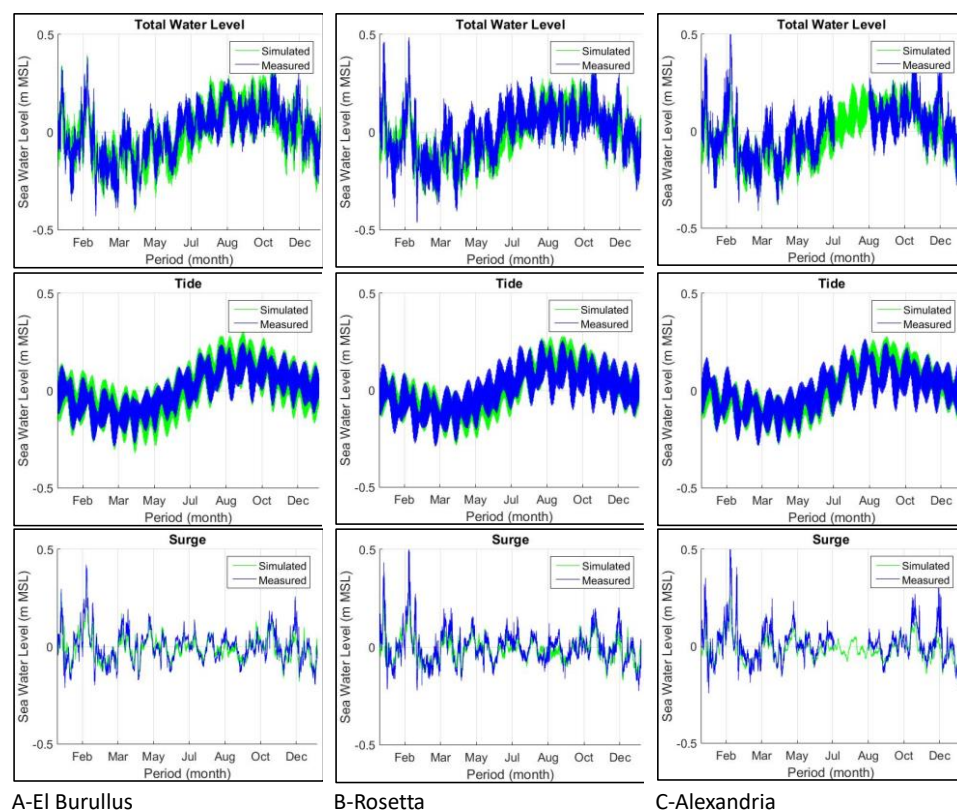


Figure 4 Harmonic analysis results showing the tidal and surge water levels during 2015. after the calibration process at: a- El Burullus, b- Rosetta, and c- Alexandria, Egypt

## **CONCLUSIONS AND RECOMENDATIONS**

Storm surge is an important coastal process for the design of coastal infrastructure primarily because it increases the design still water level and allows waves to attack higher elevations. A calibrated Delft3D FM model is used to simulate water level along the Egyptian Mediterranean coast from 2019 to 2023 in addition to three distributed stations used to extract surge height from measured data using T\_TIDE software package.

Tidal range along the Egyptian Mediterranean Coast increases gradually from 0.188 m (west) to 0.448 m (east), due to the existence of an amphidromic (zero tide) at the eastern basin south of Greece [3] which increases the tidal height outwards away from it and for this reason the tidal range increases eastward along the Egyptian coast. The maximum positive and negative surges obtained is about 0.68 and -0.5 m, respectively. The maximum expected positive and negative surge heights occurring once in fifty years at the most important stations along the Egyptian Mediterranean coast, Rosette, Burullus and Damietta are 0.81 to -0.67, 0.9 to -0.57 and 0.77 to -0.68 respectively. It is recommended to take the effect of the climate change on simulation consideration to determine its influence on the surge height.

## **REFERENCES**

- [1] Pawlowicz R, Beardsley B, Lentz S.: 'Classical tidal harmonic analysis including error estimates in MATLAB using TDE'. *Comput Geosci.*, 2002;28, (8), pp. 929-937.
- [2] Isaacson, M. de St., and MacKenzie, N.: 'Long-Term Distributions of Ocean Waves: A Review', *Journal of the Waterway, Port, Coastal and Ocean Division.*, 1981; 107, (2), pp. 93–109.
- [3] Pugh, D.: 'Tides, Surges and Mean Sea Level': 'A Handbook for Engineers and Scientists' , (1987), PP. 1-472.

**Theme 4: Actions for Water and Climate Adaptations and  
Resilience  
Day 4**



## The Impact of Different Climate Change Scenarios on Water and Crop Productivity of Wheat in Jenin Governorate, Palestine (Case Study)

Imad Ghanma\*<sup>1</sup> and Ibtesam Abu-alhaija<sup>2</sup>

<sup>1</sup>[Director of soil and land classification, [Imad\\_ghanma@yahoo.com](mailto:Imad_ghanma@yahoo.com), 00970598922768, Palestinian Ministry of Agriculture (MoA), Ramallah, Palestine.

<sup>2</sup>[Head division of water harvesting, [abuhaijaibtisam@yahoo.com](mailto:abuhaijaibtisam@yahoo.com), 00970598999758, Ministry of Agriculture Palestinian, Ramallah, Palestine.

**Keywords:** Deficit irrigation, Aqua crop, Climate change scenarios, Water productivity.

### ABSTRACT

The State of Palestine is vulnerable to the impacts of climate change with severe implications for its economy. Palestine as other Arab countries in the region is located in the one of the arid and semi-arid areas in the world; most recent assessments have concluded that arid and semiarid regions are highly vulnerable to climate change (IPCC, 2007a).

Impacts significant to the region include decreased precipitation, significant warming and more frequent extreme weather events, the recent climatic studies indicated that the global surface air temperature increased from 1850 to 2005 by 0.76°C. Moreover, the linear warming trend over the last 50 years is recorded by 0.13°C per decade (IPCC, 2007b). Regarding the Arab countries, recent studies found that the Arab region experienced an uneven increase in surface air temperature ranging from 0.2 to 2.0°C that occurred from 1970 to 2004 (IPCC, 2007a). These could lead to greater water scarcity and decrease agricultural productivity. Palestine expects that climate change will most severely affect water and agricultural sectors that will lead to higher insecurity levels for food and water.

Wheat is one of the most strategic cultivated rainfed crop in Palestine, according to the (MoA statistics 2021), the total cultivated area with wheat was 11000 Hectare. which is considered 42% of the total rainfed crops, with the total estimated production was 25926 ton, 54% of the total production was in Jenin governorate as the main governorate of planting filed crops, while in Hebron and tubas it was 16% and 11% respectively.

Recently due to climate change conditions, with increase of temperature, the shift in the rain season from October to December, a combined with a decrease in the number of rainy days, and the rain stops by late march, yield and water productivity of the wheat became low and economically not feasible to be grown as a rainfed crop.

In Palestine cultivating irrigated wheat is very difficult due to scarcity of water resources and continues controlling Palestinian water resources by Israeli occupation of more than 85% according to (PWA 2017), therefore, supplementary irrigation can be one of the solutions to improve wheat productivity and water productivity in the area where additional water resources can be available and the cultivated land also can be irrigable.

In cooperation with ESCWA, ACSAD, FAO the Ministry of Agriculture, carried out a simulation case study using Aqua Crop software in in Marj ben Amer plain in Jenin governorate which is located in the northern part of west bank, Marj ben Amer consider one of the most fertile internal plain in Palestine with total area of 361 Km<sup>2</sup>, the cropping pattern are varies due to unique climatic conditions and availability of water resources.

The main objective of the research was to study and to evaluate the impact of expected climate change scenarios (RCP 8.5 and RCP 4.5 for both fixed CO<sub>2</sub> and increased CO<sub>2</sub>), on crop and water productivity from (1985 - 2005) as base years, from 2020 - 2030 and 2040 – 2050 years.

The comparison between both scenarios regarding the minimum and maximum temperature shows an increase in maximum and minimum temperatures with a difference in the rate of increase, 8.5 scenario shows that the increase in maximum temperature ranges from 0.95 - 1.75, while in scenario 4.5 the increase ranges between 0.7 - 1.3 while the increase in minimum temperatures ranges between 0.72- 1.4 for scenario 8.5 and 0.4-1 for scenario 4.5.

To run the simulation model, detailed crop data was collected from the specialists of plant production and the collected data was verified by researchers from national agriculture research center (NARC), while soil data was collected from soil department from MoA, planting date was 1<sup>st</sup> of March, soil fertility was near optimal with 60% and the weeding control was 85%.

The result indicates that water productivity of wheat in scenario RCP 8.5 and RCP 4.5 increased CO<sub>2</sub> was the two best scenarios comparing with the fixed CO<sub>2</sub> due to the availability and the importance of CO<sub>2</sub> for photosynthesis operation.

RCP 8.5 increased CO<sub>2</sub> scenario gave the best results, where the crop productivity and water productivity in the base year was 1.7 ton/h and 0.6 Kg/m<sup>3</sup> respectively and it was 2.35 ton/h and 2.63 ton/h for crop productivity and 0.8 kg/ m<sup>3</sup> and 1kg/ m<sup>3</sup> for Water productivity in the years of 2020 - 2030 and 2040 -2050 respectively as indicated in the table 1 additionally to the average of the expected changes in the production, averages of the growing season length, averages of reference and actual evapotranspiration and water productivity of the wheat.

In table 2, RCP 4.5 increased Co2 scenario indicate that the crop productivity and water productivity was 1.64 ton/ha and 0.6 kg/M3 respectively additionally to the average of the expected changes in the production, averages of the growing season length, averages of reference and actual evapotranspiration and water productivity of the wheat.

Table 1. RCP 8.5 increased CO2 main results

<b>Monitored parameters</b>	<b>1985-2005</b>	<b>2020-2030</b>	<b>2040-2050</b>
Total production in base year ton/ha	1.7		
Absolute change ton/ha		0.656	0.932
Relative change		38.55	54.72
Length of growing season (day)	150	152	152
Reference Evapotranspiration(mm)	574	556	540
Actual evapotranspiration (mm)	266	283	273
Water productivity kg/m3	0.6	0.8	1

Table 2 RCP 4.5 increased CO2 main results

<b>Monitored parameters</b>	<b>1985-2005</b>	<b>2020-2030</b>	<b>2040-2050</b>
Total production in base year ton/ha	1.64		
Absolute change ton/ha		0.29	0.49
Relative change		17.8	30
Length of growing season (day)	150	151	151
Reference Evapotranspiration(mm)	574	562	548
Actual evapotranspiration (mm)	268	289	280
Water productivity kg/m3	0.6	0.68	0.76

It was clearly noticed in all climate change scenarios of the wheat that, the crop productivity as well as water productivity was increased while the reference evapotranspiration of the wheat is decreased, also, it was noticed that the percent of increased in crop productivity and water productivity in the increased RCP 8.5 CO2 scenario and RCP 4.5 CO2 scenario more that the fixed one.

Due to the phenomena of climate change over the world and especially in the same region or in the neighboring countries, water scarcity, irrigation water shortage, it is highly important to follow the next recommendations to improve irrigation water management water productivity under different climate change adaptation or mitigation scenarios.

1. Exchange all required data and the obtained results of the Aqua crop for all tested crops between the other countries who have similar climatic conditions in order to increase the accuracy of the obtained results.
2. Full cooperation between the ministry of agriculture and the national agricultural research center as well as the academic agricultural researchers to provide a precise data of the crops and local soil properties to ensure run the program with high performance.

**Acknowledge:** The others would like to express appreciation for the support of the sponsors project Number **40**.

### **References.**

1. IPCC, 2007b. Climate Change 2007: The Scientific basis, Summary for Policymakers – Contribution of working Group I to the IPCC Fourth assessment report 2007.
2. IPCC, 2007a. Climate Change 2007: Impacts, Adaptation and Vulnerability Contribution of Working Group II to the Fourth Assessment Report of the Intergovernmental Panel on Climate Change, Cambridge University Press, Cambridge, UK, 2007.
3. Ministry of agriculture statistics, 2021.
4. PWA, 2018 Database.

## **Application of the Interactive Flood Risk Analysis Dashboard for Hamburg, Germany A GIS, Remote Sensing and AHP Approach**

Ahmed Abuzeid<sup>1</sup>, Noha Kamal\*<sup>2</sup>, and Christoph Schüth<sup>3</sup>

<sup>1,3</sup>Institute of Applied Geosciences, Technische Universität Darmstadt, Darmstadt, Hesse, Germany.

(Email: [ing.ahmedabuzeid@gmail.com](mailto:ing.ahmedabuzeid@gmail.com))

<sup>2</sup>Nile Research Institute - National Water Research Center, Cairo, Egypt.

(Email: [noha\\_kamal@nwrc.gov.eg](mailto:noha_kamal@nwrc.gov.eg), [noha\\_kamal2002@hotmail.com](mailto:noha_kamal2002@hotmail.com))

### **ABSTRACT**

Floods are among the most destructive natural disasters, causing significant loss of life, property damage, and economic disruption. Hamburg, being one of the largest port cities in Germany, is particularly vulnerable to flood risks due to its geographical location and climate change effects. Interest in flood mitigation measures have been implemented after the flood incident in 1962 which caused immense damage and loss of lives and assets. Despite the advancements in flood risk management, there is a need for more comprehensive and precise flood risk analysis tools to aid in disaster preparedness and mitigation. Geographic Information Systems (GIS) and Remote Sensing (RS) have emerged as powerful tools in environmental management and disaster risk reduction. They offer the ability to collect, process, and analyze spatial data, making them invaluable in flood risk analysis. However, their application in flood risk analysis in Hamburg has been limited.

This study is set against this backdrop, aiming to fill this gap by conducting a comprehensive Flood Risk Analysis in Hamburg using GIS and Remote Sensing techniques. The research will leverage the Analytic Hierarchy Process (AHP) and multi-criteria decision method (MCDM) with ArcGIS Pro to calculate the weights and effects of ten layers. According to the results, all medical facilities in Hamburg's St. Georg district, for instance, are 100% at medium risk. Additionally, 40% of social facilities are classified as high risk, and 60% as medium risk. Furthermore, 50% of police and fire stations will be in high- and medium-risk categories. The results have been presented in an operational interactive dashboard that displays risk areas, infrastructure affected, and risk levels, among other metrics, in different scenarios based on user input.

**Key words:** Flood Risk, Dashboard, AHP, GIS, MCDM, Hamburg.

## METHODOLOGY

In this research, Hamburg, Federal state of Germany was used as the study area (Figure 1). The Advanced Spaceborne Thermal Emission and Reflection Radiometer (ASTER) Digital Elevation Model (DEM) [1] offers impressive accuracy and resolution, providing detailed elevation data with a vertical accuracy of around 15 meters and a horizontal resolution of approximately 30 meters for Hamburg as shown in Figure 2. Also, WorldClim version 2 open source data was used, which accumulates precipitation averages from 1970 to 2000 [2], leaving the chance to use more recent data to derive climate induced flood risk mapping. The precipitation data is available at the spatial resolution of 30 seconds, which translates to 1 square kilometer in raster. This study aimed to assess the flood risk analysis in Hamburg through the utilization of an innovative methodology that integrated the AHP and MCDM to calculate the weights and effects of ten different layers, namely Elevation, Slope, Topographic Wetness Index, Curvature Analysis, Precipitation Analysis, NDVI Analysis, Landuse and Landcover Analysis, Distance to Stream Analysis, Drainage Density Analysis, and Geomorphology Analysis. A multi-step methodology was used to achieve this goal, as shown in Figure 3.

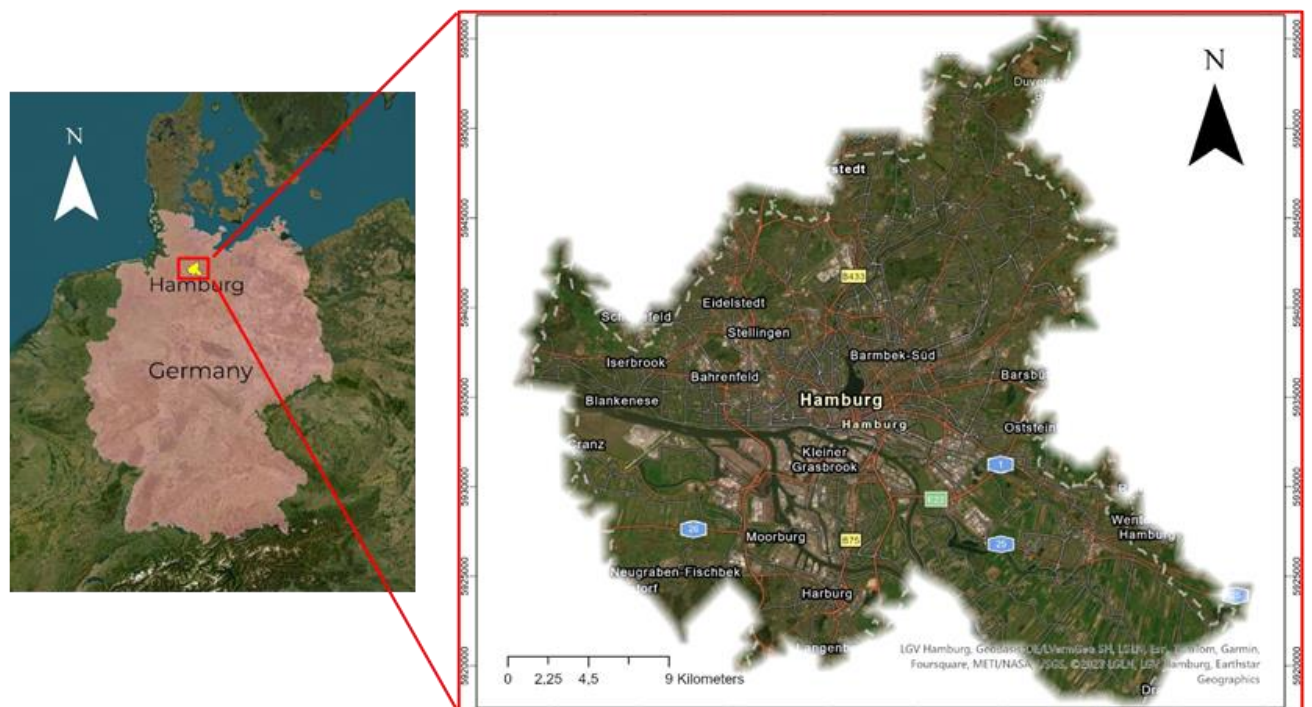


**Figure 1.** Location study area of a Federal State of Hamburg in Federal Republic of Germany.



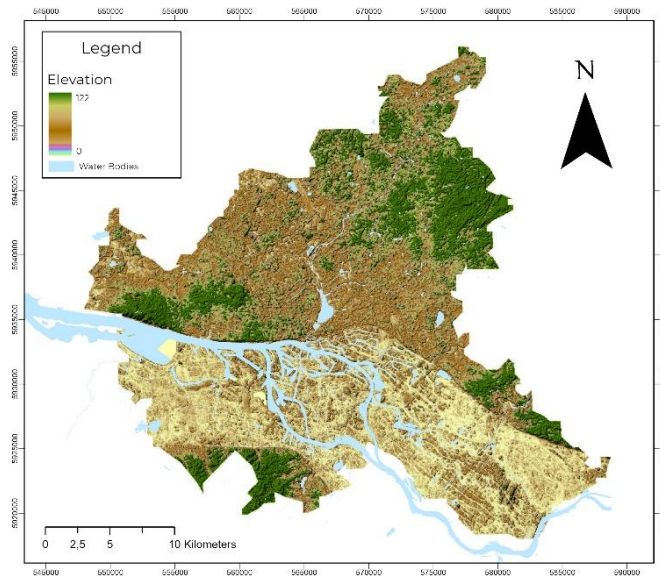


**Figure 2.** Digital Elevation Model of Hamburg.

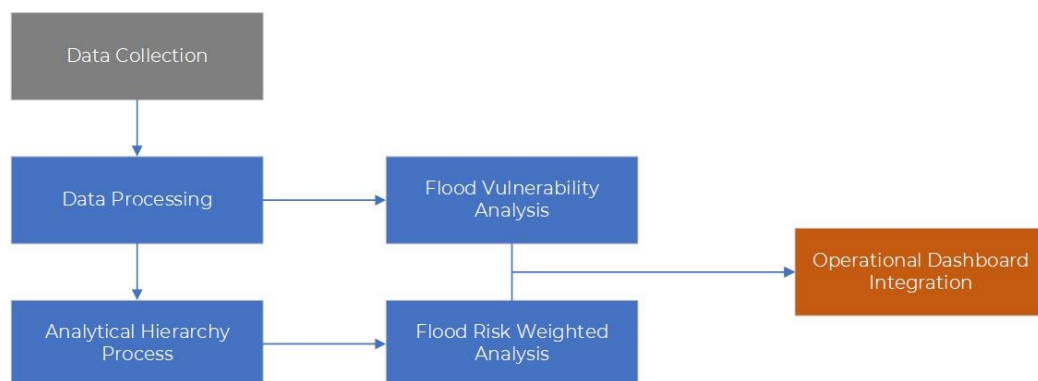


**Figure 3.** Flowchart of the proposed methodology

## RESULT

The results support the premise that integrating AHP and GIS approaches may efficiently use spatial data for decision-making in flood hazard mapping. A flood risk map is the result of integrating two features: hazard and vulnerability [3]. Figure 4 depicts the Flood Risk dashboard developed using ArcGIS Pro 3.3. Figure 5 shows that the Barmbek-Süd district in Hamburg has the highest flood risk percentage at 76%.

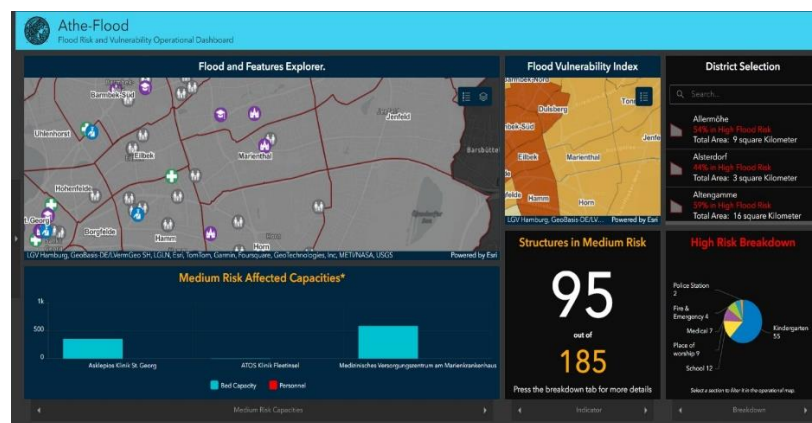


**Figure 4.** The developed Flood Risk Analysis Dashboard for Hamburg

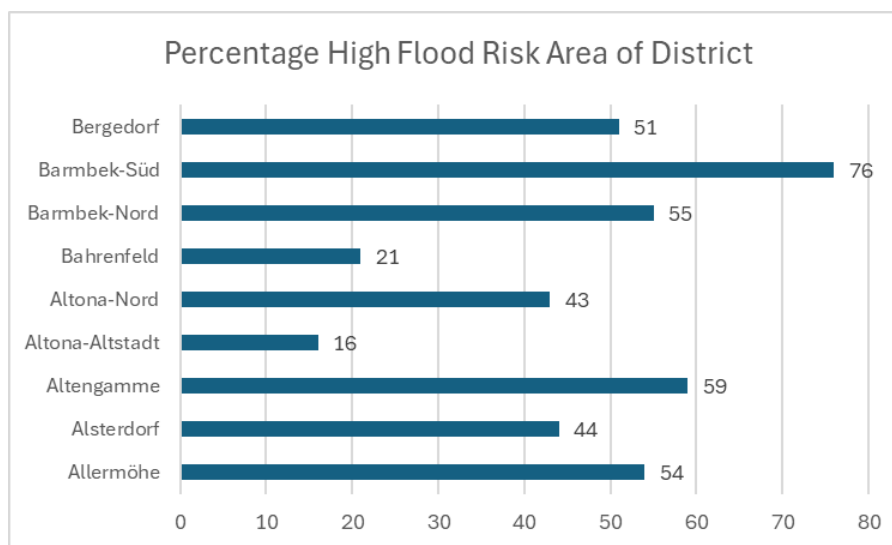


**Figure 5.** Example of Percentage High Flood Risk of total district area from 9 districts

## CONCLUSION


The flood risk dashboard was developed using a multi-criteria analysis technique that included both hazard and vulnerability aspects. According to the developed dashboard, 76% of Barmbek-Süd district is at high flood risk. The high flood risk percentages for other districts are as follows: 51% for Bergedorf, 55% for Barmbek-Nord, 21% for Bahrenfeld, 43% for Altona-Nord, 16% for Altona-Altstadt, 59% for Altengamme, 44% for Alsterdorf, and 54% for Allermöhe.

The analysis of flood risk zones and vulnerability is not a novelty, but limited access and the slow introduction of public information are, in many cases, causes imprecise resource allocation and hence weak management in flood scenarios. The introduction of open-source data analysis opens a door for virtually all the world's municipalities and towns to implement such an analysis and present it in a dashboard that is navigable and equally informative for decision-makers as well as the public

## REFERENCES

- [1] NASA Earthdata. (n.d.). New Version of the ASTER GDEM. Retrieved April 18, 2024, from <https://www.earthdata.nasa.gov/news/new-aster-gdem>.
- [2] <https://www.worldclim.org/data/index.html>
- [3] Ouma, Y. O. & Tateishi, R. 2014 Urban flood vulnerability and risk mapping using integrated multi-parametric AHP and GIS: methodological overview and case study assessment. *Water* 6 (6), 1515–1545. <https://doi.org/10.3390/w6061515>.
- [4] Statista. (2021, August 13). Opinions on assistance for flooding victims in Germany 2021. ZDF Politbarometer. <https://www.statista.com/statistics/1268478/flooding-disaster-victims-assistance-opinions-germany/>
- [5] Radio Hamburg. (2012, February). Rückblick auf Hamburger Flutkatastrophe - 50. Jahrestag der Sturmflut 1962. <https://www.radiohamburg.de/Nachrichten/Hamburg-aktuell/Panorama/2012/Februar/Rueckblick-auf-Hamburger-Flutkatastrophe-50.-Jahrestag-der-Sturmflut-1962>
- [6] Hagos, Y.G., Andualem, T.G., Yibeltal, M. et al. Flood hazard assessment and mapping using GIS integrated with multi-criteria decision analysis in upper Awash River basin, Ethiopia. *Appl Water Sci* 12, 148 (2022). <https://doi.org/10.1007/s13201-022-01674-8>
- [7] NASA Landsat Program. (n.d.). Landsat 8. Retrieved April 18, 2024, from <https://landsat.gsfc.nasa.gov/satellites/landsat-8/>
- [8] Esri. (n.d.). Land Cover Explorer. Retrieved April 18, 2024, from <https://livingatlas.arcgis.com/landcoverexplorer/#mapCenter=9.99567%2C53.51458%2C11.788648581718112&mode=step&timeExtent=2017%2C2023&year=2023&renderingRule=4&month=9>
- [9] Sentinel Hub. (n.d.). NDVI - Normalized Difference Vegetation Index. Retrieved April 18, 2024, from <https://custom-scripts.sentinel-hub.com/custom-scripts/sentinel-2/ndvi/>

# Flash Flood Hazard Assessment in the Amlog Valley Basin, North-West Galala City, Egypt, Based on a morphometric approach using GIS Techniques

Ali Hagraš\*<sup>1</sup> 

<sup>1</sup> Ph.D., Egyptian General Survey Authority, Ministry of Water Resources and Irrigation, Egypt.  
[alihagras@alexu.edu.eg](mailto:alihagras@alexu.edu.eg) - [ali\\_hagras23@yahoo.com](mailto:ali_hagras23@yahoo.com)- [alihagras87@gmail.com](mailto:alihagras87@gmail.com).

## Abstract

Flash Floods are one of the natural threats that arise as a result of temporary surface runoff. The Amlog Valley Basin is characterized by the lack of rain and the prevalence of drought, but it is exposed to sudden rains that lead to surface runoff in its dry valleys in a way that results in threats to infrastructure and spatial development in the coastal region. Within this framework, the purpose of this research is to investigate the possible areas of flood hazard by using geographic information systems (GIS) techniques based on morphometric assessment parameters to determine the risk level of specified subbasins from a digital elevation model (DEM). In this regard, the hazard of the study basin's flash flood susceptibility was mapped by measuring the mean for each of the individual parameter weights (the highest weight is 11 and the least is 1) and re-ranking the flood hazard classification into very low, low, moderate, high, and very high risk. The results showed that the SB1, Sb11, SB2, and SB9 subbasins have the largest hydrodynamic risk. Consequently, large torrents may occur after heavy rainfalls in those basins in the study area. Therefore, care needs to be taken in these subbasins by creating areas for collecting water, making flood walls and flood gates, and establishing early flood warning systems by relying on Remote Sensing and GIS data.

**Keywords:** Amlog Valley Basin, Climate Adaptations, Egypt, Flood hazard, GIS, Morphometric assessment.

## Introduction

Flash floods are one of the main natural disasters in Egypt. As a result of climate change affecting the rainfall regime where different regions of the world are exposed to flash floods [1]. Moreover, if they are not better managed, flash floods cause significant losses in people, property, the economy, society, and the environment [2]. Despite the lack of rainfall received by the study area and the current drought, it is exposed to sudden torrential rains that lead to a torrent flow in the dry valleys particularly on steep mountainous terrain, in a way that leads to the destruction of roads in addition destruction of tourist

areas and vital establishments. The objectives of this research are therefore to identify potential flood risk areas using geographic information systems and remote sensing methods and assess the prioritization of hydro-conservation and groundwater recharge potentials of the catchments in the Amlog Valley Basin. Moreover, the final map aims to help planners and decision-makers create hydro-mitigation strategies.

### **Study area**

Amlog Valley basin is located on the western side of the Suez Gulf, Eastern Desert, Egypt. In this regard, the study area is located between Latitude 29° 26' 00"- 29° 32' 50" North and longitudes 32° 18' 00" - 32° 23' 30" East, It occupies an area of approximately 53.14 Km<sup>2</sup> (Figure 1).

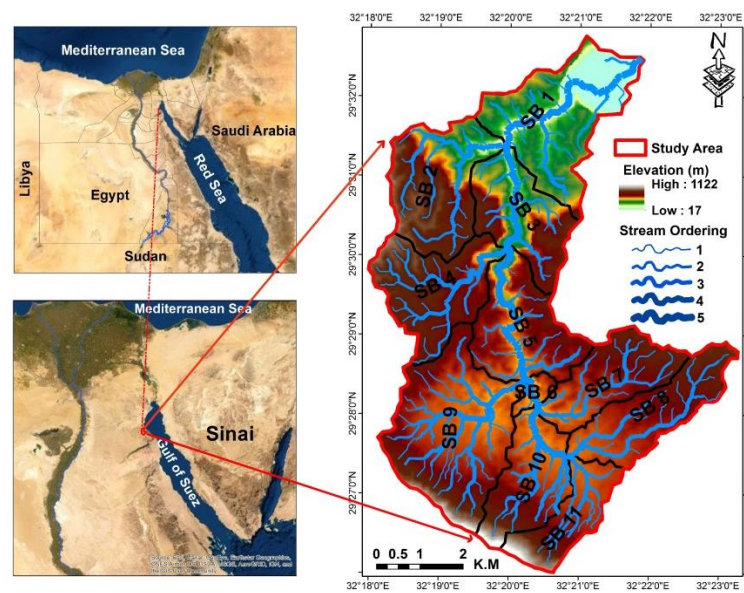


**Figure 1** Location map of Amlog Valley basin

### **Materials and Methods**

Many maps are extracted for terrain analysis using a DEM where the required thematic terrestrial layers were automatically derived, which include flow direction (Figure 2A), flow accumulation (Figure 2B), slopes (Figure 2C), aspects of slopes (Figure 2D), stream density (Figure 2E) and hill shade (Figure 2F).



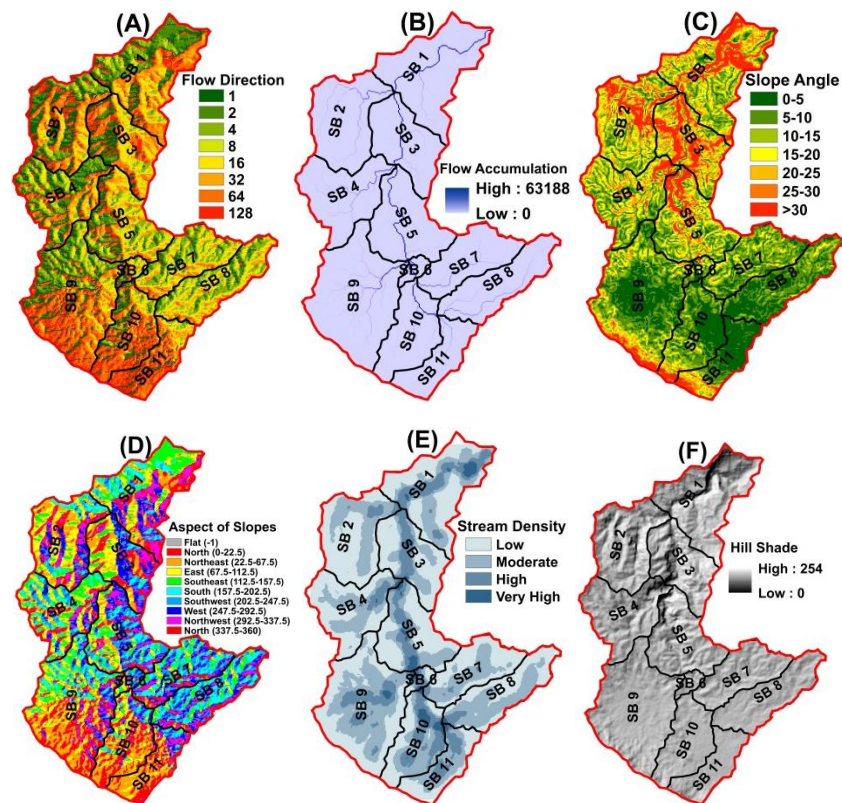


**Figure 2** Extracted hydrological from DEM **A** Flow Direction, **B** Flow accumulation, **C** Slope Angle, **D** Aspects of slope, **E** Stream density, **F** Hill shade

## Results and Discussion

Former listed morphometric parameters were numerically calculated in the software of Excel and prepared in GIS environment and the Parameters of morphometric include Stream order ( $S_u$ ), Stream number ( $N_u$ ), Bifurcation ratio ( $R_b$ ), Drainage density ( $D_d$ ), Stream frequency ( $F_s$ ), Drainage texture ( $T_d$ ), Relief ratio ( $R_r$ ), Ruggedness number ( $R_n$ ), Form factor ( $F$ ), Elongation ratio ( $E_b$ ), Compactness index ( $C$ ), Lemniscate ratio ( $K$ ), Circularity ratio ( $R_c$ ), and Basin relief ( $H_r$ ) (Figure 3).

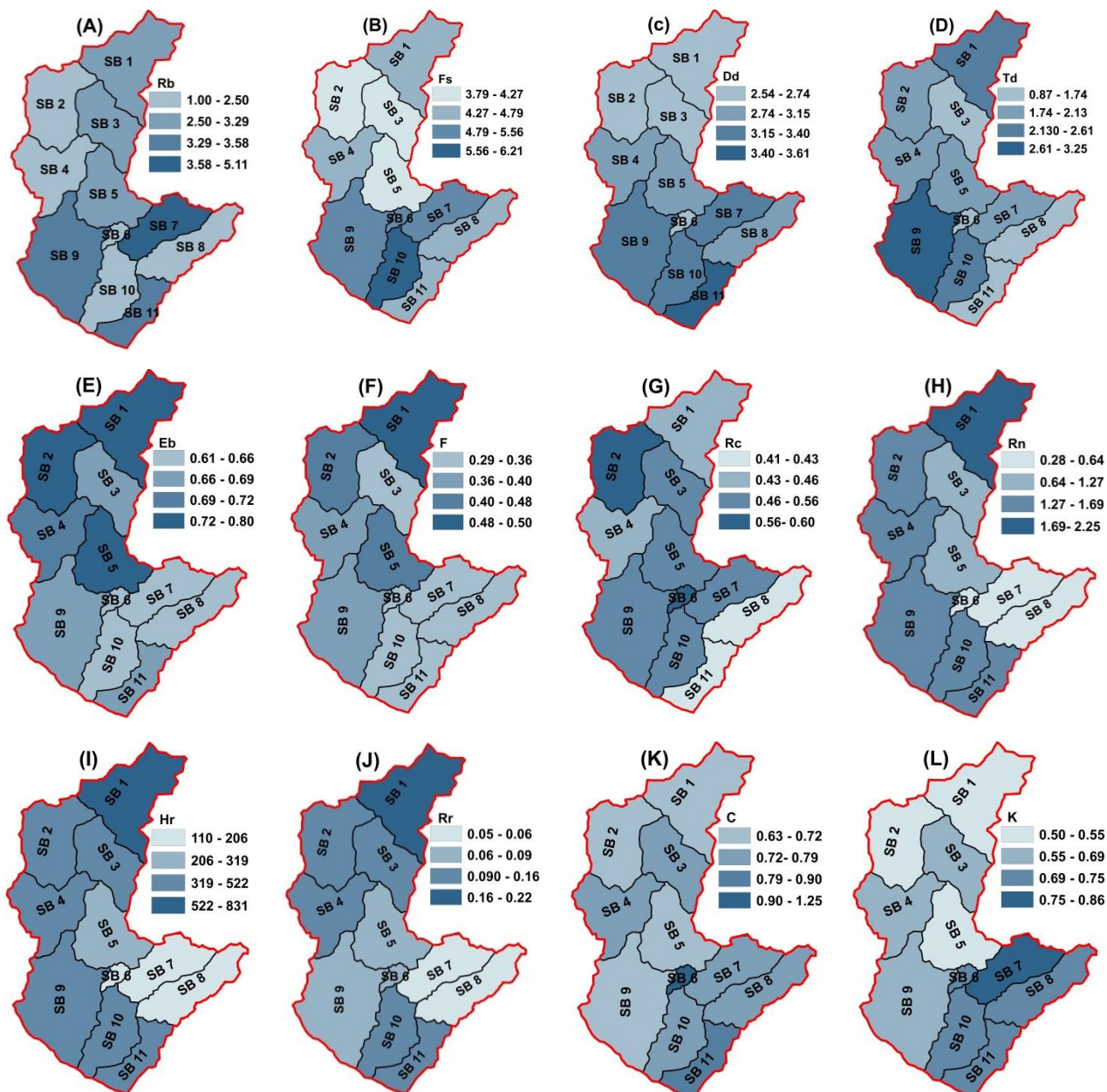


**Figure 3** Morphometric parameters **A:** ( $R_b$ ), **B:** ( $F_s$ ), **C:** ( $D_d$ ), **D:** ( $T_d$ ), **E:** ( $E_b$ ), **F:** ( $F$ ), **G:** ( $R_c$ ), **H:** ( $R_n$ ), **I:** ( $H_r$ ), **J:** ( $R_r$ ), **K:** ( $C$ ), **L:** ( $K$ ).

In the present assessment, the Hydro-prioritizing for each sub-basin was identified and mapped in a GIS environment based on Cf (Figure 4). Whatever, the Compound factor (Cf) assessment implies that the sub-basin (SB1) in the upper north of the study area among the studied sub-basins was the riskiest, (weight = 8.00).

However, this sub-basin has been specified at the front of the basins that need to be taken care of and set priorities for hydro-prioritization of flood mitigation steps to be adopted. In addition, SB1, SB11, SB2, SB9, SB10, SB4, and SB5 sub-basins have the largest Cf values.



## Conclusions

Analysis of the future results of flash flood risk is an aspect of planning and development. In a way that contributes to protecting the places most affected by the dangers of floods in the subbasins in the study area. Moreover, the role of GIS appears to be an effective, accurate, and rapid tool for analyzing flood hazards. In addition, the case study results utilized five evaluation degrees, very low, low, moderate, high, and very high to interpret the flood danger (Figure 4), where this evaluation can help make decisions to protect the places most affected by the dangers of floods in the subbasins in the study area.

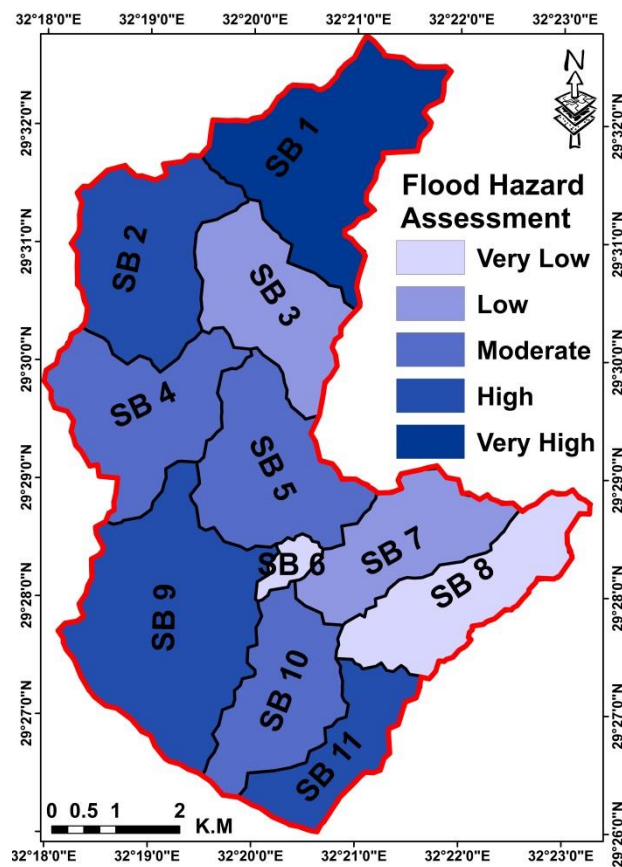


**Figure 4** Flood risk susceptibility map of sub-basins with their pairing ranks in the Amlog Valley basin for hydro-prioritization

## References

- [1] Negm AM et al. Flash floods in Egypt. Springer International Publishing (2020). [https:// doi. org/ 10.1007/ 978-3- 030- 29635-3](https://doi.org/10.1007/978-3-030-29635-3)
- [2] Kundzewicz ZW et al. Flood risk and climate change: global and regional perspectives. Hydrol Sci J, (2014), 59, (1):1-28. [https:// doi. org/ 10.1080/ 02626 667. 2013. 857411](https://doi.org/10.1080/02626667.2013.857411)

## Vulnerability of Groundwater Quantity for an Arid Coastal Aquifer under the Climate Change and Extensive Exploitation

Karim Soliman<sup>1</sup> Doaa Amin<sup>2</sup>

1 Karim Mohamed Ahmed Soliman, Water Resources Research Institute, National Water Research Center, Egypt (E-mail: karim\_soliman@nwrc.gov.eg)

2 Doaa Mohamed Amin El-Sayed, Water Resources Research Institute, National Water Research Center, Egypt (E-mail: doaa\_amin@nwrc.gov.eg)

### ABSTRACT

Groundwater is the primary water source in arid climate regions. However, climate change and extensive groundwater exploitation are expected to significantly stress these resources in the coming decades. Consequently, it is crucial to assess both the quantity and quality of groundwater under these stressors. In this study, we focused on groundwater quantity, specifically groundwater recharge and storage (using groundwater levels as an indicator), to predict the system's vulnerability under the impacts of climate change and extensive exploitation. The northern portion of El-Qaa Plain was selected as a case study because it is coastal arid aquifer, and naturally replenished by precipitation events. Groundwater in this area is the main water source used for agricultural purposes. To project groundwater recharge, the WetSpa model was employed, and climate ensembles were bias-corrected using the Delta

Change Factor (DCF) method. The MODFLOW model was applied to project groundwater levels. The findings of this study indicate that groundwater resources will be severely impacted by climate change, with groundwater recharge expected to decrease significantly during the far 21st century by 35% to 75 % under moderate to severe climate change scenarios. Mean groundwater levels are projected to decline by 7 to 8 meters by 2100 under the same scenarios.

In terms of over-exploitation, the maximum drawdown is projected to increase to 16 meters if the abstraction rate remains unchanged, and to 36 meters if the abstraction rate increases, but it will stabilize by around 7 meters from 2040 to 2100 if the annual abstraction rate was decreased to 11.5 Mm<sup>3</sup> by year 2040. The results of this study can assist decision-makers and stakeholders in developing sustainable water resource management plans for the study area.

**Keywords:** Arid climate aquifer, Climate change, Groundwater, Sustainable management of water resources.

## **METHODOLOGY**

The aim of this study is to investigate the impact of climate change on groundwater resources, particularly in the context of extensive groundwater exploitation. The study focuses on groundwater quantity, specifically by measuring two key variables: groundwater recharge and groundwater level (storage). To achieve these objectives, two models were implemented: the hydrological mass balance model (WetSpas) developed by [1] to project groundwater recharge under climate change conditions, and the groundwater flow model (MODFLOW) developed by [2] to assess changes in groundwater storage.

To set up the models, comprehensive data acquisition was conducted, including hydrogeological data (such as aquifer geometry, past and present abstraction rates, current groundwater recharge, aquifer hydraulic properties, and observed groundwater levels), meteorological data (precipitation, temperature, wind speed), and geomorphological data (land-use/land cover maps, and soil texture data). The two models were calibrated and validated according to the methods described by [3] and [4], respectively.

The impacts of climate change were quantified using ensembles of Regional Climate Models (RCMs) obtained from the CORDEX project, forced by moderate and worst-case emission scenarios: RCP4.5 and RCP8.5. The Delta Change Factor (DCF) method was applied to perform bias correction for these ensembles. Groundwater recharge and groundwater level anomalies were used as indicators to assess changes in groundwater resources under the influence of climate change.

## **RESULTS/FINDINGS**

Overall, the results suggest a high degree of uncertainty in the spatial variability of groundwater recharge. Figure 1 illustrates the spatial distribution of hydrological components under the severe change scenario. The findings indicate that this scenario causes a division of the study area into two distinct regions based on changes in soil texture and land cover. In the mid and far periods of the severe change scenario, all hydrological components, including recharge, are projected to decrease significantly, with reductions ranging from approximately 35 % to 75 %.

The future groundwater levels of the El-Qaa Plain Aquifer were projected for different General Circulation Models (GCMs) and emission scenarios under climate change for the period 2026– 2100, assuming a constant groundwater abstraction rate of 23 Mm<sup>3</sup>/year. Figure 2 illustrates the anomaly in projected groundwater levels (i.e., the difference between simulated groundwater levels in future and baseline periods),

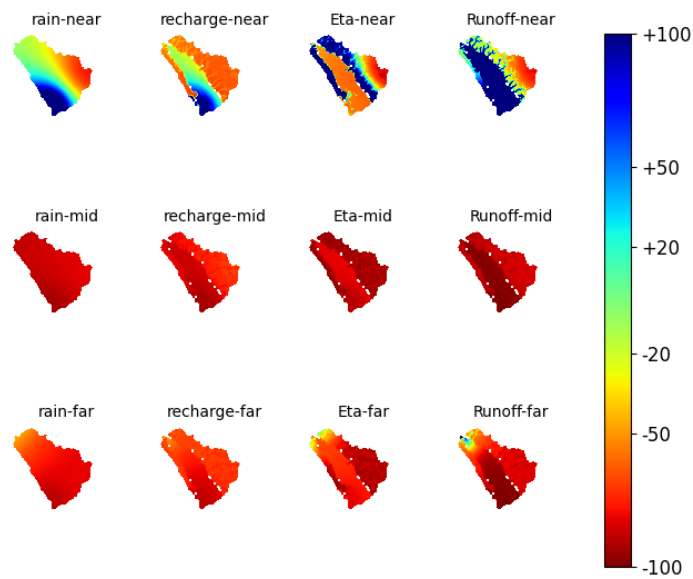


Figure 1: Relative change of the spatial distribution of the hydrological components with respect to baseline period for RCP8.5 for severe change scenario in percentage.

showing the spatial distribution for the severe change scenario - RCP8.5. The results indicate a general decline in groundwater levels, with the anomaly decreasing gradually across all scenarios. The severe scenario (RCP8.5) during the far century period records the maximum drawdown, reaching approximately 17 meters by the year 2100. The figures also show that the cone of depression expands gradually, particularly in areas where pumping wells are concentrated.

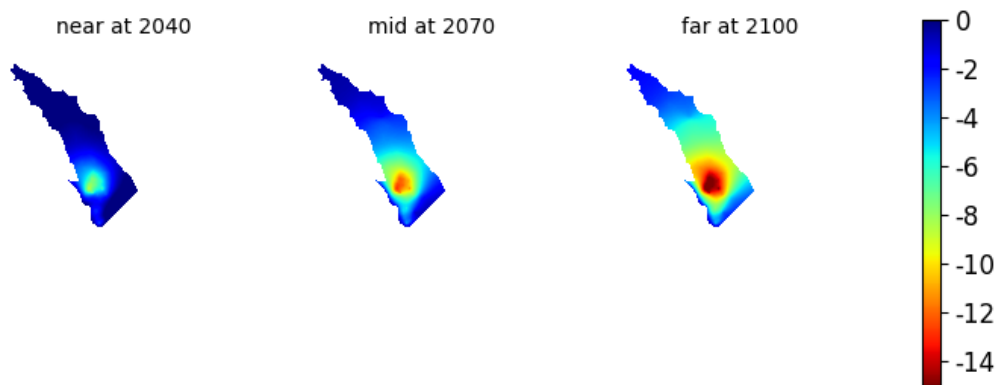


Figure 2. Groundwater level anomaly in meter under climate change for RCP 8.5 for the severe change scenario.

## **CONCLUSIONS AND RECOMENDATIONS**

The impact of climate change on groundwater recharge and levels has been evaluated. For both mid- and far-century periods, under moderate and severe emission scenarios, the results indicate a decline in recharge across most periods and scenarios, with reductions ranging from approximately 35% to 75%. Groundwater levels are projected to decrease, with maximum drawdowns ranging from about 14 to 17 meters under these scenarios. Additionally, the mean groundwater level, which reflects changes in groundwater storage, is expected to drop by 7 to 8 meters, potentially deteriorating groundwater quality due to seawater intrusion. To mitigate potential future water scarcity, it is recommended to implement a sustainable groundwater management plan. Key measures could include reducing current abstraction rates (to a recommended 11.5 Mm<sup>3</sup>/year) and introducing Managed Aquifer Recharge (MAR) using non- conventional water resources as a water source.

**ACKNOWLEDGMENT** The authors would like to express appreciation for the support of Water Resources Research Institute (WRRI) for providing the data

## **REFERENCES**

- [1] Batelann, O., De Smedt, F.: 'WetSpas: a Flexible, GIS Based, Distributed Recharge Methodology for Regional Groundwater Modelling', IAHS Publ., 2001, 269 (1), pp.
- [2] MacDonald, M. G., Harbaugh, A. W.: 'A modular three-dimensional finite-difference groundwater flow model', 1988, USA.
- [3] Soliman, K., Amin, D., Bekhit, H.M., Hafiz, M.G., 'Estimating the natural groundwater recharge taking into consideration temporal and spatial variability for an arid unconfined aquifer', 2024, Water Sci., 38 (1), pp. 359–377
- [4] Soliman, K., Hafiz, M.G., Amin, D., Bekhit, H.M., 'Specifying the hydrogeological parameters range for a groundwater flow model in El-Qaa Plain aquifer, Sinai, Egypt', 2022, Arab. J. Geosci., 15, (21), pp. 1–12

## Role of HydroSOS in Climate Actions (139)

Sulagna Mishra<sup>1</sup>, Washington Otieno<sup>1</sup>, David Kataratambi<sup>2\*</sup>

<sup>1</sup>World Meteorology Organization, Geneva, Switzerland

(Email: [smishra@wmo.int](mailto:smishra@wmo.int), [wotieno@wmo.int](mailto:wotieno@wmo.int)),

<sup>2</sup>Ministry of Water and Environment, Uganda

(Email: [davidkataratambi44@gmail.com](mailto:davidkataratambi44@gmail.com))

### ABSTRACT

Climate change poses significant threats to food, water, and human security, and is a driving factor for migrations. In response, the World Meteorological Organization (WMO) Members developed the Hydrological Status and Outlook System (HydroSOS) to address water-related challenges within the framework of sustainable development, climate change adaptation, and disaster risk reduction. Water-related issues are consistently identified as top priorities by WMO Member Countries. HydroSOS provides an integrated global mechanism for assessing hydrological status and outlooks, involving National Meteorological and Hydrological Services (NMHSs), transboundary basin organizations, and modeling centers. This system enhances decision-making by delivering current hydrological status overviews, appraisals of deviations from the norm, and future outlooks. Ongoing initiatives, such as those in the Nile Basin, support the implementation of HydroSOS, aiming to strengthen countries' capacities to produce relevant hydrological information

The HydroSOS framework comprises three interdependent work components to establish a Hydrological Prediction System. It specifies global assessment processes, modeling methods, and the minimum viable product requirements for hydrological status. These requirements include key variables like streamflow, groundwater levels, soil moisture, and more. Guidelines for seasonal hydrological predictions, best practice specifications, and a forecast verification framework have been established. A proof-of-concept comparison validated these guidelines. HydroSOS facilitates the linkage between monitoring and decision-making at the national level, helping NMHSs provide actionable water resource information to stakeholders, improving national hydrological systems, and integrating products across regions. Ultimately, HydroSOS aids countries in adapting to climate change, enhancing climate actions, and supporting the development of National Adaptation Plans.

**Keywords:** Adaptation, Climate action, Hydrological status and forecasts, National capacity



## METHODOLOGY

The HydroSOS Pilot Study Area covers the entire Lake Victoria Basin (LVB), stream flow data was collected, analyzed and hydrological Streamflow Status and Outlook Products were produced through hands on training of staff from National Meteorological and Hydrological Services. Guidelines for hydrological prediction and Calculation of Climate Normals were used to guide generation of products and the WMO HydroSOS Streamflow Status Product Methodology was followed and has the following steps: (i) Calculating monthly mean flow, (ii) Calculating monthly mean flow as a percentage of average, (iii) calculating rank percentiles and assigning percentile to a category. The R- Software was also used in the generation of the streamflow products.

## RESULTS

Figure (1) Demonstrates Lake Victoria Basin hydrological status and outlook of Streamflow and furthermore shows the months with normal stream flows, above normal stream flows and below normal stream flows. Capacity building of staff from NMHS is also illustrated.

### Equations

The Weibull distribution was used in WMO HydroSOS Streamflow Status Product Methodology and is shown as equation (1).

$$\frac{i}{N + 1} \tag{1}$$

Where  $i$  is the rank of the current month and  $N$  is the number of months in the period of record.

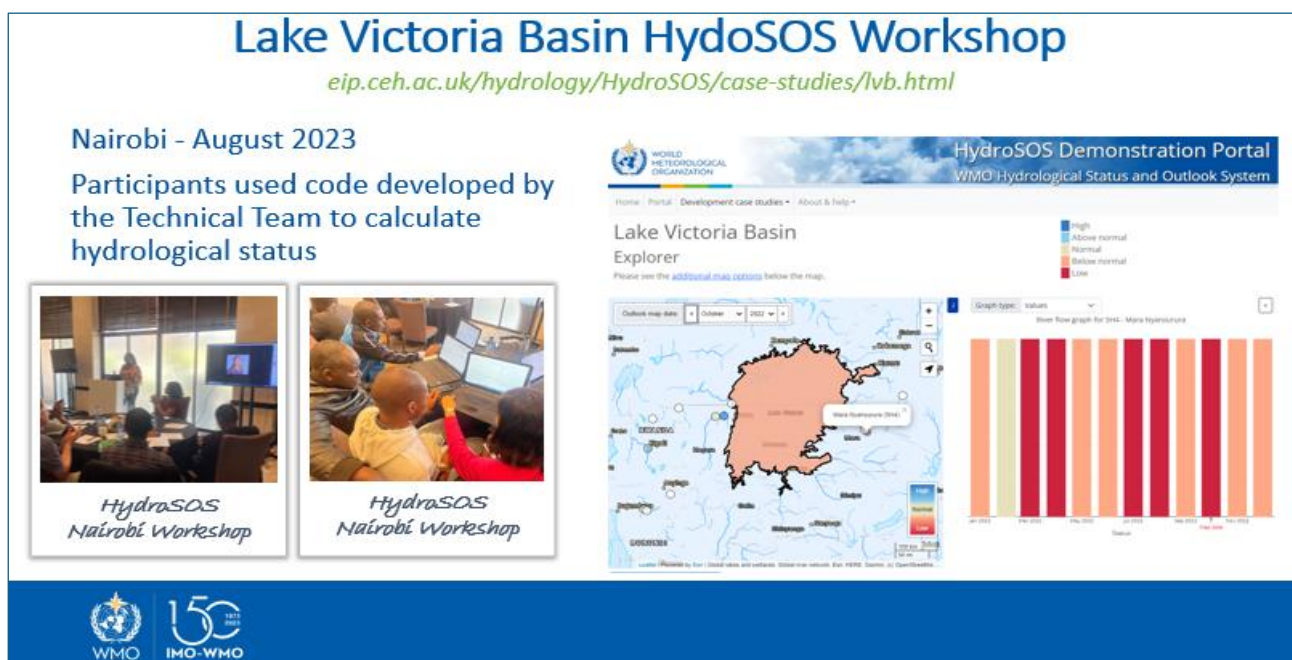


Figure 5: Lake Victoria Basin – Streamflow status



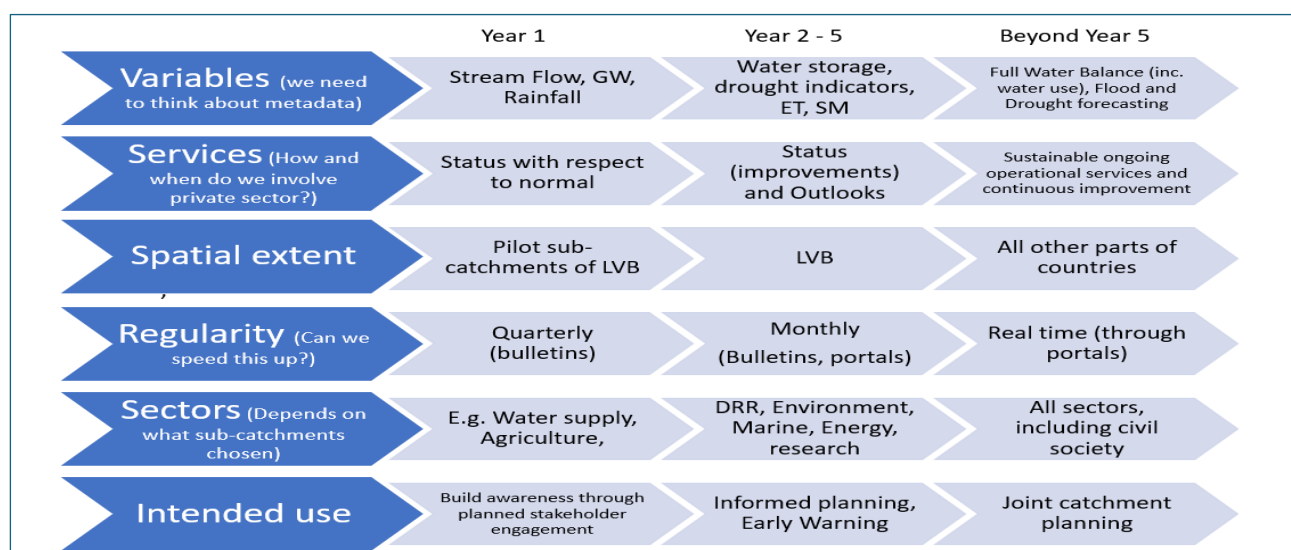


Figure 6: HydroSOS Work Plan

## CONCLUSIONS AND RECOMENDATIONS

From Figure (1), it may be concluded that HydroSOS provides a link between monitoring and decision making, thereby assisting countries in their adaptation to climate change and could also boost literally all climate actions and also help Government Departments in development of National Adaptation Plans.

## ACKNOWLEDGMENT

The authors would like to express appreciation for the support of the HydroSOS technical team, Lake Victoria basin countries and focal points.

## REFERENCES

- [1] WMO Guidelines on the Calculation of Climate Normals (2017 edition)
- [2] WMO Guidelines on Seasonal Hydrological Prediction (2021 edition)
- [3] WMO Hydrological Status and Outlook System (HydroSOS), Dr. Sulagna Mishra et al
- [4] WMO HydroSOS Streamflow Status Product Methodology

**Theme 5: Climate-Smart Communities Planning and  
Legislation  
Day 5**

## Meta- analysis on the Mitigation Measures of Methane Emission in Rice Cultivation Worldwide

Eman A. Hasan

Drainage Research Institute, National Water Research Center, Egypt

(E-mail: Dr\_eman30@hotmail.com)

### ABSTRACT

Rice is a vital staple food for much of the world's population and has critical economic and cultural significance in many developing countries. However, rice is responsible for about 1.5% of global greenhouse gas (GHG) emissions and 48 % of total GHG emissions from croplands, including methane. Methane (CH<sub>4</sub>), as the second most prominent greenhouse gas on a global scale, has assumed a critical role in global climate action due to its heightened warming potential. Meta-analysis was carried out to evaluate five identified methane mitigation technologies worldwide based on data from field experiments. Methane mitigation effects vary in descending order, as Water and fertilizer management > cultivation > Management of crops and fertilizer > Water management > Soil amendment. In particular, the water-fertilizer coupling management could reach a CH<sub>4</sub> reduction of 67.27 %, while methane reduction in the case of system of rice intensification (SRI) equaled 61.1%. Intermittent and alternate wetting and drying irrigation have high abatement potential in southern China. In Amazonian, applying Charcoal as soil amendment derived from the Babassu palm nut reduced methane emission by 43.8% in intensely fertilizer-flooded rice without affecting rice grain yield. In Thailand, the co-application of wood vinegar and biochar significantly mitigated CH<sub>4</sub> emissions by 42.6% in 2016 and 35.3% in 2017, respectively. Based on the research results, CH<sub>4</sub> emission can best be reduced by water-fertilizer coupling management, system of rice intensification, and crop–fertilizer management respectively. The application of Charcoal as soil amendment was better than wood vinegar and biochar in reducing methane emission without affecting rice grain yield.

**Keywords:** Emission, Intermittent irrigation, Methane, Mitigation , Mideason drainage, Rice cultivation,

## **INTRODUCTION**

The Inter-governmental Panel of Climate Change (IPCC) report highlights that methane emissions have contributed to raising global temperatures by 0.5 °C out of the 1.1 °C increase compared to pre-industrial levels [1]. Rice cultivation accounts for approximately 30% of the total annual global agricultural CH<sub>4</sub> emissions in 2017. These emissions are projected to rise 7 % by 2030 and 6 % by 2050 [2]. Hence, mitigating methane emissions in rice cultivation is crucial in tackling global climate change. China is the largest rice producer and, thus, a significant contributor to methane emissions. In 2020, the total methane emissions from rice paddies in China was 149.26 MtCO<sub>2</sub> eq., representing 21.75 % of the global total methane emissions from rice cultivation [3]. Several factors impact methane emissions from rice cultivation, including rice varieties, soil conditions, climate factors, and agricultural practices. Methane mitigation strategies primarily encompass three dimensions: water management, fertilizer management, and cultivation practices [4]. Water management includes intermittent irrigation, midseason drainage, and Alternating Wetting and Drying irrigation (AWD).

Meta-analysis was carried out to evaluate five identified methane mitigation technologies worldwide based on data from field experiments.

## **METHODOLOGY**

Meta-analysis for peer-reviewed research articles on the mitigation of CH<sub>4</sub> from rice cultivation was carried out using the Scopus database from 2004 to 2024 and led to 107 research papers. The keyword combinations of ("Mitigation" or "reduction") and "methane emission" and "rice cultivation" and PUBYEAR > 2003 and PUBYEAR < 2025 and (LIMIT-TO (LANGUAGE, "English")) were instrumental in retrieving the relevant studies. The following criteria were employed to select studies for inclusion: (1) studies were required to be designed as paired-plot field experiments in paddy fields; (2) absolute CH<sub>4</sub> emissions could be calculated or measured; (3) detailed descriptions of treatments and controls were required; and (4) the experiment's location was specified. The mitigation technologies mainly focus on Cultivation, management of water and fertilizer, Management of crops and fertilizer, Water management, and Soil amendment. Twelve mitigation measures were evaluated for their impact on CH<sub>4</sub> emissions and rice yields. These twelve assessed mitigation measures encompass: (i) Intermittent irrigation, AWD and Midseason drainage as water management, (ii) Cellulose Acetate-mixed Ethephon, Biochar, Wood vinegar and biochar, Bacterial consortium, Charcoal as soil amendment, (iii) Rice direct dryland seeding and SRI are related to cultivation, (iv) Management of water and fertilizer, and (v) Management of crops and N fertilizer.

## RESULTS

The meta-analysis revealed that China has the highest publication records in mitigating methane emissions from rice cultivation, followed by the USA and Japan, as shown in Figure (1). The relation between the 12 methane mitigation measures in rice cultivation, methane mitigation and yield increase percentage is shown in Figure (2); it is clear that midseason drainage has the largest reduction of methane emission, 52.4% from rice cultivation as a water management technique in China, [5] . Intermittent irrigation demonstrates a remarkable CH<sub>4</sub> reduction of 43.83% compared to continuous flooding irrigation [7]. Meanwhile, AWD techniques effectively reduce CH<sub>4</sub> emissions by 39% and increase rice yield by 7.5% [10]. The application of Charcoal as a soil amendment has the largest methane reduction percentage of 43.8 in Amazonian [8]. CH<sub>4</sub> emission can best be reduced by the water-fertilizer coupling management that reaches a reduction of 67.27 % and an increase in rice yield by 10%, while the reduction of methane in the case of SRI equaled 61.1% and the increase of rice yield is 7% [9]. Management of crops and N fertilizer reduces methane emission by 59.8 % and increases rice yield by 35% [13], while Bacterial consortium reduces methane emission by 42% and increases rice yield by 33.55% [12].

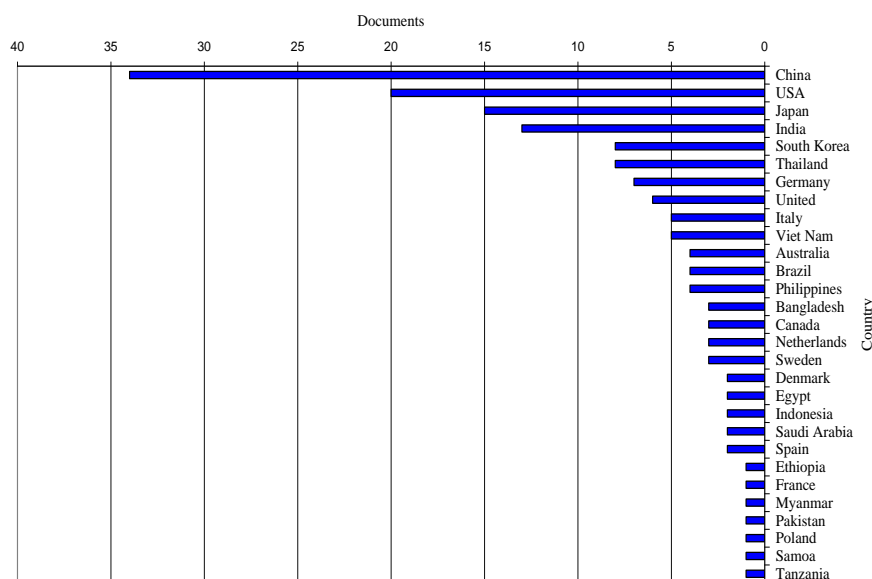


Figure 1 Publication records (documents) in mitigating methane emissions

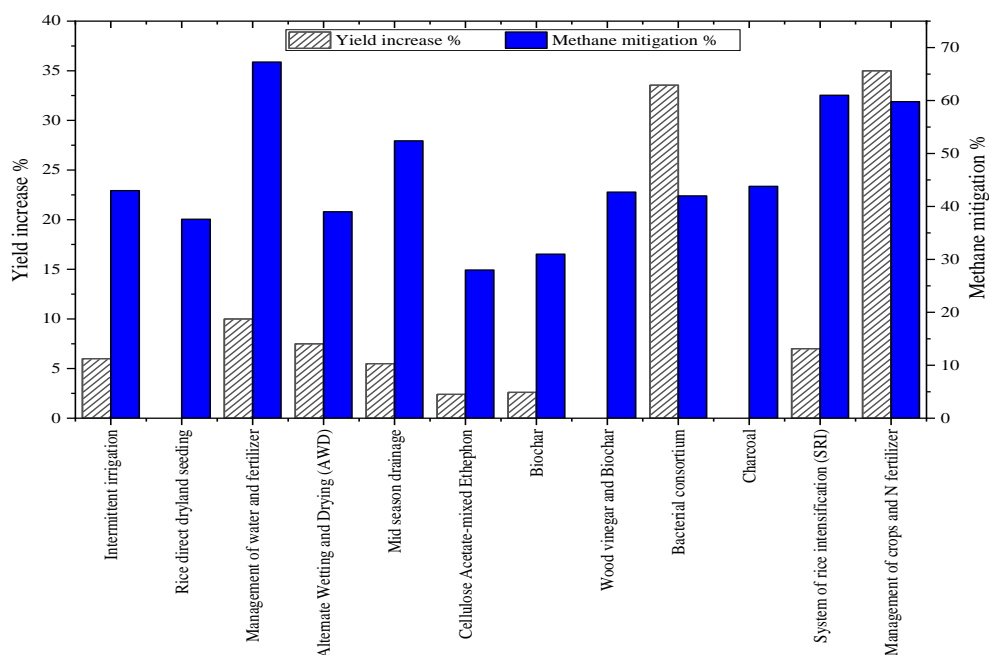


Figure 2 Results of meta-analysis on methane mitigation from rice cultivation

## CONCLUSIONS AND RECOMMENDATIONS

Methane emissions from rice cultivation have contributed to raising global temperatures, causing global warming and climate change. The present study confirms the capacity of the water-fertilizer coupling management technique to effectively mitigate CH<sub>4</sub> emissions by 67.27 % in the rice growing season with increasing yield by 10%. SRI and Management of crops and N fertilizer mitigate methane emission by about 61% and 59.8% and increase rice yield by 7% and 35%, respectively. Midseason drainage has the highest methane reduction of about 52.4 % as a water management technique.

Meanwhile, Charcoal application is the best soil amendment technique to mitigate methane emission from rice cultivation by 43.8% . It could be concluded that the best technique to mitigate methane emission from rice cultivation without decreasing rice yield is the Water-fertilizer coupling management followed by SRI and Management of crops and N fertilizer. It is recommended to use low methane-emitting varieties of rice worldwide. Nitrification inhibitors can lead to a significant reduction in methane emissions from rice cultivation.



## **REFERENCES**

- [1] IPCC, 2021. Summary for Policymakers, Climate Change 2021: The Physical Science Basis, pp. 3–32. Cambridge.
- [2] Saunio, M., Stavert, A.R., Poulter, B., Bousquet, P., Zhuang, Q., 2020. The global methane budget 2000–2017. *Earth Syst. Sci. Data* 12 (3), 1561–1623.
- [3] FAO STAT, 2021. <https://www.fao.org/faostat/en/#data/GT>.
- [4] Wang, B., Cai, A., Song, C., Qin, X., Liu, S., Li, Y., 2022a. CH<sub>4</sub> reduction in rice paddy: technology, challenge and strategy. *Chin. J. Agric. Resour. Reg. Plann.* <https://kns.cnki.net/kcms/detail//11.3513.s.20221207.20221726.20221012.html>.
- [5] X.Liu et al., 2019. Effect of midseason drainage on CH<sub>4</sub> and N<sub>2</sub>O emission and grain yield in rice ecosystem: A meta-analysis. *Agricultural Water Management* 213 (2019) 1028–1035
- [6] Corton et al., 2000. Methane emission from irrigated and intensively managed rice fields in Central Luzon (Philippines). *Nutrient Cycling in Agroecosystems* 58: 37–53, 2000. © 2000 Kluwer Academic Publishers. Printed in the Netherlands
- [7] Ma et al., 2024. A meta-analysis on the mitigation measures of methane emissions in Chinese rice paddy. *Resources, Conservation & Recycling* 202 (2024) 107379
- [8] Brbosa et al., 2014. Charcoal in Amazonian paddy soil–nutrient availability, rice growth and methane emission. *Journal of plant nutrition and soil science*, volume 177, issue 1.
- [9] Niveta Jain, Rachana Dubey, D.S.Dubey and Jagpal.2013. Mitigation of greenhouse gas emission with system of rice intensification in the Indo Gangetic Plains. *Paddy and Water Environment*, DOI 10.1007/S10333-013-0390-2.
- [10] Prangbang et al.(2020). Climate Based Suitability Assessment for Methane Mitigation By Water Saving Technology in Paddy Fields of the Central Plan of Thailand. *Frontiers in Sustainable Food Systems*, Volume4.
- [11] Sriphirom et al.(2021). Effects of biochar on methane emission, grain yield, and soil cultivation in Thailand. Volume 12, issue 2.
- [12] Pratiwi, etty, A Akhdiya and J Purwani, 2021. Impact of methane –utilizing bacteria on rice yield, inorganic fertilizers efficiency and methane emissions. *IOP Conference Series Earth and Environmental Science*,648(1):012137, DOI:10.1088/1755-1315/648/1/012137.
- [13] Mboyerwa PA, Kibebew K, Mtakwa P and Aschalew A, 2022. Greenhouse gas emissions in irrigated paddy rice as influenced by crop management practices and Nitrogen Fertilization Rates in Eastern Tanzania. *Front Food Syst*.6:868479 , DOI:10.3389/Fsufs.2022.868479.
- [14] Cho S., Verma P P and Das S., 2022. A new approach to suppress methane emissions from rice cropping systems using Ethephon. *The Science of the total environment*, Volume 804(1):150159, DOI:10.1016/J.scitotenv.2021.150159.

## Implications of Climate Change for Managing Water-Related Risks in Developing Countries: Examples from Three African States

Saber Abdelaal\*<sup>1</sup> and Matthias Fritz <sup>1</sup>

<sup>1</sup> Hydraulic Engineering Department, CES Consulting Engineers Salzgitter GmbH, Nordstraße 23, 38106 Braunschweig, Germany. (E-mail: [\\*abd@ces.de](mailto:*abd@ces.de), [frt@ces.de](mailto:frt@ces.de) )

### ABSTRACT

Climate Change (CC) imposes extra hydraulic loads on water infrastructure worldwide. Global warming drives an increase in frequency and intensity of extreme weather events leading, among others, to: (i) accelerated coastal erosion and extreme coastal flooding in coastal areas, (ii) an increase in water needs for agricultural and domestic purposes, (iii) long-lasting hydrological drought and frequent extreme floods. While developed countries are relatively prepared for CC impacts due to their strong and well-managed infrastructures, ongoing, and future water-related projects in developing countries need to consider CC-driven additional loads in order to enhance their resilience to CC and help vulnerable communities cope with climate-related risks with minimal residual risks. This study presents cases from three African states (South Sudan, Tanzania, and Mozambique) where proper indices and climate change projections are applied to identify the severity of CC impacts, identify vulnerable regions, and map future risks as an essential element of managing extreme events and adapting to CC. As a result, proactive interventions are applied to enhance the resilience of projects' zones in the three states against the impacts of CC. It is found that the approach applied in each different state depends on the regional CC conditions as well as the hydraulic boundaries. However, the lessons learned are transboundary and still applicable in other African states that have similar drivers. For instance, the methods applied, and the measures implemented to mitigate coastal erosion and flooding in Inhambane, Mozambique, (e.g., construction of coastal dikes of low permeable sands) are still valid to protect Egyptian coasts from the same risks.

**Keywords:** Adaptation; Climate Change; Coastal Management; Flood modeling; Risk Mapping; Regional Projections

## METHODOLOGY

CC impacts refer to those phenomena that occur due to global warming induced by increased emissions of greenhouse gases (GHG), e.g. changes in precipitation patterns and intensity, rising sea levels, and increased evapotranspiration [1]. Impacts also include tangible/nontangible consequences of the latter phenomena e.g. increased coastal/fluvial flooding, coastal erosion, and saltwater intrusion [2-4]. Predicting the latter consequences requires analysis of both historical climatic data (e.g., precipitation) as well as future projections of this data under different emission scenarios. Projections are often obtained from outcomes of climatic models that simulate, among others, the changes in climatic phenomena under different future Shared Socio-economic Pathways (SSPs) that consider different emission scenarios, mitigation efforts, and international development paths. Climatic models are coordinated internationally by the World Climate Research Program (WCRP) through the Coupled Model Inter-comparison Projects (CMIPs). Thus, CMIPs provide climate projections that support (i) essential WCRP activities and climate science worldwide, and (ii) decision and policy-makers communities, in its objective to understand past, present, and future climate changes.



Figure 7. Inundation map for both of Zanzibar islands under the emission scenario SSP5-8.5 of a sea level rise of 80 cm until 2100

CMIPs and their associated data infrastructure have become essential to the Intergovernmental Panel on Climate Change (IPCC) and other international and national climate assessments. The sixth phase of CMIPs (known as CMIP6) consists of 134 models of different spatial resolutions which 53 international modeling centers are constantly developing [5]. Individual outputs of the latter models are accessible from many institution's

portals e.g., German Climate Computing Center (DKRZ)<sup>1</sup> and thematic information services e.g., Copernicus Earth Observation Programme of the European Union<sup>1</sup>. Moreover, the Climate Change Knowledge Portal (CCKP) provides a multi-model ensemble of outcomes of latter models at national, sub-national, and watershed scales with a resolution of 0.25° x 0.25. The CCKP<sup>1</sup> supports the integration of scientific climate data into the design of projects or policies, particularly those related to the World Bank Group. The methods employed in this study are based on the analysis of historical and projected CMIP6 data to assess climate change impacts on three water-related projects in Northern Bahr El Ghazal (NBeG) and Western Equatoria (WEQ) states in South Sudan, Zanzibar (Tanzania) and Mozambique. The employed historical data are first calibrated with available field data, showing acceptable coincidence. Thus, the multi climatic model ensemble data are then used to run flood models to identify vulnerable regions and map future risks, particularly under the worst CC scenario SSP5 8.5, as an essential element of managing extreme events and adapting to CC.

## **RESULTS/FINDINGS**

Analysis of many factors related to climate change impacts (e.g., precipitation, evapotranspiration, and sea level rise) showed that Zanzibar may be subject to long-term droughts and excess water demand for domestic and irrigation purposes. Among the main reasons for the increase in demand is the increase in evapotranspiration rates due to the regional warming induced by increased GHG emissions. Moreover, long-term rise of sea levels combined with episodic increases driven by episodic events (e.g., tropical storms and subsequent surges) will lead to large inundations of nearshore areas, as shown in Figure 1. The coastal inundation will lead, among others, to increased lateral and vertical saltwater intrusion.

In South Sudan, many micro-catchments (e.g., in Figure 2) that belong to the great Bahr El Ghazal catchment in the states of NBeG and WEQ are hydrologically modeled for the purpose of integrated catchment management in the light of flood modeling and CC impacts. The analysis of climate change projections of precipitation showed that the frequency of extreme precipitation (e.g., 100-year precipitation as an adaptation indicator of CC) will increase as an impact of CC while the intensity of extreme precipitation events will remain almost stable. Other insights into CC impacts on other micro catchments in NBeG and WEQ and Inhambane, Mozambique will be shown in the presentation.

---

<sup>1</sup> Under the link <https://esgf-data.dkrz.de/projects/cmip6-dkrz/>

<sup>1</sup> Under the link <https://cds.climate.copernicus.eu/cdsapp#!/dataset/projections-cmip6?tab=form>

<sup>1</sup> Under the link <https://climateknowledgeportal.worldbank.org/>

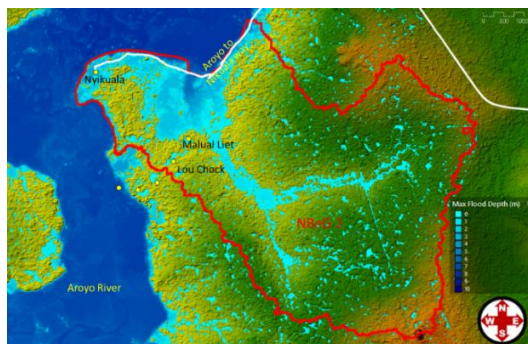


Figure 8. Inundation map for one of the micro-catchment near Aroyo city, in NBeG, under the 100-year flood storm.

## CONCLUSIONS AND RECOMMENDATIONS

CC will impose episodic and long-term effects on water resources, food security and sustainable development of African states and worldwide. Therefore, ongoing, and future water-related projects need to consider CC-driven additional loads in order to enhance their resilience to CC and help vulnerable communities cope with climate-related risks with minimal residual risks. To avoid maladaptation to CC impacts, future projections of relevant factors (e.g., precipitation and sea levels) should be considered to evaluate the increase of hydraulic loads imposed by CC impacts. Although the increase in the hydraulic loads depends on the regional climate projection, the methods applied, and the measures implemented are transboundary and still applicable in other African states.

## ACKNOWLEDGMENT

South Sudan and Zanzibar projects are financed respectively by the GIZ and KFW on behalf of the German government. The project in Mozambique is financed by the World Bank Group. CES is the consultant for the three projects.

## REFERENCES

- [1] S. L. Burch and S. E. Harris, *Understanding climate change: Science, policy, and practice*, second edition. 2021.
- [2] S. M. Elsayed Abdelaal and H. Oumeraci, "Modelling and mitigation of storm-induced saltwater intrusion: Improvement of the resilience of coastal aquifers against marine floods by subsurface drainage," *Environmental Modelling and Software*, vol. 100, 2018, doi: 10.1016/j.envsoft.2017.11.030.
- [3] S. M. Elsayed Abdelaal, H. Oumeraci, and N. Goseberg, "Erosion and breaching of coastal barriers in a changing climate: Associated processes and implication for contamination of coastal aquifers," *Proceedings of the Coastal Engineering Conference*, vol. 36, no. 2018, 2018, doi: 10.9753/icce.v36.papers.107.
- [4] S. M. Elsayed Abdelaal, H. Oumeraci, and N. Goseberg, "Effects of soil properties on erosion and breaching of natural coastal barriers under extreme storm surges," *Shore & Beach*, vol. 92, no. 4, p. 26, 2024.
- [5] V. Eyring et al., "Overview of the Coupled Model Intercomparison Project Phase 6 (CMIP6) experimental design and organization," *Geoscientific Model Development*, vol. 9, no. 5, pp. 1937–1958, May 2016

## Application of Virtual Reality on Water Resources

**Management** Djamel Berkaoui\*

<sup>1</sup>, Florian Balmes<sup>2</sup>, Richard Gramlich<sup>3</sup>

<sup>1, 2, 3</sup> Academic and Research Department Engineering Hydrology, UNESCO Chair of Hydrological Change and Water Resources Management, RWTH Aachen University, GERMANY.  
(E-Mail: [berkaoui@lfi.rwth-aachen.de](mailto:berkaoui@lfi.rwth-aachen.de), [balmes@lfi.rwth-aachen.de](mailto:balmes@lfi.rwth-aachen.de), [gramlich@lfi.rwth-aachen.de](mailto:gramlich@lfi.rwth-aachen.de).)

### ABSTRACT

Climate change is causing an increase in extreme events related to the vital resource of water. These changes impact cultures, communities, and ecosystems globally.. To respond effectively, mitigation and adaptation measures are needed. Raising awareness of these challenges is essential. Hence, interdisciplinary knowledge transfer between different actors at a global level is indispensable. Extreme events like droughts and floods lead to environmental, economic, and social changes significantly affecting sustainable development. A variety of impacts can be observed, including infrastructural changes like lacking crop yields, limited access to fresh water and hygiene and thus to human health.

By implementing Avatar-based Teaching and Learning in Virtual Reality [2] (ABTAL VR) scenarios displaying flood protection infrastructure or holistic Water-Energy-Food Nexus models including photovoltaic, desalination and agricultural components not only awareness can be raised, also practical trainings can be simulated in ABTAL VR so that their actual trainings can be shortened or in some cases completely replaced. Recent research showed that in a case study to construct a mobile flood protection unit, theoretical knowledge is gained and a positive reception towards the usage of the Virtual Reality tool can be achieved [3].

**Keywords:** Climate Change, Droughts, Education, Heavy Rainfall, Virtual Reality



## **METHODOLOGY**

A multi-level ABTAL VR scenario is being developed to teach the concept and functioning of various components of a seawater desalination plant (Figure 1, left). The ABTAL VR scenario is structured in three levels (beginner, intermediate, advanced), which consider the different prior knowledge of students. In order to enable the best possible assignment of students, a catalogue of questions is created which is completed by students. The answers are used to assess prior knowledge and assign students to the appropriate level. As this is one ABTAL VR scenario, the three levels do not differ in terms of their basic structure and visualization. However, the levels differ in terms of the level of detail and complexity of the functionalities and the use of specialized terminology. There are also different levels of assistance and explanations such as videos.

Another use case is in the field of mobile flood protection unit (Figure 1, right) (MFPU). During hazardous events, when flood waves are announced, highly skilled and well-trained professionals are needed to construct mobile flood protection units within a short matter of time. Practical training on actual mobile flood protection walls however cannot be easily done due to availability problems. A comparative study (publication in progress) with an experimental group (48 students) was used to conduct the experiment using VR tutorials and traditional instructional videos. Firstly, the variable being analysed was defined: In this case, the use of VR technology. Secondly, the desired effects of this variable were measured and when the method can be categorised as a success was determined. This was measured on the basis of a questionnaire that the two groups needed to fill out after the experiment. The effectiveness of these teaching tools was evaluated in terms of both theoretical and practical knowledge transfer. In addition, the students' personal perception of the use of the VR software was evaluated [1].



Figure 1. Actual footage of the ABTAL VR scenes. The area of the desalination plant, agriculture and photovoltaic fields on the left. The partly constructed mobile flood unit in an urban area on the right.

## RESULTS/FINDINGS

The ABTAL VR scenario is divided into successive phases. All stages have milestones at certain points in the processing of the ABTAL VR scenario, at which the level of knowledge is tested through small tasks and a self-assessment is carried out by the students. Based on this, students are recommended to change levels if the ABTAL VR scenario was too easy or too difficult for them in the corresponding processing phase. The evaluation is carried out automatically by analyzing the data collected during the course. Students can collect experience points by completing the course, which are credited to their learning account and thus unlock new areas of the ABTAL VR scenario. The learning success, especially of the MFPU scenario is assessed by comparing two test groups of students. For this purpose, identical tests are carried out with the two test groups. One test group will work on the MFPU scenario, while the other test group will learn the same content in the form of a conventional lecture or media.

Initial results (Figure 2) on the evaluation of the effectiveness of the ABTAL VR scenario for the mobile flood protection unit indicate a positive effect on theoretical knowledge transfer and favorable student reception of the VR tool. However, further studies are needed to gain more insight into its impact on practical skills.

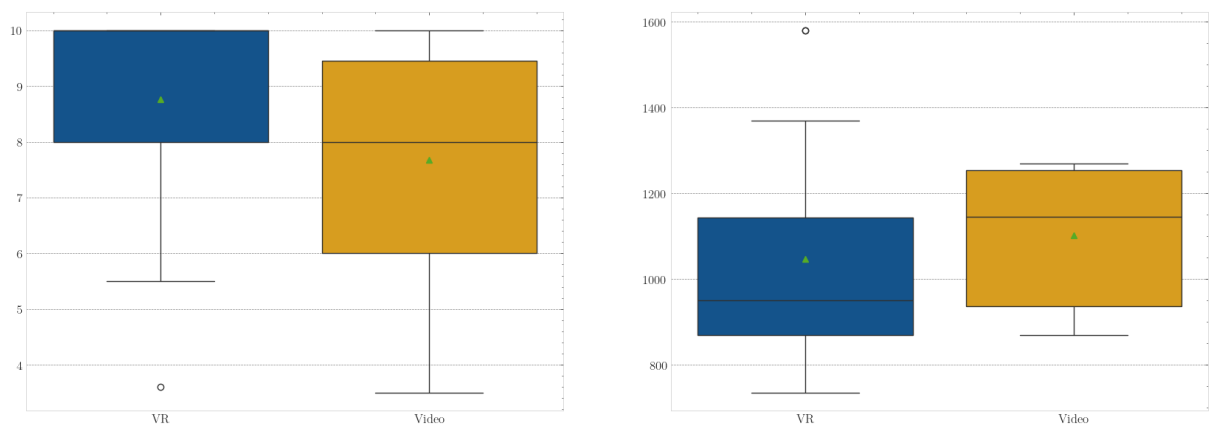


Figure 2. Comparison of test results (theoretical assessment) of the VR group and the video group (left). Comparison of time needed to construct (practical assessment) the MFPU per team of 3 students in the VR group and the video group (right).

## **CONCLUSIONS AND RECOMENDATIONS**

The ABTAL VR scenario on the desalination plant introduces a multi-level learning approach based on Gamification. This not only improves the personal motivation for the students but also the competitive dynamic of the group. Additionally, the scenario gives each student the possibility to adjust the difficulty of the scenario to their specific need.

Since damages from flooding are a core problem in various places of the world, adequate protection and training are important to face future challenges. For the mobile flood protection unit, the VR training helped to build the mobile flood protection unit in a realistic manner, which concluded in a significant gain in theoretical knowledge. Some technical difficulties were identified like motion sickness for some participants.

For both scenarios, neglection of the upper limit on the group size in the face-to-face training, the outreach to the target groups however are outperforming aspects to continue research and development in this direction.

## **REFERENCES**

- [1] Theyßen, H.: 'Methodik von Vergleichsstudien zur Wirkung von Unterrichtsmedien', Methoden in der naturwissenschaftsdidaktischen Forschung., 2013
- [2] Berkaoui, D. et al.: MyScore – Avatar-Based Teaching and Learning., 2022
- [3] Querl P. et al.: Does Self-paced Learning in Mobile Flood Protection Unit Construction in Virtual Reality Have Advantages Over Traditional Measures? (unpublished, in progress)

**POSTER**  
**Day 4**

## Adapting to climate change by quantifying optimal allocation of water resources & socio-economic interlinkages (ACQUAOUNT)

M. Debolini<sup>1</sup>, S. Mereu<sup>1</sup>, M. Funaro<sup>1</sup>, R. Padulano<sup>1</sup>, G. Rianna<sup>1</sup>, E. Depliazzo<sup>1</sup>, A. Kandarakis<sup>2</sup>, V. Constantianos<sup>2</sup>, T. Fanni<sup>3</sup>, F. Martini<sup>3</sup>, G. Foddis<sup>3</sup>, J. Pijuan<sup>4</sup>, L. Viñe<sup>4</sup>, F. Wassar<sup>5,\*</sup>, F. El Mokh<sup>5</sup>, M. Ben Zaied<sup>5</sup>, K. Nagaz<sup>5</sup>, M. Lo Cascio<sup>6</sup>, C. Sirca<sup>6</sup>, S. Marras<sup>6</sup>, S. Asgharinia<sup>7</sup>, M. Onorati<sup>7</sup>, I. Jomaa<sup>8</sup>, N. Mazahrih<sup>9</sup>

<sup>1</sup>FONDAZIONE CMCC Fondazione Centro Euro-Mediterraneo sui Cambiamenti Climatici, Italy

<sup>2</sup>Global Water Partnership - Mediterranean (GWP-Med), Athens, Greece

<sup>3</sup>ABI ABINSULA SRL, Sassari, Italy

<sup>4</sup>EUT FUNDACIO EURECAT, Barcelona, Spain

<sup>5</sup>Institut des Régions Arides, Médenine, Tunisia

<sup>6</sup>UNISS University of Sassari, Italy

<sup>7</sup>Nature4 Nature 4.0 Soc. Benefit Srl, Sassari, Italy

<sup>8</sup>National Agricultural Research Center, Amman, Jordan

<sup>9</sup>Lebanese Agriculture Research Institute, Lebanon

The efficient use of water is a critical issue impacting multiple sectors, with high potential returns when managed properly. Integrated Water Resource Management (IWRM) is a key approach to address these challenges, but its development varies widely among countries, especially in the Mediterranean region. Climate change predictions suggest reduced and degraded water resources in these areas, alongside increasing irrigation demands driven by population growth and climate-related factors. Given that agriculture is the most significant consumer of water, enhancing farm-level efficiency is crucial to sustainable IWRM. Beyond the agricultural sector, broader resource management strategies are essential, including effective allocation of various water sources like groundwater and grey water, to support a balance between all sectoral needs and ecosystem preservation. Digitalization in the water sector can play a pivotal role in managing these complex systems. It can help track water resources, foster inter-sector coordination, and speed up the implementation of new policies. The ACQUAOUNT project aims to tackle these challenges by deploying a Web of Things (WoT) platform. This platform integrates data from digital sensors at both farm and basin levels, along with remote sensing, geographic databases, and socio-economic information, to provide a comprehensive view of water resource dynamics. It offers two key real-time services: one for farmers to optimize irrigation schedules, and another for water managers to monitor and project water demands and supplies, helping to identify and mitigate potential issues. Moreover, the embedded model in the WoT platform supports decision-makers by allowing them to simulate various scenarios and make informed long-term plans for climate change adaptation. ACQUAOUNT demonstrates this IWRM model at a basin scale in four Mediterranean countries: Italy, Jordan, Lebanon, and Tunisia.

**Keywords:** real-time services, Business models for digital water, Decision Support tools for long-term planning and adaptation, Basin level demonstration, Multi-actor approach, smart agriculture, food security.

## Chitosan-g-polyacrylonitrile ZnO nano-composite, synthesis and characterization as new and good adsorbent for Iron from groundwater

Abdelrahman O.A. Eldenary <sup>a</sup>, H.M. Abd El-Salam <sup>a,\*</sup>, Abeer Enaiet Allah <sup>b</sup>

<sup>a</sup> Department of Chemistry, Faculty of Science, Polymer Research Laboratory, Beni-Suef University, 62514 Beni-Suef City, Egypt ([abdoosman1312@gmail.com](mailto:abdoosman1312@gmail.com) , [hanafy011246@sci.bsu.edu.eg](mailto:hanafy011246@sci.bsu.edu.eg) )

<sup>b</sup> Department of Chemistry, Faculty of Science, Beni-Suef University, 62514 Beni-Suef City, Egypt ([abeer.abdelaal@science.bsu.edu.eg](mailto:abeer.abdelaal@science.bsu.edu.eg) )

**Keywords:** Adsorption, Chitosan, composite, Polyacrylonitrile, Zinc oxide.

### ABSTRACT

The highly poisonous, non-biodegradable heavy metals present serious concern in wastewater environmental sustainability and human health. Using adsorption is an effective technology for the treatment of this kind of water. Therefore, developing efficient and cost-effective adsorbents considers a significant and an emerging topic in the field the water purification. Chitosan grafted polyacrylonitrile (Cs-g-PAN) was facially fabricated via graft polymerization using ammonium persulfate (APS) as the initiator. The simple ultrasonic technique was used for doping ZnO nanoparticles into the Cs-g-PAN matrix to prepare chitosan-grafted polyacrylonitrile/ZnO (Cs-g-PAN/ZnO). For comparative study, pure ZnO and nanocomposite of PAN doped with ZnO (PAN/ZnO) were also prepared. XRD, FTIR, SEM, TEM, BET, EDS, and TGA measurements were conducted to confirm the morphological and structural properties of the prepared materials. Cs-g-PAN/ZnO possesses a specific surface area of 20.23 m<sup>2</sup> /g with a pore size of 31.58 nm and pore volume of 0.16 cm<sup>3</sup> g<sup>-1</sup>. The adsorption behavior toward Fe (II) as a pollutant for groundwater was studied for the synthesized materials.

The effect of pH (4–8), contact time (5–60 min), adsorbent dose (0.01–0.3 g), and different temperature degrees (278, 288, 298, 308, and 318 K) on the removal of iron (II) has been conducted. The removal efficiency was achieved 100 % under the optimum condition, at pH = 7, contact time 30 min, adsorbate concentration 0.93 mg/ L, and adsorbent dosage 0.05 g/L at room temperature. Langmuir and Freundlich's isothermal and kinetic studies have been analyzed to determine the adsorption mechanism of Fe(II) ions on the synthesized nanomaterials. The adsorption process of Fe(II) over the surface of prepared catalysts proceeded via the Langmuir model and pseudosecond-order reaction kinetics with  $R^2 > 0.99$ . Suggesting the formation of Fe(II) monolayer over the adsorbent surface and the rate-limiting step is probably controlled by chemisorption through sharing the electrons between Fe<sup>+2</sup> and the prepared catalyst.



## AIM OF WORK

The goal of the current study was to discover a fast, affordable, and safe process for removal of iron from ground water. Where the excessive iron (II) content in drinking water can cause lifethreatening problems including, siderosis, anorexia, hypothermia, diphasic shock, metabolic acidosis, oliguria, diarrhea, heart failure, diabetes, and even death. For this reason, the World Health Organization WHO fixed the tolerance limit of Fe(II) concentration in drinking water as  $<0.3$  mg/ L. So the authors try to present a safe and economic solution by preparing chitosan-grafted polyacrylonitrile/ZnO (Cs-gPAN/ZnO) and use it for removal of iron from ground water.

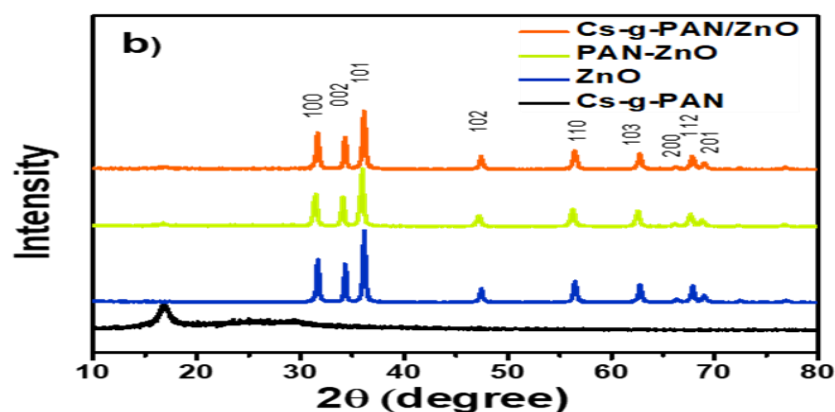
**Materials** Chitosan, Methanol, Ammonium persulfate, zinc acetate, Acrylonitrile and Sodium hydroxide. Twice distilled water was used as a medium for all the polymerization reactions. All reagents were used without further purification.

## Methods

### Preparation of Chitosan-Graft-PAN/ZnO(CS-g-PAN/ZnO) and Poly Acrylonitrile/ ZnO (PAN /ZnO) composites

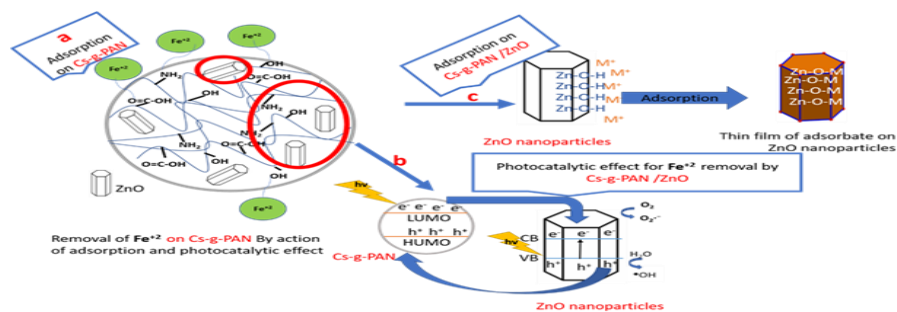
- 1- 1 g of Cs-g-PAN has immersed in a 50 mL zinc acetate solution of 6% with a weight ratio of 1:3 Cs-g-PAN: zinc acetate. The solution was sonicated for 2 hours at  $70^{\circ}\text{C}$ .
- 2- PAN /ZnO composite was prepared by the same previously described method by replacing Cs-g-PAN with PAN.

**Figure 1: XRD of the prepared samples.**



The diffractograms of pure chitosan sample shows the intense peak at  $2\theta = 17^\circ$  is due to the crystal planes of PAN. The broadening of the peak at  $24^\circ$  is due to the amorphous nature of the polymer. The small intensity of this peak is ascribed to the grafting of PAN onto chitosan. Pure ZnO the characteristic peaks at  $2\theta = 31.87^\circ, 34.55^\circ, 36.35^\circ, 47.59^\circ, 56.66^\circ, 62.89^\circ, 66.40^\circ, 67.89^\circ, 69.17^\circ, 72.59^\circ$  and  $77.00^\circ$ .

### Scheme 1: Mechanisms for removal of Fe(II) by Cs-g-PAN/ZnO



The presence of a negative charge on the surface creates active adsorptive sites for the attachment of positively charged heavy metal ions of Fe(II). When radiation of the light strikes ZnO nanoparticles, it causes electrons in the valence band to become excited and move into the conduction band. This results in the formation of highly active electrons in the conduction band and holes in the valence band, which leads to the generation of radicals.

### Conclusions:

The prepared superior adsorbent Cs-g-PAN/ZnO was characterized using XRD, FTIR, SEM, TEM, and TGA and resulting data proved the successful grafting of polyacrylonitrile on the surface of chitosan and growth of ZnO nanoparticles on the chitosan surface using ultrasonic technique. The obtained results from the adsorption experiment demonstrated that Cs-g-PAN/ZnO showed the highest adsorption capacity toward Fe(II) compared to bare Cs-g-PAN, ZnO, and PAN-ZnO. The adsorption behaviors of Cs-g-PAN/ZnO were investigated, which confirmed that the introduction of ZnO significantly improves the adsorption capacity in a short time, over a wide pH range, using a small quantity of adsorbent. The isotherm and kinetic data for the Fe(II) adsorption onto the prepared adsorbents fit well to the Langmuir model with  $R^2 > 0.99$  and pseudo-second-order reaction. Cs-g-PAN/ZnO considers an environmentally friendly promising candidate for the removal of highly toxic pollutants from aqueous media such as heavy metal Fe(II) due to its high adsorption efficiency, and low cost.

**Acknowledgment:** The authors extend their thanks and appreciation to the Faculty of Science, Beni Suf University for its financial and logistical support during the completion of this work.

**References:**

- Abd El-Salam, H. M., Kamal, E. H. M. & Ibrahim, M. S. Synthesis and Characterization of Chitosan-Grafted-Poly(2-Hydroxyaniline) Microstructures for Water Decontamination. *J. Polym. Environ.* **25**, 973–982 (2017).
- Ghrab, S. *et al.* Removal of Iron from Groundwater onto Raw Clay (Ka-II). 309–311 (2019) doi:10.1007/978-3-030-72543-3\_69.
- Zhang, X. *et al.* Advanced Modified Polyacrylonitrile Membrane with Enhanced Adsorption Property for Heavy Metal Ions. *Sci. Rep.* **8**, 1–9 (2018).
- Hebeish, A. A., Ramadan, M. A., Montaser, A. S. & Farag, A. M. Preparation, characterization and antibacterial activity of chitosan-g-poly acrylonitrile/silver nanocomposite. *Int. J. Biol. Macromol.* **68**, 178–184 (2014).
- Kim, K. *et al.* Physicochemical properties of surface charge-modified ZnO nanoparticles with different particle sizes. *Int. J. Nanomedicine* **9**, 41–56 (2014).
- Le, A. T., Pung, S. Y., Sreekantan, S., Matsuda, A. & Huynh, D. P. Mechanisms of removal of heavy metal ions by ZnO particles. *Heliyon* **5**, e01440 (2019).

## **Integrated approach for sustainable utilization of groundwater resources in the Western Desert**

Khalid Zahran\*<sup>1</sup>, Mohamed Sultan<sup>2</sup>, Abdullah Ibrahim<sup>2</sup>, Karim Abdelmohsen<sup>3</sup>, Mustafa Emil<sup>2</sup> and Hamada Saadalla<sup>1</sup>

<sup>1</sup> National Research Institute of Astronomy and Geophysics, Egypt.

<sup>2</sup> Department of Geological and Environmental Sciences, Western Michigan University, Kalamazoo, MI 49008, USA.

<sup>3</sup> School of Sustainability, Arizona State University, Tempe, AZ 82581, USA.

### **ABSTRACT:**

Previous studies indicated that Lake Nasser is the primary source of recent recharge to the Dakhla subbasin and that rapid turbulent groundwater flow occurs along an extensive network of faults and karst topography. The network provides preferred pathways for groundwater flow that carries the infiltrated waters tens to hundreds of km across the Western Desert. We are conducting the following research activities to identify the distribution of preferred pathways: (1) delineate the regions across which preferred groundwater flow from Lake Nasser occurs using GRACE and GRACE-FO, (2) conduct structural analysis over the GRACE-defined preferred groundwater flow regions, using multi-spectral satellite observations (Sentinel-2, and field observations to generate connectivity and permeability maps from which the preferred pathways are being identified , (3) compare the temporal and spatial variations in groundwater levels in monitoring wells proximal to, or distant from, the structurally-defined preferred pathways in search of hydrologic evidence supporting the presence of the structurally-identified preferred pathways , (4) collect groundwater samples from pumping wells proximal to, or distant from, the structurally-defined preferred pathways in search of geochemical (solute chemistry) and isotopic evidence in support of the structurally-identified preferred pathways. Primary results shows that NS-EW fault system intersections perform a preferred pathways for groundwater flow. The 3-year project (2024-2027) is funded by the Science Technology & Innovation Funding Authority (STDF) and the US–Egypt Science and Technology Joint Fund from the US Agency for International Development administered by the National Academy of Sciences (NAS).

**Keywords:** Ground water, Nubian Aquifer.

## METHODOLOGY:

Until recently, it was believed that the Dakhla subbasin does not receive any recent recharge. In other words, it is not a sustainable water resource. We recently published two major articles, one in *Science of the Total Environment* [1] and another in *Earth Science Reviews* [2] that refute this concept. In the current research we proved that the Dakhla subbasin is not made entirely of fossil water, it is receiving recent recharge, and Lake Nasser is the main source of recent recharge. These findings were based on observations extracted from the Gravity satellite (Gravity Recovery and Climate Experiment; GRACE) data that measures temporal mass variations over areas of interest. These mass variations, hereafter referred to as GRACE terrestrial water storage (GRACETWS) are commonly attributed to changes in water content in one or more of the water compartments (surface water, groundwater, soil moisture). In arid regions, such as the Dakhla subbasin, the variations in GRACETWS values is mainly related to the temporal changes in groundwater storage with negligible contribution from the other water compartments. Examination of seasonal GRACETWS measurements over the Dakhla subbasin and Lake Nasser for years 2006 to 2015 (Fig. 1).

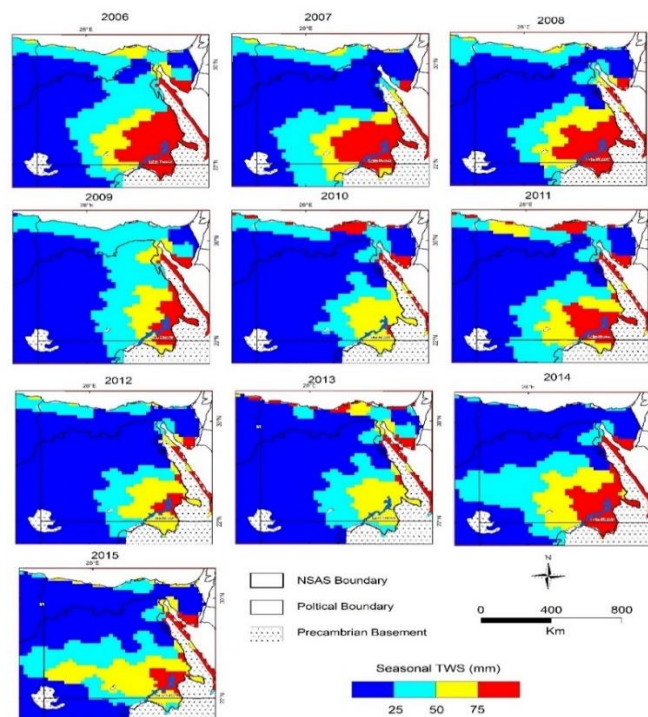


Figure 1. SD<sub>TWS</sub> image over the Dakhla subbasin for 2006 through 2015 centered over Lake Nasser.

To accomplish the main objective of the current study, the following tasks have been considered:

- (1) Delineate the regions where preferred groundwater flow from Lake Nasser occurs using GRACE and GRACE-FO data.



- (2) Conduct structural analysis over GRACE-defined preferred groundwater flow regions to generate connectivity and permeability maps from which the preferred pathways will be identified using high-resolution satellite data (30 cm).
- (3) Verify the identified preferred pathways using hydrological data where the surface water levels in Lake Nasser are compared with the groundwater levels and the distribution of faults and damage zones.

**RESULTS/FINDINGD:** Data of GRACE and GRACE-FO over Lake Nasser Region shows a large increase in seasonal TWS correlates with the distribution of faults/karst, namely along E-W trending Kalabsha and Sayal fault systems and their extension to the west, Fig. 2. The Figure shows high propagation of water mass along an E-W trending Kalabsha and Sayal fault system its extension to the west (polygon outlined by green and black dashed line). Conduct structural analysis over GRACE-defined preferred groundwater flow regions using high-resolution satellite data (30 cm) was able to generate connectivity and permeability maps from which the preferred pathways have been identified. The mapped faults and fracture together with topological network were able explain the preferred groundwater flow mechanism. Comparison hydrological well data to the surface water levels in Lake Nasser and the groundwater levels and the distribution of faults and damage zones, shows that rise in Lake Nasser's surface water level is accompanied by increased groundwater levels in the wells, indicating a groundwater flow from the Lake towards the surrounding areas. On the other hand, well nearest to the fault damage zone shows higher water level, even they are and farthest from the Lake.

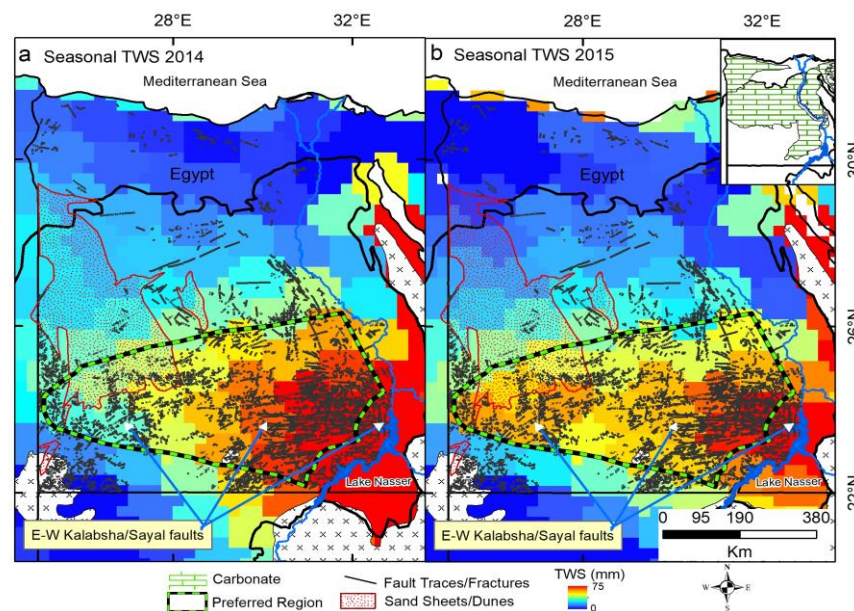


Fig. 2 Comparison of the distribution of areas witnessing large increase in  $GRACE_{TWS}$  (seasonal increase in TWS) with the distribution of faults/karst.



**CONCLUSIONS AND RECOMENDATIONS:** This research aims to develop scenarios for sustainable utilization of groundwater resources in the Western Desert by identify preferred pathways for groundwater flow from Lake Nasser (source) into the Dakhla subbasin. Data of GRACE and GRACE-FO over Lake Nasser Region shows a large increase in seasonal TWS correlates with the distribution of faults/karst. structural analysis using high-resolution satellite data was able to generate connectivity and permeability maps from which the preferred pathways have been identified. As a continuation for this research, it is recommended to Verify the identified preferred pathways using geochemical and isotopic data and to conduct geophysical survey to verify subsurface structures (i.e., faults) and the presence of water within them.

**ACKNOWLEDGMENT** This research is funded by the Science Technology & Innovation Funding Authority (STDF) and the US–Egypt Science and Technology Joint Fund from the US Agency for International Development administered by the National Academy of Sciences (NAS).

[Project Number = C21-88].

## **REFERENCES**

- [1] Abdelmohsen, K., Sultan, M., Ahmed, M., Save, H., Elkaliouby, B., Emil, M., Yan, E., Abotalib, A., Krishnamurthy, R.V., AbdeImalik, K., Earth and Planetary Science Let., 2019, Response of deep aquifers to climate variability, Science of the Total Environment, <https://doi.org/10.1016/j.scitotenv.2019.04.316>
- [2] Abdelmohsen, K., Sultan, M., Save, H., Abotalib, A., Yan, E. 2020, What can the GRACE seasonal cycle tell us about lake-aquifer interactions? Earth Science Reviews, <https://doi.org/10.1016/j.earscirev.2020.10339>

## Flood Risk Assessment in Wadi Ghwieba Under climate Change Impacts

Azza Ewis\*<sup>1</sup>, Radwa Bakr<sup>1</sup>, Khaled Gaber<sup>1</sup>, Doaa Amin<sup>1</sup> and Elsayed M. Abu El Ella<sup>2</sup>

<sup>1</sup> Water Resources Research Institute, National Water Research Center, Cairo, Egypt

<sup>2</sup> Geology Department, Faculty of Science, Assiut University, Assiut71516, Egypt

[Azza.Ewis@yahoo.com](mailto:Azza.Ewis@yahoo.com), [rm29\\_9@yahoo.com](mailto:rm29_9@yahoo.com), [khaledgaber890@gmail.com](mailto:khaledgaber890@gmail.com), [doaa\\_amin@nwrc.gov.eg](mailto:doaa_amin@nwrc.gov.eg)  
[elsayed.abdelaziz@science.au.edu.eg](mailto:elsayed.abdelaziz@science.au.edu.eg), [abuelellaem@gmail.com](mailto:abuelellaem@gmail.com)

### ABSTRACT

The Northwest Gulf of Suez region presents a great potential for development programs. especially at wadi Ghoweiba. The water resources in this area play an increasing important role in providing a source of potable water for the economic zone and construction of new settlements. Moreover, the area is embedded within a network of active watersheds, which are subjected to recurrent flash flooding. These flash floods damage the infrastructure industrial zones and a great economic loss. To ensure the sustainable development in this region an assessment for water resources management, and vulnerability of the watersheds located in this region should be carried out under climate change impacts to get optimum utilization of every possible drop of water. In this research different Global climate models (GCMs) namely (IPSL-IPSL-CM5A-MR, MOHC-HadGEM2-ES, MPI-M-MPI-ESM-LR, NCC-NorESM1-M and CNRM-CERFACS-CNRM-CM5) were used to represent recent climate over the domain of the study area up to 2100 after downscaled by Regional Climate model (RCA4) with resolution of 0.11° (10km) for all (GCMs). Direct runoff hydrograph for Mid/Far-Century due to two scenarios (RCP4.5, RCP8.5) was investigated for all climate models. The results for all Climate models showed that the direct Runoff hydrograph for wadi Ghoweiba increase due to scenarios RCP4.5 and RCP 8.5 for Mid/ Far-century periods compared with historical period. Also, the hazard degree maps were investigated which showed that the existing infrastructure at the outlet of Wadi Ghwieba will be susceptible to flood hazards in various future climate change scenarios. These maps help in the water resources management plans in the study area.

**Keywords** flood hazard maps, GCMs, Wadi Ghoweiba,

## METHODOLOGY

Studying the impact of climate change on flash floods involves a specific methodology to understand how changing climatic patterns affect the frequency, intensity, and spatial distribution of these rapid-onset floods [1, 2]. Here's a structured approach to conducting such a study:

### Data Collection:

- **Meteorological Data:** Global Precipitation Measurement (GPM) data
- **Climate Projections:** Utilize different GCMs to acquire future projections of rainfall patterns, and extreme weather events under different emission scenarios (e.g., RCP 4.5, RCP 8.5) [3, 4, 5, and 6].
- **Statistical analysis** is carried out for daily satellite rainfall data (GPM) from (2000-2022) to predict the rainfall values for return period 2, 5, 10, 25,30, 50, 100 and 200-year using Hyfran Plus statistical analysis program.
- **Bias Correction** was conducted for climate rainfall data by applying Delta change method. The method is based on the use of a change factor, the ratio between a mean value in the future and historical data. then this factor is applied to the observed time series to transform this series set into time series that is representative of the future climate.

### 2. Hydrological Modeling:

- **Model Selection:** Watershed Modeling Simulation (WMS) model was selected for Runoff hydrograph estimation until 2100.

### 3. Topographical and Geospatial Analysis:

- **Digital Elevation Models (DEMs):** Acquire high-resolution DEMs to delineate watershed boundaries, analyze terrain characteristics, and model flood inundation extents.
- **GIS Analysis:** Use Geographic Information Systems (GIS) to integrate meteorological, hydrological, and topographical data for spatial analysis and mapping of flash flood hazard zones.

### 4. Risk Assessment:

- **Quantitative Risk Analysis:** Evaluate flash flood risks by combining hazard maps with vulnerability assessments to prioritize areas for mitigation and adaptation strategies.
- **Risk Mapping:** Produce maps depicting different levels of flash flood risk based on hazard exposure and vulnerability indicators.

The Delta flood hazard map for Wadi Ghweba indicates the location of various hazard zones. These zones, classified as high, medium, and low, are defined based on the level of danger they pose to the average person due to floodwater depths.

## 5. Climate Change Impact Analysis:

- **Impact Scenarios:** Analyze how climate change influences flash flood characteristics (e.g., magnitude, frequency, seasonality) using climate projections and hydrological modeling results.

### Results and Discussion

This research focuses on studying the impact of climate change on flash flood in wadi Ghoweiba due to Mid/ Far century for different scenarios.

- **Mid-century for RCP 4.5 and RCP 8.5 Scenarios**

The results of the hydrologic analysis for Mid-Century period from (2041-2070) due to two scenarios RCP4.5 and RCP8.5 showed that the maximum runoff occurs from Wadi Ghoweiba derived from (NorESM1-M) model due to RCP 4.5 and RCP8.5 compared with peak discharge for historical period from (2000-2022).

On the other hand, the lowest value of runoff developed from (IPSL) model due to RCP4.5 and from (MOHC) model due to RCP8.5 compared with historical Runoff.

Overall, All Climate models results showed that Runoff values for wadi Ghoweiba increase due to RCP4.5 and RCP 8.5 for Mid- century period as shown in figure (1).

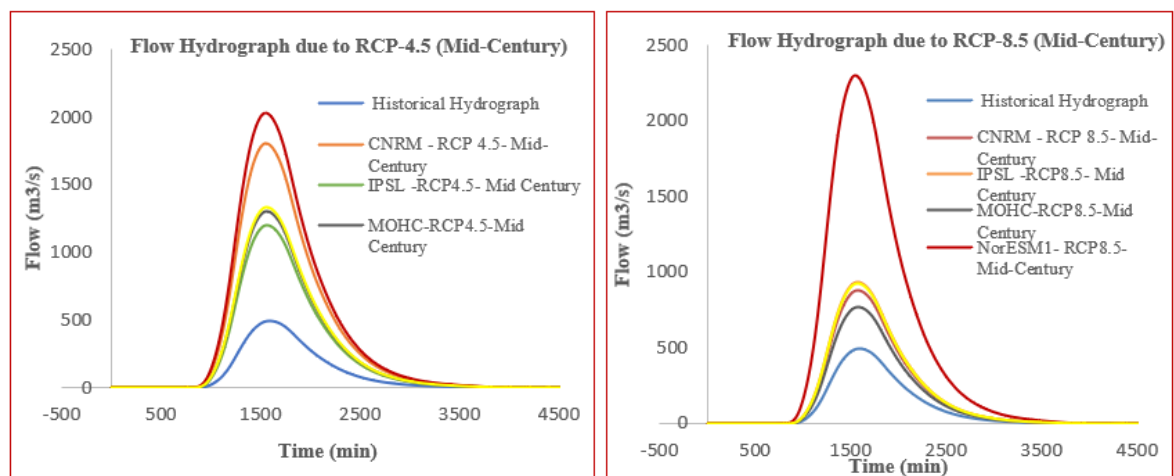


Figure 1. Runoff Hydrographs of wadi Ghoweiba due to RCP 4.5 and RCP 8.5 (Mid-Century)

- **Far-century for RCP 4.5 and RCP 8.5 Scenarios**

The results of the hydrologic analysis for far-Century period from (2071-2100) due to two scenarios RCP4.5 and RCP8.5 showed that the maximum runoff occurs from Wadi Ghoweiba derived from (MOHC) model due to RCP 4.5 and max discharge due to (NorESM1-M) model for RCP8.5 compared with historical period from (2000-2023).

On the other hand, the lowest value of runoff developed from (IPSL) and CNRM models due to RCP4.5 and from (CNRM) model due to RCP8.5 compared with historical Runoff.

Overall, All Climate models results showed that Runoff values for wadi Ghoweiba increase due to RCP4.5 and RCP 8.5 for Far- century period.

**Flood hazard mapping.**

The hazard maps clearly indicate that the existing infrastructure at the outlet of Wadi Ghowiba exposed to flood hazards in all future climate change scenarios as shown in Figure (2) as example.

Therefore, it is crucial to propose mitigation works that aim to minimize potential damage to the infrastructure and investments.

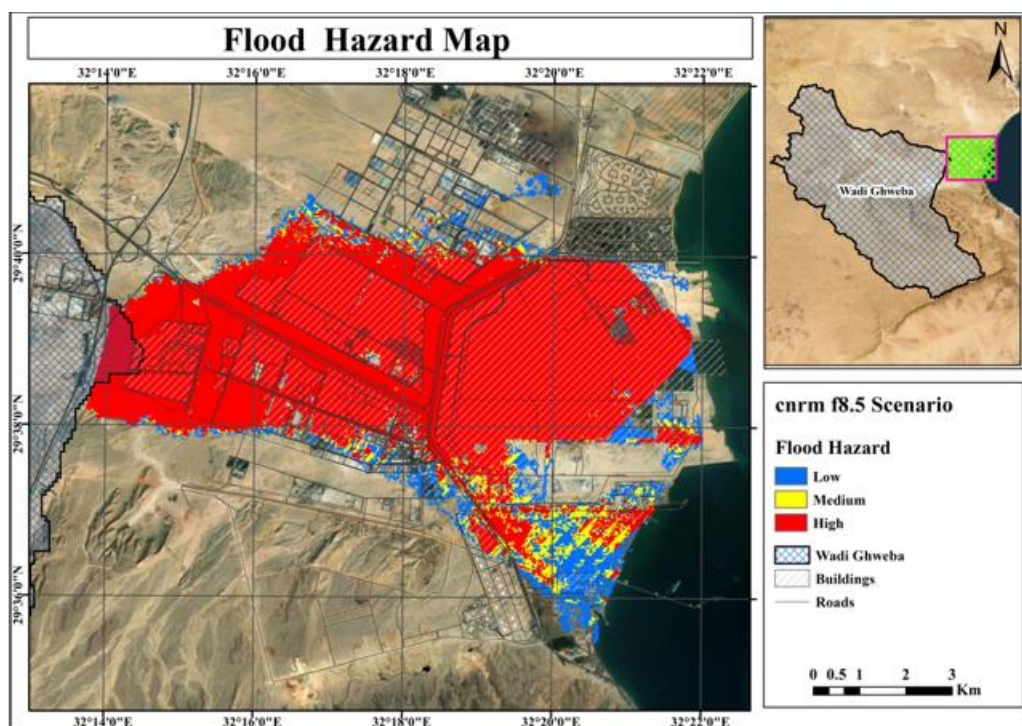


Figure (2): Flood Hazard classification for CNRM F 8.5 Scenario

## **CONCLUSIONS**

- This research has focused on investigation different sources of (GCMs) models in comparison with the satellite data (GPM).
- Bias correction was performed to estimate future corrected rainfall data (projected) for Mid/Far-century under two different scenarios (RCP4.5 and RCP8.5) in wadi Ghoweiba to Investigate the impact of climate change on rainfall –runoff hydrograph up to 2100.
- Finally, investigate the locations that may be most affected and produce more reliable flood hazard maps which will help in the water resources management plans in the study area.

## **References**

- [1] IPCC. (2007). IPCC Fourth Assessment Report: Climate Change, 2007. Contribution of Working Group I to the Fourth Assessment Report of the Intergovernmental Panel on Climate Change. D. Q. S. Solomon, M. Manning, Z. Chen, M. Marquis, K.B. Averyt, M. Tignor and H.L. Miller. Cambridge, United Kingdom and New York, NY, USA: IPCC.
- [2] Prusty, R.M., A. Das, and K.C. Patra, Climate Change Impact Assessment under CORDEX South-Asia RCM Scenarios on Water Resources of the Brahmani and Baitarini River Basin, India. 2018.
- [3] Hansen, J.W., Challinor, A., Ines, A., Wheeler, T., Moron, V., 2006. Translating climate forecasts into agricultural terms: advances and challenges. *Clim. Res.* 33, 27–41.
- [4] Sharma, D., Das Gupta, A., Babel, M.S., 2007. Spatial disaggregation of bias corrected GCM precipitation for improved hydrologic simulation: ping river basin, Thailand. *Hydrol. Earth Syst. Sci.* 11 (4), 1373–1390.
- [5] Chen, J., Brissette, F.P., Leconte, R., 2011. Uncertainty of downscaling method in quantifying the impact of climate change on hydrology. *J. Hydrol.* 401 (3–4), 190–202.
- [6] Salvi, K., Kannan, S., Ghosh, S., 2013. High resolution multi-site daily rainfall projections in India with statistical downscaling for climate change impact assessment. *J. Geophys. Res. Atmos.* 118, 3557–3578.



## Setting up a groundwater model with land subsidence simulation using Python

Hend Samir Atta<sup>1</sup>, Amany Tammam Eid <sup>2</sup>, Enas Ahmed Elemy <sup>3</sup>, Mamdouh Al-Sittawy<sup>4</sup>, Eman Ragab Nofal<sup>5</sup>, Suhyb Salama<sup>6</sup> and Mostafa Gomaa Daoud <sup>7</sup>

<sup>1\*</sup> Hend Samir Atta, Research Institute for Groundwater (RIGW), National Water Research Centre (NWRC), Egypt. (E-mail: [hendatta09@yahoo.com](mailto:hendatta09@yahoo.com))

<sup>2-5</sup> Research Institute for Groundwater (RIGW), National Water Research Centre (NWRC), Egypt.

<sup>6</sup> Suhyb Salama, Faculty of Geo-Information Science and Earth Observation, University of Twente, Netherland. (E-mail: [s.salama@utwente.nl](mailto:s.salama@utwente.nl))

<sup>7</sup> Mostafa Gomaa Daoud, Faculty of Geo-Information Science and Earth Observation, University of Twente, Netherland. (E-mail: [m.g.m.daoud@utwente.nl](mailto:m.g.m.daoud@utwente.nl))

### ABSTRACT

The objective of the research is to investigate the effect of groundwater abstraction on land subsidence at Rasheed, Nile Delta, Egypt. The findings reveal a notable impact of groundwater abstraction on water levels within the study area, indicating a reduction of more than half a meter through the period from 1990 to 2019. The interaction between groundwater abstraction and rainfall recharge has led to temporal fluctuations in land subsidence. The observed vertical displacement ranges from +5.1 to -9.9 mm through the period from 1990 to 2019, underscoring the dynamic nature of subsidence processes. Notably, storage and hydraulic parameters These findings underscore the importance of sustainable water management practices to mitigate the adverse impacts of groundwater abstraction on land subsidence. In addition, this tool can be utilized by stakeholders to develop effective strategies for preserving the region's infrastructure and environment. The top layer plays a pivotal role in discerning the patterns of subsidence behavior.

**Keywords: Groundwater, Land subsidence, MODFLOW, Python**

### INTRODUCTION

Vertical ground movement is caused by natural factors and human activities such as groundwater extraction. These effects are more pronounced in lowlands, like the Nile Delta in Egypt.

According to [1], an alternative method for developing models using Python scripting. Plotting, array manipulation, optimization, and data analysis are just a few of the many tools that Python offers to make the process of developing a model easier. In this study, the authors developed FloPy package to build model input files, execute the model, and read and plot simulation results for models based on MODFLOW. Using Python in conjunction with FloPy and the available scientific packages makes

these tasks easier. [3] Applied MODFLOW 6 code with presenting the standard and new capacities of MODFLOW 6 in transient simulation of the interaction between the surface water / groundwater of Sardon catchment in Spain, also apply a novel cascade-routing and re-inflation (CRR) concept to improve surface–unsaturated-zone interactions and also surface-water/groundwater interactions. There have been few researchers that focused on the using of FloPy, a Python package, for setting up MODFLOW-based model and land subsidence resulting from groundwater pumping. Also, there is no specific research presented this issue by using MODFLOW 6 code and Python environment to model groundwater aquifers especially in the coastal area of Egypt.

So, this research employs MODFLOW 6 code and Python environment to model groundwater aquifers and its relation to land subsidence in Rasheed area, north of Egypt's Nile Delta as shown in Figure (1). Given the land subsidence issue in the Nile Delta, particularly in the Rashid area, this study focuses on simulating its relation to groundwater extraction. A MODFLOW 6 model is constructed using both in-situ and remote sensing data to account for groundwater pumping's impact on land subsidence.

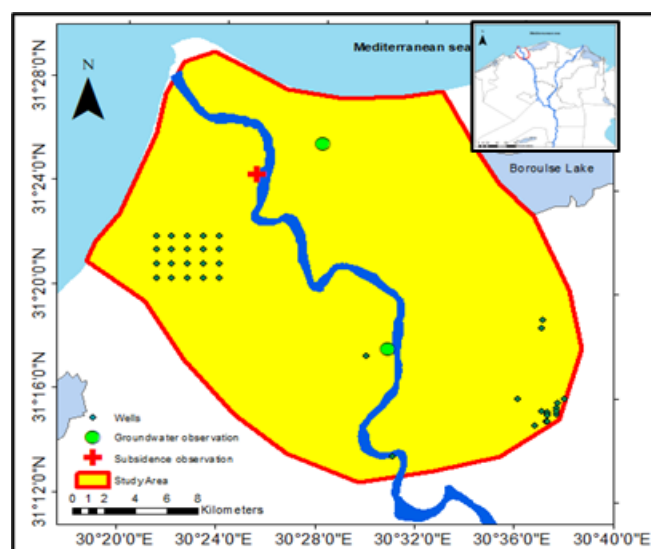


**Figure (1): Location of study area of Rasheed**

## **METHODOLOGY**

FloPy, a Python package, is utilized for setting up MODFLOW-based model and land subsidence to tackle groundwater challenges [1,2]. To attain the main objective the following methodology was done:

First, the grid was identified as a quadtree grid, the model layers, the model boundary and the main hydrogeological features were defined using python code. After that compaction and land subsidence were defined using CSUB package that includes the simulation of coarse-grained

aquifer materials and no- delay and delay interbeds and the effective stress from the previous time step used to calculate specific storage values. Also, initial elastic coarse-grained material specific storage and initial porosity were identified and given an average number. Then packages of MODFLOW were defined using python code such as wells, river and observation wells. Compaction and land subsidence packages were defined. At the end, the model was run. The results given for the total subsidence at the observation point equals to the sum of subsidence from all layers.

## **RESULTS**

The investigation of Rasheed's study area involved the utilization of a groundwater model implemented with MODFLOW 6 code and the FloPy & Pandas Python packages. The findings reveal the following:

- ✓ A notable impact of groundwater abstraction on water levels within the study area, indicating a reduction of more than half a meter as shown in Figure (2).
- ✓ An observation well situated to the north of the study area demonstrated a decline in water levels from 1.1 m above mean sea level in 1990 to approximately 0.52 m in 2019.
- ✓ The interaction between groundwater abstraction and rainfall recharge has led to temporal fluctuations in land subsidence.
- ✓ The observed vertical displacement ranges from +5.1 to -9.9 mm, underscoring the dynamic nature of subsidence processes. Notably, the storage parameters and the hydraulic parameters of the top layer play a pivotal role in discerning the patterns of subsidence behaviour.

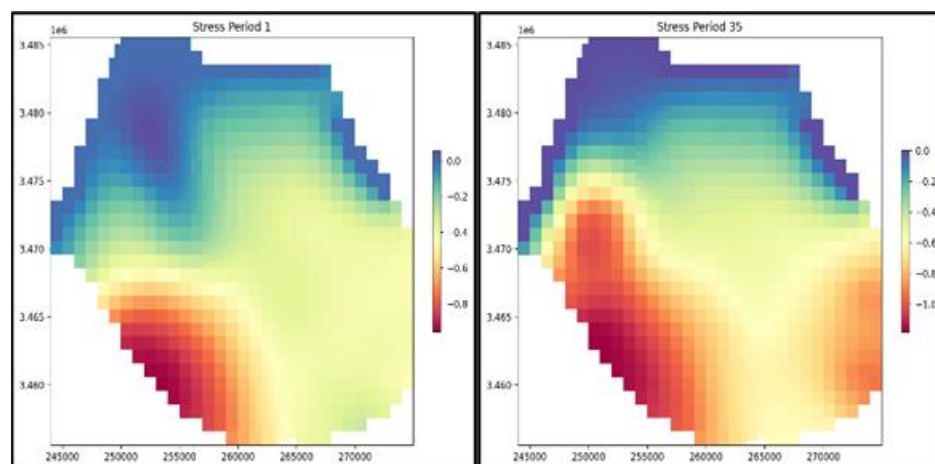


**Figure (2): Groundwater levels in 1990 (First model stress period 1) and in 2023 (Last stress period 35)**

## **CONCLUSIONS & RECOMENDATIONS**

The integration of advanced modelling techniques facilitated a comprehensive understanding of the complex interplay between groundwater dynamics and land subsidence in the Rasheed study area. Land subsidence is affected by hydraulic parameters of the top layer mainly.

These findings underscore the critical importance of sustainable water management practices to mitigate the adverse impacts of groundwater abstraction on land subsidence. In addition, policymakers and stakeholders can utilize these insights to develop effective strategies for preserving the region's infrastructure and environment.

## **ACKNOWLEDGMENT**

- ✓ Sincere thanks to NUFFIC for funding EO4C training project where the skills needed to conduct the work were acquired.
- ✓ Heartfelt gratitude to the University of Twente for providing this opportunity of training, especially to Dr. Suhyb Salama and Dr. Mostafa Gomaa.
- ✓ Sincere thanks to Dr. Manal Abdel Monem, Director of RIGW, and Dr. Eman Nofal, Deputy Head of RIGW, for their invaluable contributions.

## **REFERENCES**

- [1] **Bakker, M., Post, V., Langevin, C. D., Hughes, J. D., White, J. T., Starn, J. J., & Fienen, M. N.** 'Scripting MODFLOW model development using Python and FloPy', *Groundwater*, 2016, 54, (5), pp. 733-739.
- [2] **Befus, K. M., Barnard, P. L., Hoover, D. J., Finzi Hart, J. A., & Voss, C. I.** 'Increasing threat of coastal groundwater hazards from sea-level rise in California', *Nature Climate Change*, **2020**,10, (10), pp. 946-952.
- [3] **Daoud, Mostafa Gomaa, Maciek W. Lubczynski, Vekerdy Zoltan, and Alain Pascal Francés.** 'Application of a Novel Cascade-Routing and Reinfiltration Concept with a Voronoi Unstructured Grid in MODFLOW 6, for an Assessment of Surface-Water/Groundwater Interactions in a Hard-Rock Catchment (Sardon, Spain), *Hydrogeology Journal*, 2022, pp. 1–27.

## Responsive Aswan High Dam Operation Simulation Model: Dynamic Reservoir System Configuration

Rameen Abd El-Hady<sup>1\*</sup>, Sarah Mohamed Zoriek<sup>2</sup>, Hussam Fahmy<sup>3</sup>, Aref Gharieb<sup>4</sup>

<sup>1,3</sup>National Water Research Center, MWRI, EGYPT

(E-mail: [rameens@hotmail.com](mailto:rameens@hotmail.com), [hussam.fahmy@yahoo.com](mailto:hussam.fahmy@yahoo.com))

<sup>2,4</sup>Nile Water Sector, MWRI, EGYPT

(E-mail: [eng\\_saramohmed@yahoo.com](mailto:eng_saramohmed@yahoo.com), [arefgharib@yahoo.com](mailto:arefgharib@yahoo.com))

### ABSTRACT

Since the commence of GERD construction, the Aswan High Dam (AHD) reservoir operators are facing high uncertainty in forecasting inflow to Lake Nasser. Consequently, they have high difficulty in predicting the downstream impact of the operation decision they make on daily bases. The GERD (over year storage) releases are unknown as well as their effect on filling and emptying of Sudanese dams (seasonal storage). Moreover, climate change, currently ponding the Nile Basin and its sub catchment, make it impossible to forecast sub catchments natural runoff for long lead time.

None of the existing Lake Nasser simulation can support the change of the lake physical configuration or work in responsive on-line mode to simulate the operators' alternative combination of decisions variables. Typically, the AHD operators evaluate their alternative combination of decisions variables by the system state variables at the end of the simulation period (hydrologic year or several months). In this manuscript a STELLA model is constructed mimicking a detailed representation of the system. The aim of such modelling effort is to provide early evaluation of the system performance to MWRI's AHD operation committee.

**Keywords:** AHD, Dynamic modelling, GERD, Lake Nasser, STELLA

### INTRODUCTION

The past years of GERD filling based on a unilateral decision, forced the AHD operators to reconsider the long-settled operation policies. Lake Nasser storage zones were redefined on yearly bases and the indicative release schedule was subject to several modifications during the same hydrologic year (starts 1st of August and ends 31st of July). An increased flexible (dynamic) reservoir outlet capacity was added. For example, Toska spillway was operated after August 1st with width ranging from 0 to 690 meters and a saddle dam was commissioned to increase Toska depression storage capacity. In addition to that, Toska pumping station was put to operation.

Due to long experience and intuitive skills of AHD operators, they managed to make Egypt avoid serious shortages during filling years of GERD (2020-2023), by using flood management storage zone for water conservation. However, Egypt was on the verge to declare flood emergency during high flood years or when Ethiopian dam did not store the expected water volumes.

El Dardiry and Hossain (2021) [1] used a simplified dynamic programming models integrated, with satellite observations to reassess the operation of the AHD under the impacts of the GERD. This reassessment during the GERD's filling and operation phases followed a modelling blueprint that integrates satellite data into hydrological and reservoir models. The adaptation of AHD operations to GERD's phases is then evaluated by developing various scenarios considering factors such as the GERD filling period, initial storage level at AHD, natural flow variability, and downstream supply stress levels.

Fahmy (2001) [2] insisted on the importance of modification and re-calibration of the simulation model of Lake Nasser. They modified and calibrated the 1981 model using few parameters and adjustments of the mathematical formulation.

A comprehensive picture of the response of Lake Nasser under selected management alternatives is given in [3]. The reservoir target levels for each month specified by the operating policy indicated upper and lower operating rules to prevent extremely high or low values of water level in the reservoir.

Therefore, there is appalling need for a flexible reliable computational tool that can respond to physical changes to lake outlets and varying release/spilling schedules set by the AHD operators. The intended tool should be able to produce promptly state variables such as Lake Nasser ending storage/level, Toshka Depressing ending storage, or any other variable desired by the operators.

## **METHODOLOGY**

The study employs a computational approach using a STELLA (Systems Thinking, Experimental Learning Laboratory with Animation) model to simulate the operational performance of the Aswan High Dam (AHD).

### **Mass balance of Lake Nasser:**

The general mass balance equation for the lake is:

$$S_{t+1} = S_t + I_t - O_t - \text{Evap}(SA_{t+1}, SA_t) - O_{\text{Toshkaps.}} - O_{\text{Toshkadepp.}} \quad \text{Eq.(1)}$$

Simulation time increment “t” is one day; evaporation losses were calculated from fixed monthly evaporation rates. The hydrological boundaries of RAHDOSM extend up to Toshka pumping station (outlet) and Toshka depression (outlet and mass balance).



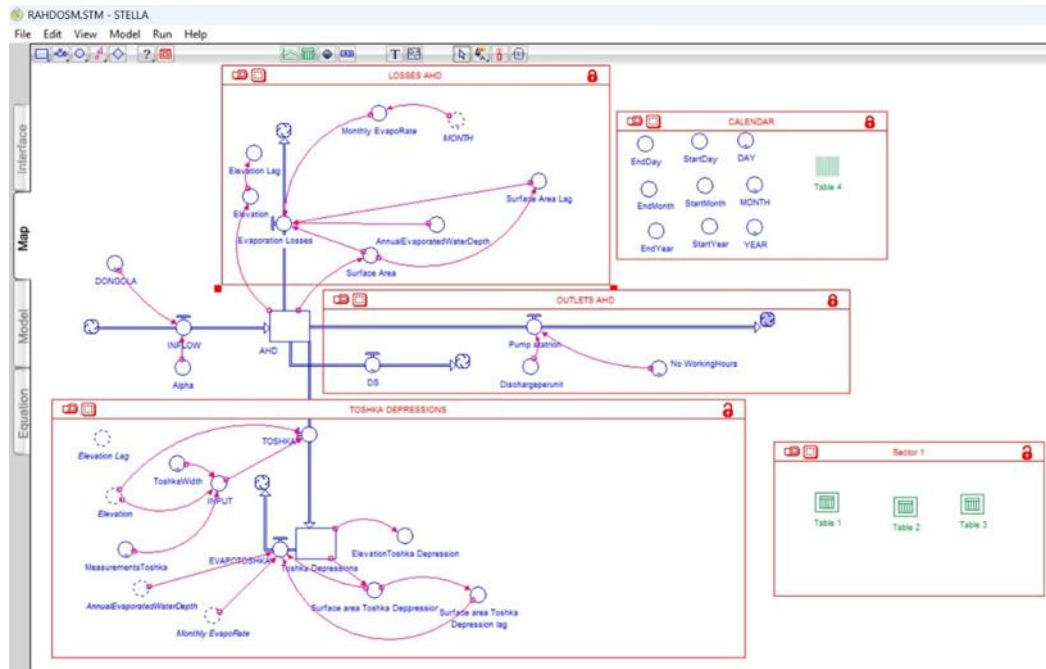


Figure 1: RAHDOSM in STELLA Modelling Environment

### EXPECTED RESULTS

Losses between Dongola and Lake Nasser inlet and annual evaporation rate are used for calibration. Selected period for calibration is from August 2020 to July 2022, while the verification period is from August 2022 to July 2024. The comparison between AHD recorded and simulated elevations is illustrated for both calibration period and verification period by Figure 2 and Figure 3. Also, Nash–Sutcliffe efficiency and the standard error in meters are displayed on the figures.

The optimal values of the calibration parameters are 2.5% and 2400 mm for the losses and annual evaporation rate, respectively.

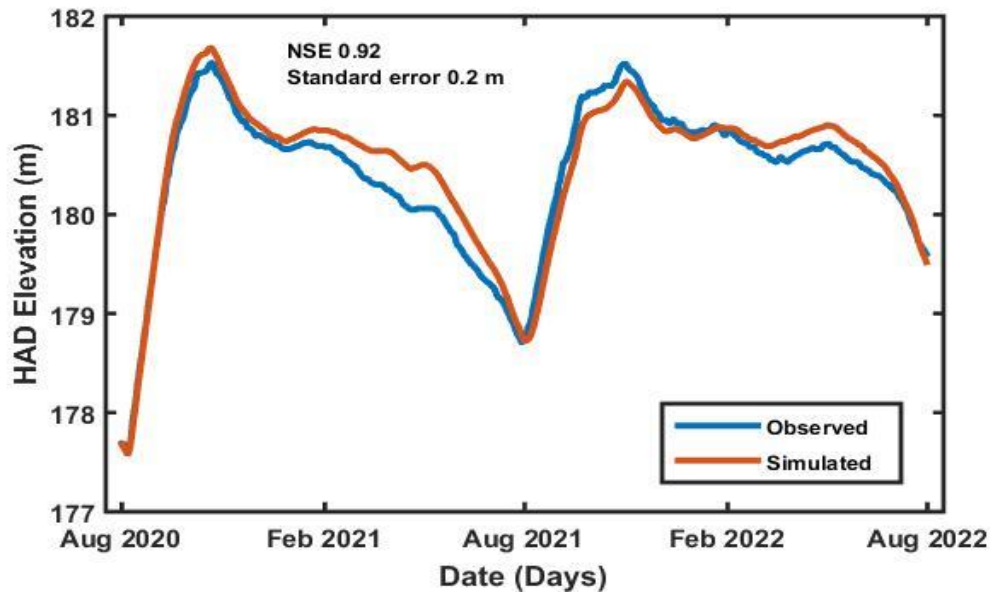


Figure 2: Recorded Vs. Simulated AHD Elevation for Calibration Period

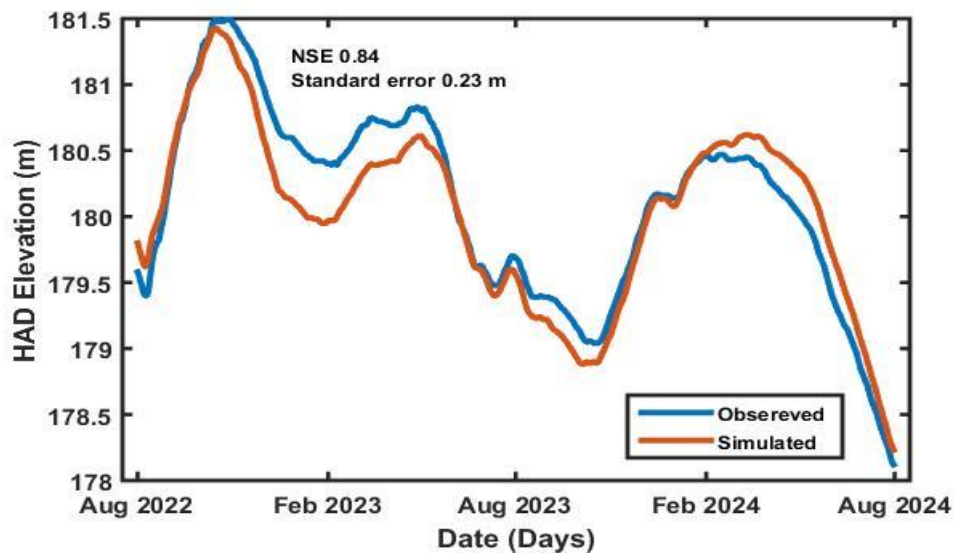


Figure 3: Recorded Vs. Simulated AHD Elevation for Verification Period

## CONCLUSION

The necessity for a flexible reliable computational tool that can respond to physical changes to lake outlets and varying release/spilling schedules set by the AHD operators became evident since the start of GERD construction. In response to that, this paper succeeded in developing a dynamic model of AHD through a sequence of formulation changes and parameters adjustments. It is recommended to add into old models the modifications of Dongola flows, new suggested area-elevation-storage equations and Toshka weir equation.

The developed STELLA model proves to be a valuable computational tool for the AHD operators. It offers a flexible and reliable platform to simulate and evaluate the effects of different decision variables on the system's state variables. This capability allows the operators to make informed decisions by understanding the potential outcomes of various operational strategies. The model's ability to produce timely and accurate predictions enhances the efficiency and effectiveness of water resource management, ensuring better planning and response to both routine operations and unexpected changes.

## **REFERENCES**

- [1] Eldardiry H, Hossain F: 'A blueprint for adapting high Aswan dam operation in Egypt to challenges of filling and operation of the Grand Ethiopian Renaissance dam', J. Hydrol., 2021 Jul 1, 598, pp.125708.
- [2] Fahmy, H.: 'Modification and Re-calibration of the Simulation Model of Lake Nasser', Water Intl., 2001, 26,(1)
- [3] MWRI, 1981. Ministry of Water Resources and Irrigation: 'Hydrological Simulation of Lake Nasser', Technical Report 14, Vol. I & II, Giza, Egypt.

## Combined electrocoagulation/flotation technique and membrane desalination for textile wastewater recycling

Heba Isawi<sup>\*1</sup>, M. A. Sadik<sup>2</sup> and F. A. Nasr<sup>3</sup>

<sup>1</sup> Water Treatment and Desalination, Hydrogeochemistry Dept., Water Resources and Desert Soils Division, Desert Research Center, 1 Mathaf Al Mataria St., Cairo 11753, Egypt..  
(E-mail: hebaessawi@hotmail.com; hebaessawi@drc.gov.eg)

<sup>2</sup> October High Institute for Engineering & Technology, Giza, Egypt.

<sup>3</sup> Water Pollution Research, National Research Centre, P.O. Box 12622, El-Behouth street, Giza, Egypt..

### ABSTRACT

The past several decades have seen a significant increase in environmental pollution as a result of toxins released by mining, manufacturing, agriculture, power generation, and urbanization [1,2]. This has resulted in a serious decline in the quality and availability of water in many regions of the world [3,4]. Because of the chemicals employed in various processes and the regular impurities in fibers, wastewater from the textile industry varies greatly in composition. Diverse dyes are produced globally for use in the textile, cosmetic, paper, leather, pharmaceutical, and food sectors, among others [5]. A novel integrated system that combined electrocoagulation/flotation (ECF) technique with membrane desalination was used for textile wastewater treatment to reduce the environmental pollution of textile wastewater. Two scenarios were examined: the first is ECF followed by membrane desalination; the second is the application of membrane desalination for treatment of raw wastewater. Iron electrodes were used in batch-wise tests to examine the effects of electrolysis time and current intensity on percentage removals. The SiO<sub>2</sub>/PA(TFC) membrane was used to treat raw wastewater and ECF effluents. As the current intensity increased from 50 mA to 600 mA, the color elimination was improved from 94 to 99% and the COD elimination improved from 59.1 to 81.5%. The findings demonstrate the efficacy of ECF in removing color and COD, although the treated wastewater sample's TDS increased from 4200 mg/L to 19400 mg/L (raw textile wastewater sample). The SiO<sub>2</sub>/PA(TFC) membrane displays the salt rejection and water flux reduction of the raw wastewater samples 95%, and 22 (L/m<sup>2</sup>.h). Corresponding results for ECF treated wastewater were 94, 93, 91% and 13, 11.5, and 10 (L/m<sup>2</sup>.h), respectively. The SiO<sub>2</sub>/PA(TFC) membrane displays the reduction of COD from 760 mg O<sub>2</sub>/L (raw) and 310 mg O<sub>2</sub>/L (ECF effluent) to zero%. Also, it proves the capabilities of SiO<sub>2</sub>/PA(TFC) membrane for the removal of TDS, COD and color. This integrated system can provide sustainable source for fresh water supply used for landscape, irrigation, industry and various purposes. Reused in many production areas of the textile dye factory.

**Keywords:** Textile wastewater, Membrane surface modification, Electrocoagulation/flotation, Color removal, Water desalination, SiO<sub>2</sub> nanoparticles.

## METHODOLOGY

Firstly, the electrocoagulation/flotation (ECF) system for water treatment consist of sacrificial electrodes within electrolytic cell are subjected to an electric current, which causes a coagulating agent and gases bubbles to form. An electrocoagulation/flotation reactor have, four Monopolar electrodes were connected to a digital DC power supply (MCH-30 3D; 30 V, 3 A); cell voltage and current are measured digitally and must be regulated in all these experiments.

The electrolysis cell consists of a borosilicate glass beaker with four iron electrodes connected in serial connections (MP-S): In the monopolar electrodes in serial connection, each pair of sacrificial electrodes is internally connected with each other, is electrically similar to a single cell with many electrodes , the same current will flow through all the electrodes. An electrolysis cell and a power supply system make up the lab-scale batch system used in the study. The electrolysis cell consists of a borosilicate glass beaker with four iron electrodes connected in series monopolar electrode design with an effective volume of one liter and 20g of sodium chloride was added as an electrolyte. Iron cathodes and anodes are made of 2.5 cm by 5 cm by 1 mm and 1 cm apart parts of iron that have been dipped in wastewater. The electrodes are connected to the positive and negative terminals of the DC power supply (Range 30V/3A).

Secondly, the SiO<sub>2</sub>/PA(TFC) nano-membrane for water desalination and purification was synthesized in three steps; (1) PS support layer was prepared using phase inversion method onto a 1.8 X 14 sheet of polyester non-woven fabric. (2) The polyamide thin film PA(TF) membranes were created by an interfacial polymerization process that involved an aqueous phase of m-phenylenediamine (MPD) and an organic phase 1,3,5-benzenetricarbonyl trichloride (TMC). Using the same method, SiO<sub>2</sub> NPs were added to TMC in n-hexane solution (0.2 wt/v%) to generate the SiO<sub>2</sub>/PA(TFC) membrane. To help with dispersion, different concentrations of SiO<sub>2</sub> NPs (0.005, 0.01, 0.02, 0.3, and 0.04 wt.%) were dispersed in n-hexane solution with TMC utilizing ultrasonic immersion at room temperature for 30 minutes.

## RESULTS/FINDINGD

Figures (1a-d), which show SEM images and EDX spectra of the SiO<sub>2</sub>/PA(TFC) membrane before and after application performances of the natural wastewater samples from textile dyeing factories, respectively. Before wastewater treatment as shown in Figure (1b), C, O, N, S, and Si were present

with respect to the  $\text{SiO}_2/\text{PA(TFC)}$  membrane. After wastewater treatment, the elemental dye and salt composition was different: C, O, N, S, Si, Na, Fe, Mg, Al, P, Ca, Mn, and Cl Figure (1d). In the newly synthesized  $\text{SiO}_2/\text{PA(TFC)}$  membrane, the signals for Na, Fe, Mg, Al, P, Ca, Mn, and Cl were missing; however, after wastewater treatment, they were visible. For  $\text{SiO}_2/\text{PA(TFC)}$  membrane after treatment shows that the appearance of new peaks related to Na, Fe, Mg, Al, P, Ca, Mn, and Cl because of the existence of fouling layer which comprises metal oxides, salts, and organic precipitate. The  $\text{SiO}_2/\text{PA(TFC)}$  membrane can be recommended to be applicable not only for water treatment from toxic elements (Fe, Al, P, and Mn), organic compounds but also it can be used for water desalination due to it can be used to remove major ions as Na, Cl, Ca, and Mg. The obtained  $\text{SiO}_2/\text{PA(TFC)}$  membrane was synthesized, and no additional contaminations were found in the EDX band, according to these results.  $\text{SiO}_2$  NPs that have been functionalized by the PA(TFC) membrane may be an advantageous material for desalination and water filtration.

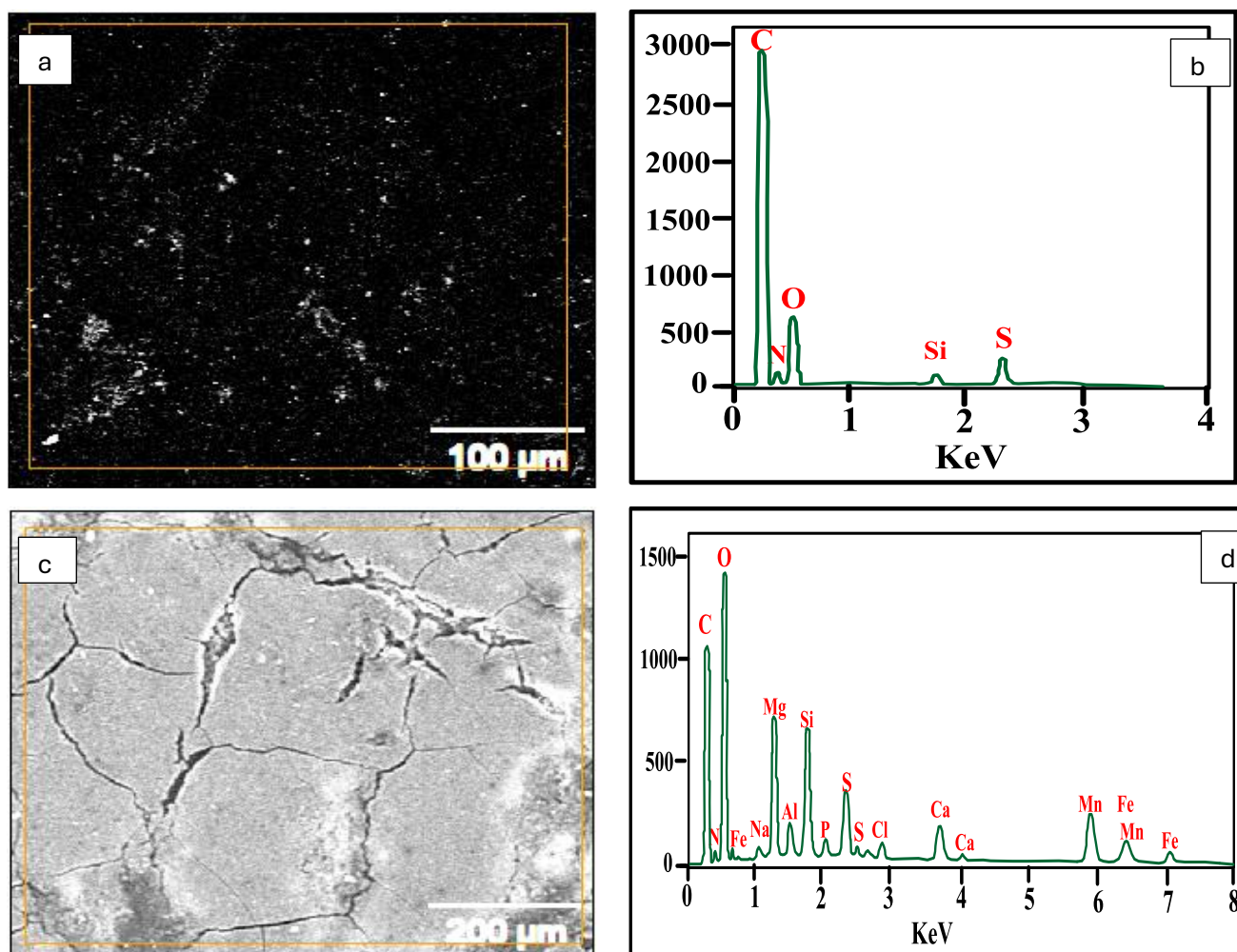


Figure 1. SEM/EDX analysis of before (a and b) and after (c and d) the separation of real treated textile water sample using  $\text{SiO}_2/\text{PA(TFC)}$  membrane.



The two systems offer a promising way for recycling textile wastewater, the treated water can be reused in many production areas of the textile dye house factory. The purpose of this study is to expand and improve the existing facilities for desalination, water treatment, and textile wastewater recycling to be used for landscape, irrigation, industry and various purposes Figure (2).

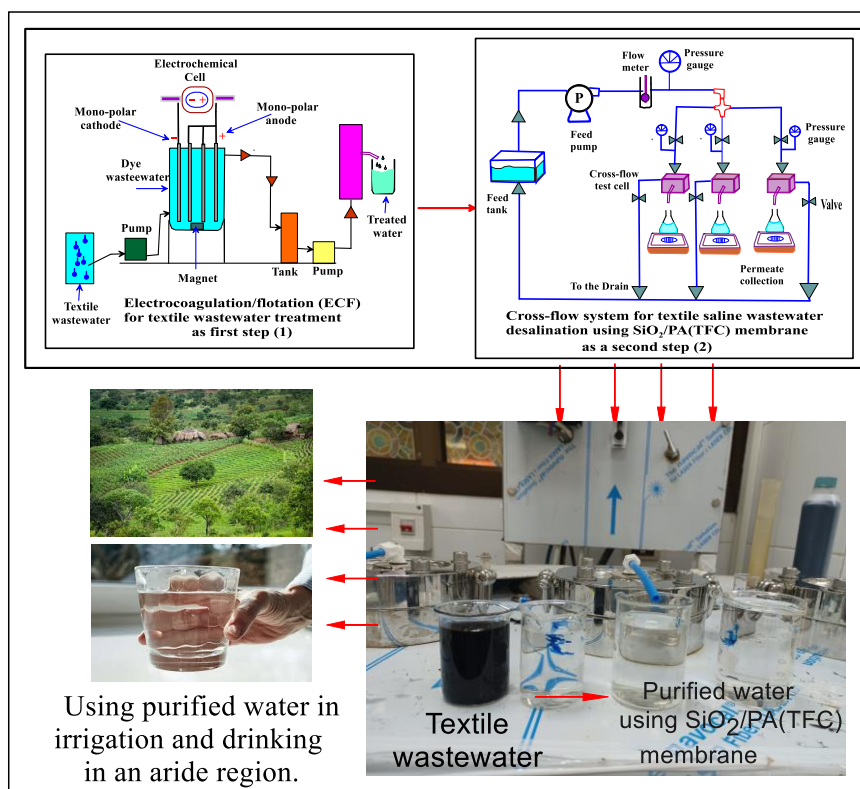


Figure (2) A novel integrated system that combined electrochemical oxidation (EC) system with membrane desalination for reuse the textile wastewater purification.

### Equations

The following equations were used to consider the water flux  $J_v$  ( $L/m^2 \cdot h$ ) and rejection  $R_s$  (%):

$$J_v = \frac{Q}{At} \quad (8)$$

$$R_s (\%) = \left[ \frac{C_f - C_p}{C_f} \right] \times 100 \quad (9)$$

where  $J_v$  ( $L/m^2 \cdot h$ ) is the water flux,  $Q$  is water permeates in liter,  $A$  ( $m^2$ ) is the membrane's surface area,  $t$  (h) is the separation time,  $R_s$  (%) is the salt retention, and  $C_f$  and  $C_p$  are the concentrations of the feed and product water, respectively.

## CONCLUSIONS AND RECOMENDATIONS

The results prove that the ECF technology is effective in color and COD removal however, the TDS increased from 4200 mg/L (raw textile wastewater sample) to 19400 mg/L (treated wastewater). As the current intensity increased from 50 mA to 600 mA, the color removal was increased from 94 to 99% and the COD removal increased from 59.1 to 81%. The TDS value has regrettably increased dramatically after the ECF treatment procedure. The second step is desalination using SiO<sub>2</sub>/PA(TFC) membrane should be applicable. The SiO<sub>2</sub>/PA(TFC) membrane for treating raw wastewater sample displays the salt rejection (95%) and water flux reduction (22 L/m<sup>2</sup>.h). The results of applying the SiO<sub>2</sub>/PA(TFC) membrane for treating ECF effluents were 94, 93, 91% for salt rejection and 13, 11.5, and 10 (L/m<sup>2</sup>.h) for water flux. The SiO<sub>2</sub>/PA(TFC) membrane displays the reducing color intensity (as COD) of the textile wastewater from 490, 140, 250, and 310 to zero% for all samples 1(raw sample), 2, 3 and 4, respectively.

I recommended that the purpose of this study is to expand and improve the existing facilities for desalination, water treatment, and textile wastewater recycling to be used for landscape, irrigation, industry and various purposes. I hope every textile factory can have its own plant to get rid of the discharge pollutant to be recycled again.

## REFERENCES

- [1] Ahmed, M.E., Isawi, H., Morsy, M., Hemida, M.H., Moustafa, H.: “Effective nanomembranes from chitosan/PVA blend decorated graphene oxide with gum rosin and silver nanoparticles for removal of heavy metals and microbes from water resources” *Surf. Interfaces*, 2023, 39 pp102980.
- [2] Bargeman, G., Miguez, O.G., Westerink, J.B., Kate, A.T.: “Chloride retention model for concentrated solutions containing sodium chloride and sodium sulfate based on thermodynamic considerations” *Desalination* 2023, 555, PP 116562.
- [3] Isawi, H.: “Evaluating the performance of different nano-enhanced ultrafiltration membranes for the removal of organic pollutants from wastewater” *Journal of Water Process Engineering* 2019, 31, PP100833.
- [4] Kim, B.-j., Shon, H.K., Han, D.S., Park, H.: “In-situ, desalination-coupled electrolysis with concurrent one-step-synthesis of value-added chemicals” *Desalination*, 2023, 551, 116431.
- [5] Bosela, R., Eissa, M., Shouakar-Stash, O., Ali, M.E.A., Shawky, H.A., Soliman, E.A.: “Potential aquifer mapping for cost-effective groundwater reverse osmosis desalination in arid regions using integration of hydrochemistry, environmental isotopes and GIS techniques” *Groundwater for Sustainable Development*, 2022, 19, PP 100853.

## Physiochemical and Microalgal Investigation of Nile River Water and a Comparison Between Seed Extract of *Moringa Oleifera* and Aluminum Sulfate in removing microalgae and turbidity from water

Mohamed T. Shaaban<sup>1</sup>, Hanaa H. Morsi<sup>2</sup>, Alshaimaa A. Aglan<sup>3\*</sup>

<sup>1,2</sup> Botany and Microbiology Department, Faculty of Science, Menoufia University, Egypt.  
(E-mail: [adel.shakdofa82@gmail.com](mailto:adel.shakdofa82@gmail.com) , [hazemeltabl@yahoo.com](mailto:hazemeltabl@yahoo.com) )

<sup>3\*</sup> Water Central Lab., Al-Menoufia Water and Wastewater Company, Menoufia, Egypt  
(E-mail: [shoshit\\_2@yahoo.com](mailto:shoshit_2@yahoo.com) )

### ABSTRACT

Egypt has the Nile River, which is the main resource of drinking water. Nile water was examined in Bahr Shebin branch (in Shebin El-kom city). The physiochemical parameters determination and algal examination were performed on raw and treated Nile water in Shebin El-kom surface water plant. The results showed various phytoplankton structures belonging to five groups, namely, Bacillariophyta, Chlorophyta, Cyanophyta, Pyrrophyta and Euglenophyta. Bacillariophyta represent the most abundant group during the period of investigation as it accounted 64.9 % of total annual crop. Chlorophyta ranked as the 2<sup>nd</sup> group with 24.3 % of the total annual crop then followed by Cyanophyta with 10.1% of total annual crop. Pyrrophyta and Euglenophyta are the remaining groups they were 0.42 % and 0.11 % of total annual stock, respectively. Coagulation of raw Nile water for algal and turbidity removal was performed with two different coagulants, chemical coagulant (aluminum sulfate) and natural coagulant (*Moringa oleifera* seeds) with and without chlorination. Coagulation with *M. oleifera* seeds extract was very effective than aluminum sulfate, as it reduced turbidity of raw water from 13.8 NTU to 2.2 NTU and the algal removal was 98.7% without chlorination, while with chlorination, it reduced turbidity of raw water from 5.5 NTU to 1.5 NTU and the algal removal was 99.1%. Aluminum sulfate reduced turbidity of raw water from 13.8 NTU to 2.0 NTU and the algal removal was 85.8 % without chlorination, while with chlorination, it reduced turbidity 5.5 NTU to 1.2 NTU and the algal removal was 96.8%.

**Keywords:** Algal Count, Aluminum sulfate, Coagulants, *Moringa oleifera*, Nile River, Phytoplankton.

## METHODOLOGY

**Scope of study:** The Nile River is the artery of life in Egypt as it considered as the main resource of drinking water. Unfortunately, Nile ecosystem is currently suffering from the discharge of contaminated agricultural wastewater, oil discharge and untreated domestic wastewater [1]. Aluminum sulfate is the most commonly coagulant that used in the developing countries. Recently, there are many studies result in its linkage with developing neurological diseases such as pre-senile dementia or Alzheimer's disease [2]. Therefore the importance of modifying new coagulants as a safe alternative to aluminum sulfate appear clearly.

**Methodology:** The recent study had been performed in three stages of examination: -

- (a) Monitoring the algal community and the physiochemical parameters of River Nile water (Shebin El-kom surface water plant) according to APHA, 2010 [3] every two months during the period from May, 2017 to March, 2018.
- (b) Preparation of new coagulant based on *Moringa oleifera* seeds extract. The natural coagulant had been used to remove the algae and turbidity of surface water under different coagulation conditions such as pH and coagulant dose.
- (c) Comparing the removal efficiency of chemical coagulant (aluminum sulfate) and natural coagulant (*Moringa oleifera* seeds).

## RESULTS/FINDINGD

The total number of phytoplankton populations during the period of investigation was ( $1694 \times 10^3$  organism \ l). The highest yield was ( $407 \times 10^3$  organism \ l) in January. On the other hand, the minimum yield was ( $191 \times 10^3$  organism \ l) in September. The counts in March and November showed moderate values with seasonal average of ( $252 \times 10^3$  organism \ l).

The phytoplankton populations encountered are included in the groups Bacillariophyta, Chlorophyta, Cyanophyta, Pyrrophyta and Euglenophyta. Bacillariophyta dominated the whole populations, as it accounted for 64.9 % of total annual crop. Chlorophyta ranked as the 2nd group with 24.3 % of total annual crop. Then the 3rd group was Cyanophyta with 10.1% of total annual crop. Pyrrophyta and Euglenophyta represented 0.42 % and 0.11 % and of total annual stock, respectively.

The total number of phytoplankton populations was ( $544 \times 10^3$  organisms). Algal removal without chlorination from raw Nile water using *M. oleifera* was very high and reached 98.7% removal, on other hand aluminum sulfate removed algae by 85.8 % removal without chlorination. Different concentrations of *M. oleifera* and aluminum sulfate were used for treatment.

Concentrations of *M. oleifera* and aluminum sulfate were used for treatment. The efficiency of treatment of different concentrations of *M. oleifera* (350 – 400 – 450 – 500 - 550 – 600) mg/l were (60.4 - 92.8 - 95.6 - 96.9 - 98.7 - 98.7) %, respectively. The most effective concentration was 550 mg/l and the result was constant in concentration 600 mg/l. while the efficiency of treatment of different concentrations of aluminum sulfate (10 – 15 – 20 – 25 – 30 – 35) mg/l were (69.7 - 75.1 - 80.1 – 80 - 85.8 - 87.5) %, respectively. As shown in figure (1) and table (1)

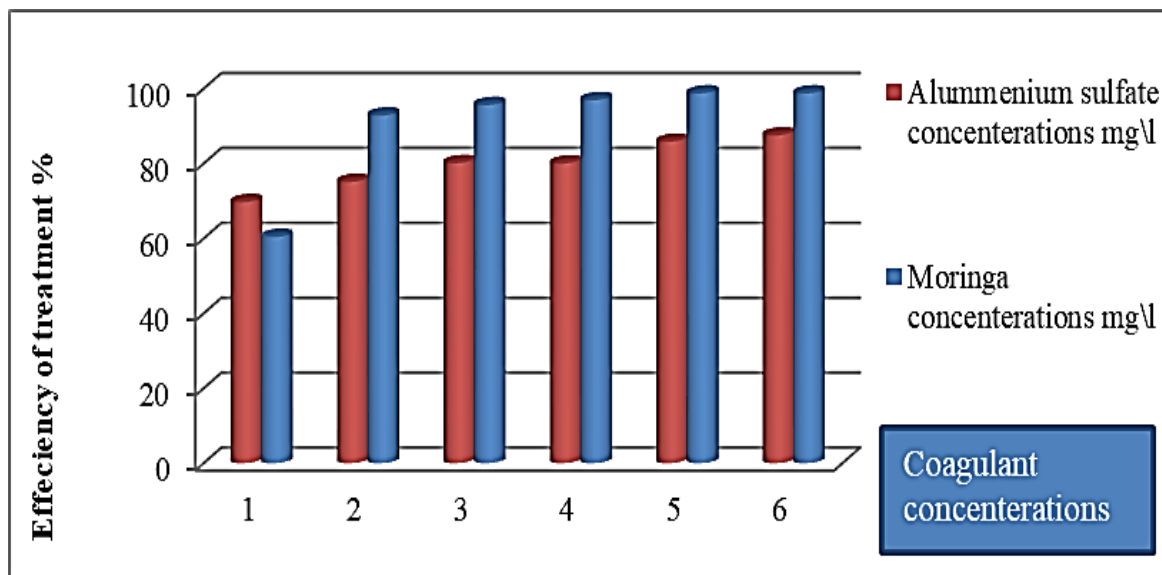


Figure 1. Comparison between the efficiency of treatment of Moringa oleifera seeds extraction and aluminum sulfate on algal count of Nile raw water without chlorination.

Table 1. Comparison between effect of Moringa oleifera seeds extraction and aluminum sulfate on total algal count of Nile raw water without chlorination

Algal groups	Raw water	<i>Moringa oleifera</i> extraction (mg/l)						Aluminum sulfate (mg/l)					
		350	400	450	500	550	600	10	15	20	25	30	35
Total algal count	544	215	39	24	17	7	7	165	135	108	105	77	68
Efficiency of treatment %		60.4	92.8	95.6	96.9	98.7	98.7	69.7	75.1	80.1	80	85.8	87.5

## **CONCLUSIONS AND RECOMENDATIONS**

It can be concluded that *Moringa oleifera* seeds extraction is an effective and safe natural coagulant in drinking water clarification and wastewater treatment due to the presence of a water-soluble cationic coagulant protein that able to reduce turbidity and remove algae and also has antimicrobial activity that affect the raw water bacteria instead of aluminum sulfate that has many side effects as it has various health problems in numerous studies, from gastrointestinal damage and phosphate deficiency to dialysis encephalopathy, renal osteodystrophy and Alzheimer's disease.

It is recommended that the *Moringa oleifera* seeds extract was more effective than aluminum sulfate in coagulation and treatment of surface water. Therefore, we recommend the use of *Moringa oleifera* seeds extract as a safe and alternative coagulant to the aluminum sulfate, as it is non-toxic and has no side effects like aluminum sulfate and can substitute aluminum sulfate in water treatment.

## **REFERENCES**

- [1] Zaghoul, F. A., Ghobrial, M. G., Hussein, N. R., et al., Long-term monitoring of water quality and phytoplankton community structure of Lake Manzala, Mediterranean Coast of Egypt. *Scientific African*, 2024: p. e02345.
- [2] Al-Jadabi, N., Laaouan, M., El Hajjaji, S., Mabrouki, J., et al., The dual performance of *Moringa oleifera* seeds as eco-friendly natural coagulant and as an antimicrobial for wastewater treatment: a review. *Sustainability*, 2023. 15(5): p. 4280.
- [3] American Public Health Association, American Water Works Association, Water Environment Federation (APHA) 'Standard Methods for the Examination of Water and Wastewater', 2010, 22th ed. American Public Health Association, Washington, DC.



## Modeling and Optimization of the water flow in pump station basins (Case study: New El-Marashda Pumping Station)

Noha Kamal<sup>\*1</sup>, Ahmed Abuzeid<sup>2</sup> and Osama Salem<sup>3</sup>

Associate Professor, Head of Information Systems Unit, Nile Research Institute, Egypt <sup>\*1</sup>

(Email: Noha\_Kamal2002@hotmail.com, Noha\_Kamal@nwrc.gov.eg)

Assistant Researcher, Institute of Applied Geosciences, Technische Universität <sup>2</sup> Darmstadt, Darmstadt, Hesse, Germany.

(Email: ing.ahmedabuzeid@gmail.com)

Researcher, Mechanical and Electrical Research Institute, Egypt <sup>3</sup>

(EMail: Engosama\_87@Yahoo.com)

### ABSTRACT

Pump station basins play a crucial role in the efficient operation of pump stations. This paper presents a comprehensive computational fluid dynamics (CFD) modeling and optimization study of water flow in pump station basins. The primary focus is on the New El-Marashda Pumping Station.

This study aims to comprehensively improve the performance and efficiency of the pumping station. To achieve this, computational fluid dynamics (CFD) modeling is employed to investigate the flow conditions in the pump sump. By optimizing the water flow patterns and minimizing disturbances, the study seeks to enhance the overall operation of the station. Additionally, control strategies are implemented to prevent potential flow issues, ensuring the reliability and effectiveness of the pumping system.

The CFD analysis reveals valuable insights into the flow behavior within the basin. The results indicate an operation limit for the New El-Marashda pumps at 64.5 m, beyond which air core vortex formation can occur, potentially compromising the station's performance. This study underscores the importance of CFD modeling in optimizing water flow in pump station basins and provides practical recommendations for enhancing the performance and reliability of these critical infrastructure components.

Furthermore, optimizing the water flow in pump station basins contributes to climate change mitigation by increasing pump efficiency, decreasing power consumption, and reducing carbon emissions. By addressing intake flow issues, the operational efficiency of the pumping station is enhanced, leading to a lower carbon footprint and supporting efforts to combat climate change.

**Key words:** CFD, pump station, pump station intake, optimization, flow behavior.

## METHODOLOGY

Pump station basins are essential components of water distribution systems, ensuring the efficient transfer of water from the source to the desired destination. The design and operation of these basins significantly impact the overall performance and reliability of the pumping station [1]. To fulfill the study's goal, the data collecting, CFD modeling, and analysis procedures should be followed.

This study focuses on the New El-Marashda Pumping Station, located in the second reach of the Nile River, between the Esna barrage and Nag-Hammadi Barrage. The New El-Marashda pumping station has a discharge of  $8.0 \text{ m}^3/\text{s}$  (one pumping unit) and a medium density of  $995.47 \text{ kg}/\text{m}^3$ . Figure 1 shows the side view of the station.

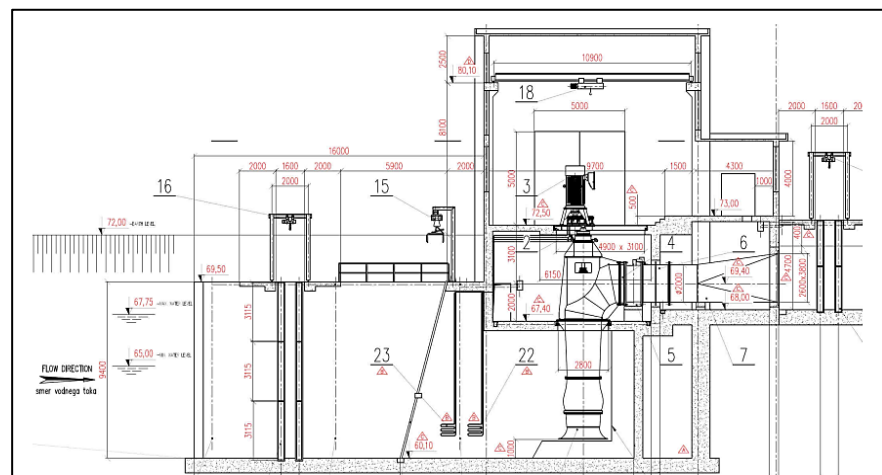


**Figure 1.** New El-Marashda station

The primary objective is to investigate the water flow patterns within the pump station basin using CFD modeling and optimize the basin design to enhance the station's performance and efficiency. A CFD model [2] was used to create the geometry and mesh for three different water level scenarios: 65 m, 64.8 m, and 64.5 m. Trash racks (weed screens) in front of the sump inlet were included in the computation. The origin of the coordinate system was placed at the center of the pump rotor, and water levels and boundary conditions for the CFD simulation were recalculated accordingly, as shown in Figure 2.

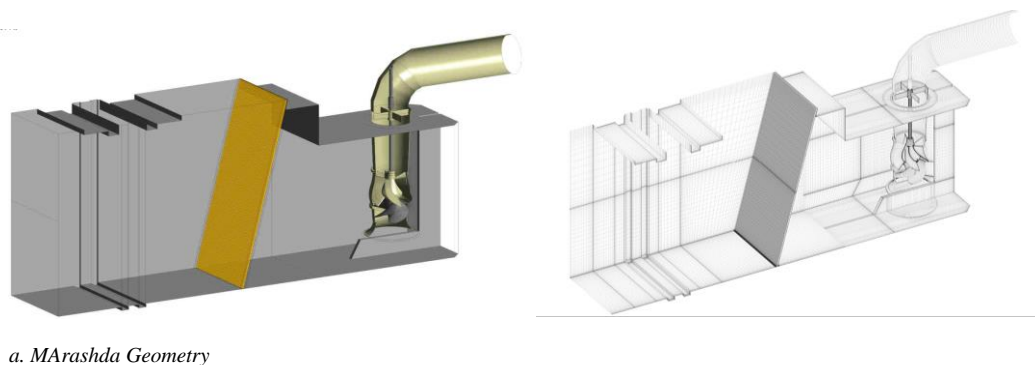


**Figure 2.** Model preparation and Mesh generation

*b. Computational mesh for CFD analysis (sump water level 65 m)*

## RESULT

Three cases of nonstationary simulation were performed, each requiring around 18 to 20 days to complete. It is important to note that no surface or subsurface vortices with an air core were present in all three scenarios.

The CFD simulations indicate a low occurrence of surface "swirl vortices" of types 1 and 2, which is considered acceptable [2]. Figure 4 shows the water velocity distribution on the xy-layer in the middle of the flow domain. The velocities are higher near the sump entrance, which could contribute to the formation of swirl vortices under specific conditions. However, as the flow moves deeper into the basin and closer to the suction bell, the velocities decrease, leading to the dissipation of these vortices.

Given these observations, a water level of 65 m should be acceptable and safe against the occurrence of "air core vortex." However, operation of the pumps at a water level of 64.5 m should be avoided, as it may lead to the formation of air core vortices, which can significantly impair pump performance. To provide a clearer understanding of the vortex dynamics, an additional set of panels has been added to Figure 3. These panels depict the flow patterns at different depths, offering better support for the description of the low occurrence of surface "swirl vortices." Figure 3. (a) Velocity distribution in the xy-plane at the middle of the flow domain; (b) Velocity profile as the flow approaches the suction bell; (c) Additional panels showing vortex dynamics at different depths.

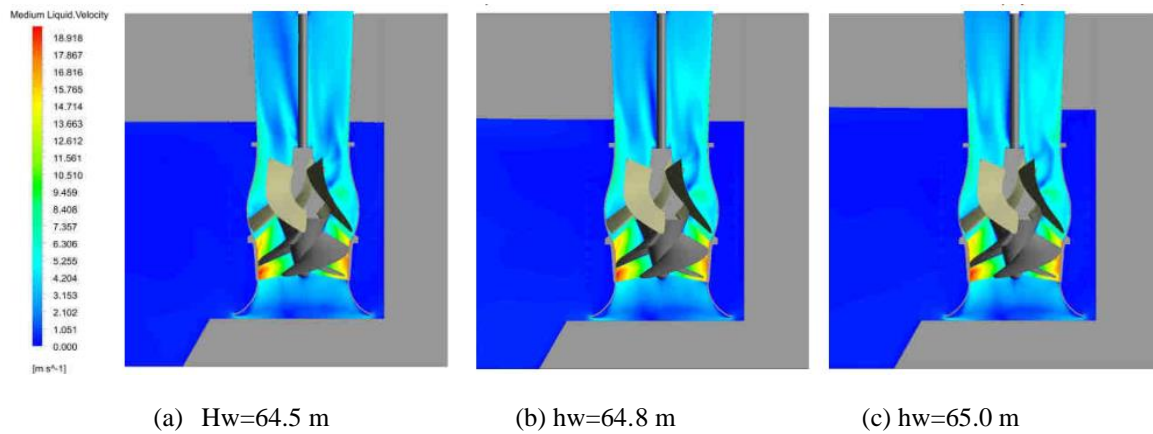


**Figure 3.** Water velocity distribution on xy-layer in middle of flow domain

### CONCLUSIONS AND RECOMMENDATIONS

This study highlights the significance of CFD modeling in optimizing water flow in pump station basins. The findings provide valuable insights into the flow behavior and offer practical recommendations for enhancing the performance and reliability of the New El-Marashda Pumping Station. Future research could explore the impact of different basin geometries and operational conditions on the flow patterns and station efficiency.

### REFERENCES

- [1] Ansys Inc. (2023). Ansys Fluent User's
- [2] Numerical and experimental analyses of Pump Intakes; A. Škerlavaj; ANSYS conference & CADFEM Austria Users Meeting 2013, Wien.
- [3] ANSI/HI 9.8 (2015) - American National Standard for Pump Intake Design; Hydraulic institute.

## Autonomous Surface Water Cleaning Robot Using AI and IoT Technology

Norhan Fathy<sup>1</sup>, Mina Zahgar<sup>1</sup>, Mahmoud Tark<sup>1</sup>, Halim M. Bassiuny<sup>1,2</sup>, Nerveen Ehab<sup>2</sup>

<sup>1</sup> Mechatronics Department, Faculty of Engineering, Heliopolis University, Egypt

Emails: nourhan191710@hu.edu.eg, mina192203@hu.edu.eg, Mahmoud191267@hu.edu.eg

Faculty of Engineering, Helwan University, Egypt

**Keywords:** Real-Time Monitoring, AI, Image Processing, Water Quality, IoT, Zero CO<sub>2</sub> Emissions

### ABSTRACT

Plastic pollution in the Nile River, dubbed the "Plastic Nile," significantly impacts the eastern Mediterranean, with an estimated annual influx of 80–106 billion microplastic particles [1]. Addressing this environmental challenge requires innovative solutions for effective water quality management. This study presents an Autonomous Surface Water Cleaning Robot designed to detect and collect floating waste using advanced AI and IoT technologies, aiming to bridge existing research gaps in efficient water pollution mitigation.

### Introduction

Despite various efforts to combat water pollution, existing systems often fall short in scalability, real-time adaptability, and energy efficiency. This research addresses these gaps by developing a robot that not only improves upon current waste collection mechanisms but also integrates renewable energy sources to enhance sustainability. The primary objectives are to:

1. Enhance waste detection accuracy through advanced AI algorithms.
2. Optimize power management for extended operational periods.
3. Improve mechanical design for efficient waste collection in diverse water conditions.

### Methodology

The robot's development involved several critical phases:

1. Design and Prototyping: Utilizing robust materials and selecting efficient propulsion mechanisms powered by rechargeable batteries supplemented with solar panels to ensure zero CO<sub>2</sub> emissions.
2. AI Integration: Implementing YOLOV8-based Convolutional Neural Networks (CNN) for precise object detection. The model was trained on a comprehensive dataset comprising various floating waste and non-waste objects, achieving a 75% accuracy rate in distinguishing waste.

3. IoT Implementation: Equipping the robot with sensors and cameras for real-time data collection on water quality parameters (turbidity, pH, dissolved oxygen). Data is transmitted to a central server via wireless modules and visualized on a user-friendly dashboard, facilitating remote monitoring and control.

4. Field Testing: Conducted in the pool at Cairo, characterized by flow depths ranging from 1 to 3 meters and velocities between 0.5 to 1.5 m/s. These tests evaluated the robot's performance in varied environmental conditions, ensuring reliability and efficiency in real-world scenarios.

### Results

- Object Detection Accuracy: The AI system achieved a 75% accuracy rate in identifying floating waste, effectively reducing false positives and negatives (Figure 2).
- Collection Efficiency: The robot successfully collected 85% of targeted floating waste across different test sites, demonstrating high efficiency even under varying flow conditions.
- Operational Capacity: With a single battery charge, the robot operates continuously for up to 2 hours. Solar panel integration extends this operational time, enabling longer cleaning cycles. The waste collection rate is 2 kg per hour. Annually, the robot is projected to clean approximately 2.5 tons of waste, showcasing its scalability.
- Cost Analysis: The initial capital cost is estimated at 30,000 EGP, making it economically viable for large-scale deployment. Challenges for local manufacturing include sourcing specialized components and ensuring quality control, which are being addressed through partnerships with local industries.

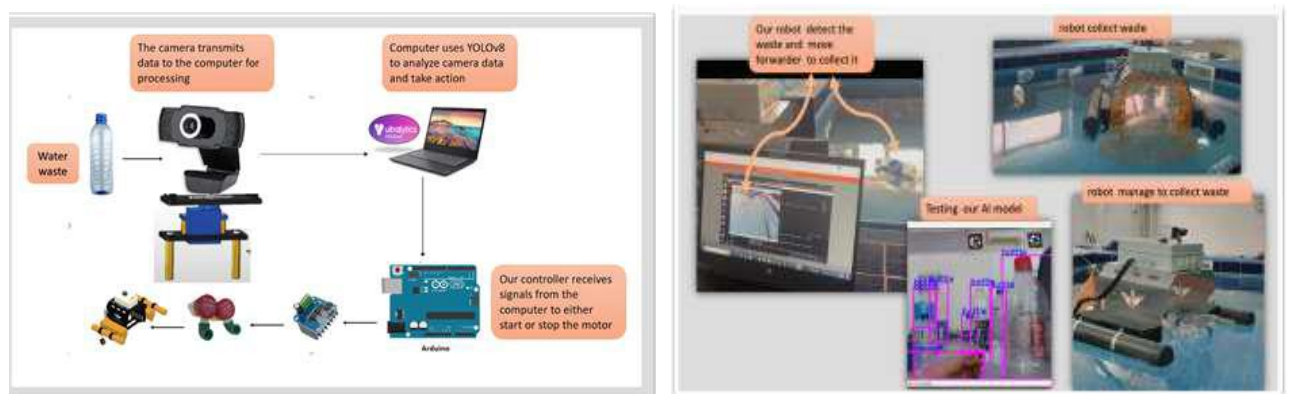


Figure 1: overview of our system software and hardware & Figure 2 : Field testing our robot, demonstrating real-time waste detection and collection.



### **Conclusions and Recommendations**

The AI and IoT-enabled autonomous surface water cleaning robot offers a scalable and sustainable solution to mitigate water pollution. Future work should focus on expanding the AI training dataset to improve detection accuracy, refining the waste collection mechanism for higher efficiency, optimizing power management for extended operations, and addressing manufacturing challenges to facilitate widespread adoption. Large-scale deployment could significantly enhance environmental impact, aligning with five UN Sustainable Development Goals (SDGs): Zero Hunger (Goal 2), Clean Water and Sanitation (Goal 6), Affordable and Clean Energy (Goal 7), Climate Action (Goal 13), and Life Below Water (Goal 14) [2].

### **REFERENCE**

- [1] Abdel-Fattah, S., G. F. El-Said, A. El-Sikaily, and N. M. Dowidar. "Heavy Metal Contamination and Ecological Risk Assessment of the Nile Estuaries into the Mediterranean Sea." *Science of The Total Environment* 873 (2023): 162055. <https://doi.org/10.1016/j.scitotenv.2022.162055>.
- [2] United Nations. "Sustainable Development Goals." Accessed July 7, 2024. <https://sdgs.un.org/goals>. <https://doi.org/10.1016/j.scitotenv.2022.162055>

## **AquaElectrica: Harnessing the Hydropower for sustainable desalination and irrigation.**

Mohamed Ehab Ahmed El-Said<sup>1</sup>, Omar Waleed Mohamed Galal<sup>2</sup>  
1, 2 Obour STEM School, EGYPT.

(E-mail: mohamed.2121030@stemkalubya.moe.edu.eg, omar.2121023@stemkalubya.moe.edu.eg)

**Keywords:** Energy production, Greenhouse gases, Hydropower, Triboelectric Nano-generators, Water desalination.

### **ABSTRACT**

The Earth's surface is predominantly covered by water, with a staggering 97.2% consisting of saline water, leaving only 2.8% as freshwater. Of this freshwater, more than 2.1% is locked in glaciers, the atmosphere, and soil moisture, leaving just 0.7% accessible for human and agricultural use [1].

The challenge of water scarcity has intensified due to inadequate integrated water resources management and the complex impacts of climate change. Greenhouse gas emissions play a pivotal role in exacerbating this global water crisis. Our research is dedicated to the urgent reduction of these emissions, with a specific focus on two dominant sectors that contribute approximately 38% of global greenhouse gas emissions: energy production and agriculture. This endeavor has drawn heightened attention to the pressing issues of global water scarcity. In Egypt, the per capita annual water supply is projected to decrease from 550 m<sup>3</sup> to just 500 m<sup>3</sup> by 2025. Given Egypt's extensive coastline of about 3,000 km, desalination has emerged as a promising solution for augmenting freshwater resources [2].

Numerous innovative approaches have been developed to enhance the sustainability of seawater desalination, reducing energy consumption while integrating electricity generation. One such approach involves the microbial desalination cell, which, although promising, faces significant challenges, including the high cost of its ion exchange membrane and relatively modest energy output. In response to these challenges, our project consists of two core components. The first component aims to harness hydropower by leveraging the triboelectric nanogenerator (TENG) principle. This involves the juxtaposition and separation of materials with substantial electronegativity differences, inducing electron flow and generating electrical current during their separation. The second component integrates an electrolytic desalination cell, meticulously designed to overcome the limitations of conventional systems.

The incorporation of a cost-effective ion exchange membrane, priced at a mere 10% of traditional counterparts, further augments our system's functionality.

In pursuit of enhanced irrigation efficiency, we introduce a sophisticated smart irrigation system equipped with soil humidity sensors. Our research methodology unfolds through two distinct phases:

#### Phase One: Implementation of the Rotary TENG System

In this inaugural stage, we meticulously constructed our rotary triboelectric nanogenerator (TENG) system. It featured a helical fan measuring 35 cm in height and 0.635 cm in diameter, ingeniously designed to channel water flow and induce fan rotation. The entire assembly was encased within a glass container measuring 45 cm in height, 20 cm in length, and 20 cm in width, with the fan securely affixed to a central shaft. Material selection was guided by the Triboelectric Series, which delineates electronegativity disparities among materials. Consequently, we opted for a combination of polytetrafluoroethylene (PTFE), copper, and aluminum. PTFE films, along with copper, were skillfully attached to the shaft to harness the kinetic energy generated by the flowing water. To ensure optimal electrical contact, a strategically positioned copper plate within the shaft facilitated charge accumulation. Further enhancing electron conduction from the PTFE/copper films to the external circuit, two carbon brushes were affixed to maintain contact with the copper plate. Subsequently, the rotating PTFE/copper plate came into contact with fixed plates arranged within a framework supported by four rods that accommodated PTFE/aluminum films.

#### Phase Two: Construction of the Electrolytic Desalination Cell

The second pivotal phase of our project focused on the construction of an electrolytic desalination cell. This meticulously crafted cell was made from acrylic sheets, measuring 45 cm in length, 15 cm in width, and 15 cm in height [3].

For the fabrication of the ion exchange membrane, we opted for a composition ratio of 2:1, blending Poly-Vinyl-Alcohol (PVA) and Poly-vinyl-pyrrolidone (PVP). The resulting solution underwent a meticulous 48-hour drying process [4]. Subsequently, we prepared a cross-linking solution, comprising 100 mL of 2% glutaraldehyde, 50 mL of HCl as a mineral acid, and 200 mL of acetone. Immersing the polymer base in this cross-linking solution, we allowed it to harden for a duration of 40 minutes. In parallel, for the functionalization of the anodic membrane, we engineered a 10 wt. % KOH solution to facilitate the anodic reaction.

Similarly, the cathodic membrane functional group was meticulously crafted using a solution containing 4 wt. % of Boric Acid, enhancing membrane selectivity [4]. The polymer base was then immersed in both the anodic and cathodic solutions, maintained at a precise temperature of 60 °C for an exacting duration of 3 hours.

Following the meticulous assembly of the prototype, comprehensive testing protocols were executed. The initial phase demonstrated the system's capacity to generate 69 V, delivering 480 watts of power output, all under a steady flow of water at a rate of 33 L/min and operating under a 10 Ω load. This significant achievement is documented in Figures 1 and 2. Subsequently, we subjected the system to a 10-day test during the second phase, during which we employed seawater. The results are comprehensively detailed in Figure 3.

**Figure 1.** Water flow rate Vs Voltage

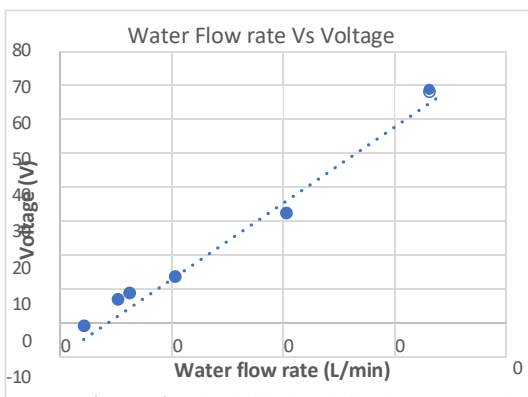


**Figure 2.** Water flow rate Vs Current

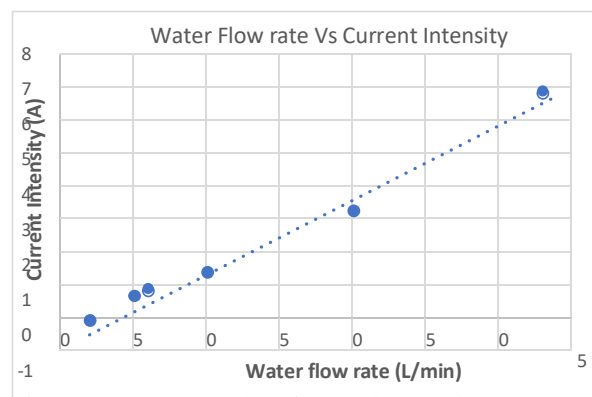
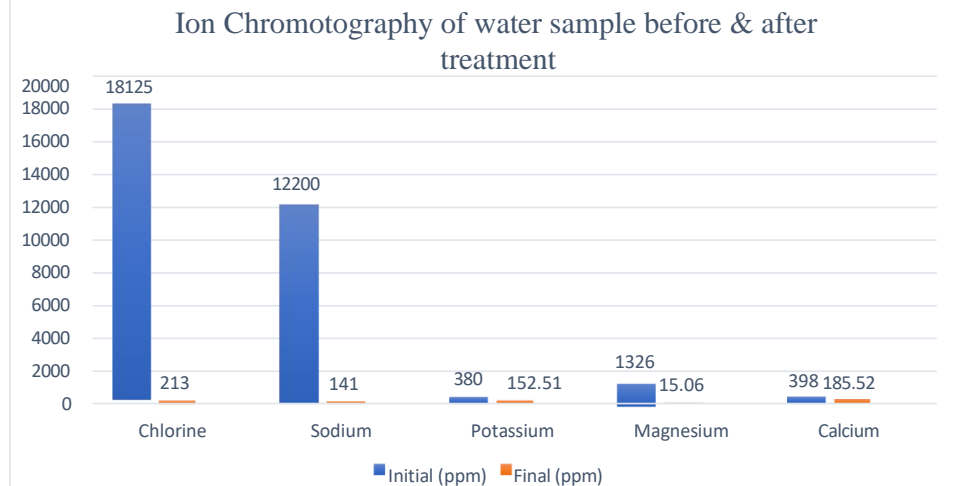


**Figure 3.** The initial and final concentration of real sea water samples after 10 days testing



In conclusion, the TENG stage is 30% more efficient than the traditional dynamo. The desalinated water is suitable for irrigation and exhibits satisfactory performance, particularly for potato crops, meeting the requirements outlined by the FAO.

**Acknowledgment:** The authors would like to thank Obour STEM school administration for their remarkable enhancement of the project, also we have to thank Allah and our parents for their support. [Project Number = CWW2024-XNY23839].

**References:**

- [1] Abdul Sattar Jatoi, Z. H. (2022, August 11). A comprehensive review of microbial desalination cells for present and future challenges.
- [2] Islam Amin, M. E. (2020, February 4). Conceptual Design and Numerical Analysis of a Novel Floating Desalination Plant Powered by Marine Renewable Energy for Egypt.
- [3] Géraldine Merle, S. S. (2012, March 30). New cross-linked PVA based polymer electrolyte membranes for alkaline.
- [4] Dandan Liu, C. W. (2018, August 21). Composite Cationic Exchange Membranes Prepared.

## Surface functionalization of cellulose nanocrystals derived from waste newspaper for highly efficient Mn (VII) sorption

F. M. Mohamed<sup>1\*</sup>, Mohamed R. El-Aassar<sup>2,3\*\*</sup>, B. Y. Eweida<sup>4</sup>, A. M. Abdulla<sup>1</sup>, H. A. Hamad<sup>5</sup>, M. F. Alrakshy<sup>6</sup>, R. E. Khalifa<sup>3</sup>

<sup>1</sup> Faculty of Earth Sciences, Beni-Suef University, P.O. 62521, Beni-Suef, Egypt.

<sup>2</sup> Department of Chemistry, College of Science, Jouf University, Sakaka 2014, Saudi Arabia

<sup>3</sup> Polymer Materials Research Department, Advanced Technology and New Material Institute, City of Scientific Research and Technological Applications (SRTA City), New Borg El-Arab City 21934, Alexandria, Egypt

<sup>4</sup> Modelling and Simulation Department, Advanced Technology and New Materials Research Institute (ATNMRI), City of Scientific Research and Technological Applications (SRTA-City), New Borg El-Arab City, 21934 Alexandria, Egypt.

<sup>5</sup> Fabrication Technology Research Department, Advanced Technology and New Materials Research Institute (ATNMRI), City for Scientific Research and Technological Applications (SRTA-City), New Borg El-Arab City, 21934, Alexandria, Egypt.

<sup>6</sup> Al -Asmaryia Islamic University, Zliten, Libya

Corresponding authors E-mail: [fathy1973@esc.bsu.edu.eg](mailto:fathy1973@esc.bsu.edu.eg);

### Abstract

The fabrication of natural polymer nanocrystals and their versatility stimulated the development of functionalized hybrid nanomaterials for the elimination of harmful contaminants. In this quest, cellulose nanocrystals (CNCs) from environmentally friendly newspapers have been functionalized using a simple two-step reaction with anionic polymer (poly hydrex 6161) to create functionalized cellulose nanocrystals (FCNCs). FTIR, XRD, and SEM are used to describe the structure of FCNCs. The impact of five factors (starting Mn (VII) concentration, contact time, pH, adsorbent dosage, and temperature) and their interactions on the removal efficiency is examined using the Response Surface Methodology (RSM). FCNC adsorption efficiency in batch mode is highly influenced by a number of variables, including pH. The innovative FCNCs hybrid composite not only demonstrated the efficient removal of Mn (VII) ions from an aqueous solution, but it also made the process easier. For the elimination of Mn (VII) ions, a mild acid (pH=2) is preferred. The pseudo-second order, intraparticle-diffusion, and Langmuir isotherm kinetic models as well as the adsorption process have been proven to be compatible. Electrostatic interaction, complexation interaction, ion exchange, and pore filling are methods that can be used to determine the adsorption mechanism on the FCNCs. At least six adsorption-desorption cycles were easily performed by the hybrid FCNCs. The hybrid composite is extremely promising as an improved adsorbent for significant potential in wastewater treatment for heavy metal removal on an industrial scale due to its special features.

**Key words:** Characterization; Adsorption; old newspaper; functionalized crystal nano cellulose; Mn (VII) removal.



## **METHODOLOGY**

### **Materials**

The old newspaper was collected from the residues of national newspaper in Egypt. Hydrex 6161 (poly acrylamide) was supplied from Veolia Company, France. Potassium permanganate ( $\text{KMnO}_4$ ) with a purity of 99.5% was obtained from Loba Chemie, India.  $\text{H}_2\text{SO}_4$  and NaOH were supplied by Al-Nasr Company.

### **Fabrication of cellulose nanocrystals (CNC) from old newspapers**

In accordance with the process described by [1], newspaper (NP) was first treated with alkali and bleached. Briefly, NP was pulverized in a grinder and then treated with 5% NaOH for 2 h at 125°C. Following that, the pulp was washed with distilled water. Then, 2% (w/v) NaOCl was added and allowed to react for another 2 h at 125°C. Finally, the suspension was dialyzed against distilled water to ensure that the pH remained consistent. The suspension obtained was sonicated for 30 minutes and then kept at 65 °C in an oven overnight. The obtained sample was referred to as CNCs.

### **Synthesis of amino functionalized cellulose nanocrystal**

Briefly, CNCs powder (5.0 g) was added to anionic polymer (poly hydrex 6161) solution at 45 °C under continuous stirring. After stirring for 4 h, the product was washed with distilled water. Finally, the product, coded as FCNCs, was freeze-dried for 24 h before use.

### **Characterization of adsorbents, and adsorption studies**

Following are summaries of the prepared FCNCs' comprehensive physicochemical characterization, adsorption tests, computer modelling, and reusability investigation.

### **Physicochemical characterization of the prepared samples.**

The functional groups, surface area, nanoscale structures, and morphology of FCNCs adsorbent, were characterized using different techniques such as Fourier-transform infrared (FTIR, Bruker Vector 33 FTIR spectrometer), Brunauer-Emett-Teller (BET, NOVA, version 11.04, Quantachrome USA), X-ray diffraction patterns (XRD, Philips APD-3720), The FCNCs were investigated by Transmission Electron Microscopy (TEM, JEOL-2100 PLUS) at 100 kV.

## RESULTS/FINDINGD

The morphology of newspapers and FCNCs before and after adsorption of Mn(VII) are shown in **Fig.1a-c** respectively. Before treatment, the old newspapers showed the long compact microstructure, where the cellulose microfibrils were observed. After treatment, it was demonstrated from the SEM images that FCNCs have a combination of small and large particle sizes, heterogeneous rough, an irregular morphology and porous surfaces with crater-like pores. These pores facilitate the diffusion of adsorbate molecules in the internal sorbent structure and subsequently it enhances the sorption process. As schematically shown in **Fig.1b**, the crystalline cellulose microfibril networks have been configured in a disorderly way [2]. TEM imaging, as shown in Figure 1d, unveiled that the catalyst particles exhibited an irregular form, with spherical particles corresponding to the FCNCs.

The crystalline micro fibrillated cellulose is converted to nanocrystalline cellulose by acid hydrolysis [1]. The initial cellulose sample, microcrystalline cellulose, as defined, contains nanocrystallite aggregates that bind local lateral crystalline contacts together. It is important to break the contacts between adjacent nanocrystallites in the aggregates of modified sample to isolate the free nanocrystalline particles.

The treatment with 60 wt.% H<sub>2</sub>SO<sub>4</sub> allows lateral contact etching and surface sulfonation of individual nanocrystallites to occur [2]. After adsorption, the SEM image revealed the closely packed morphology, and the shape did not change after adsorption due to the coverage of Mn (VII) on the pores of FCNCs when compared before adsorption (Fig. 3c). The PSA of FCNCs showed a homogenous particle size of 90 nm, which confirmed the successful synthesis of cellulose in the nano range.

### Equations

The range and levels (-1, 0, and 1) for the selected variables are coded according to Eq. (1), and summarized in **Table 1**.

$$x_i = \frac{X_i - X_0}{\Delta x} \quad (1)$$

$$Y = \beta_0 + \sum \beta_i x_i + \sum \beta_{ii} x_i^2 + \sum \beta_{ij} x_i x_j \quad (2)$$

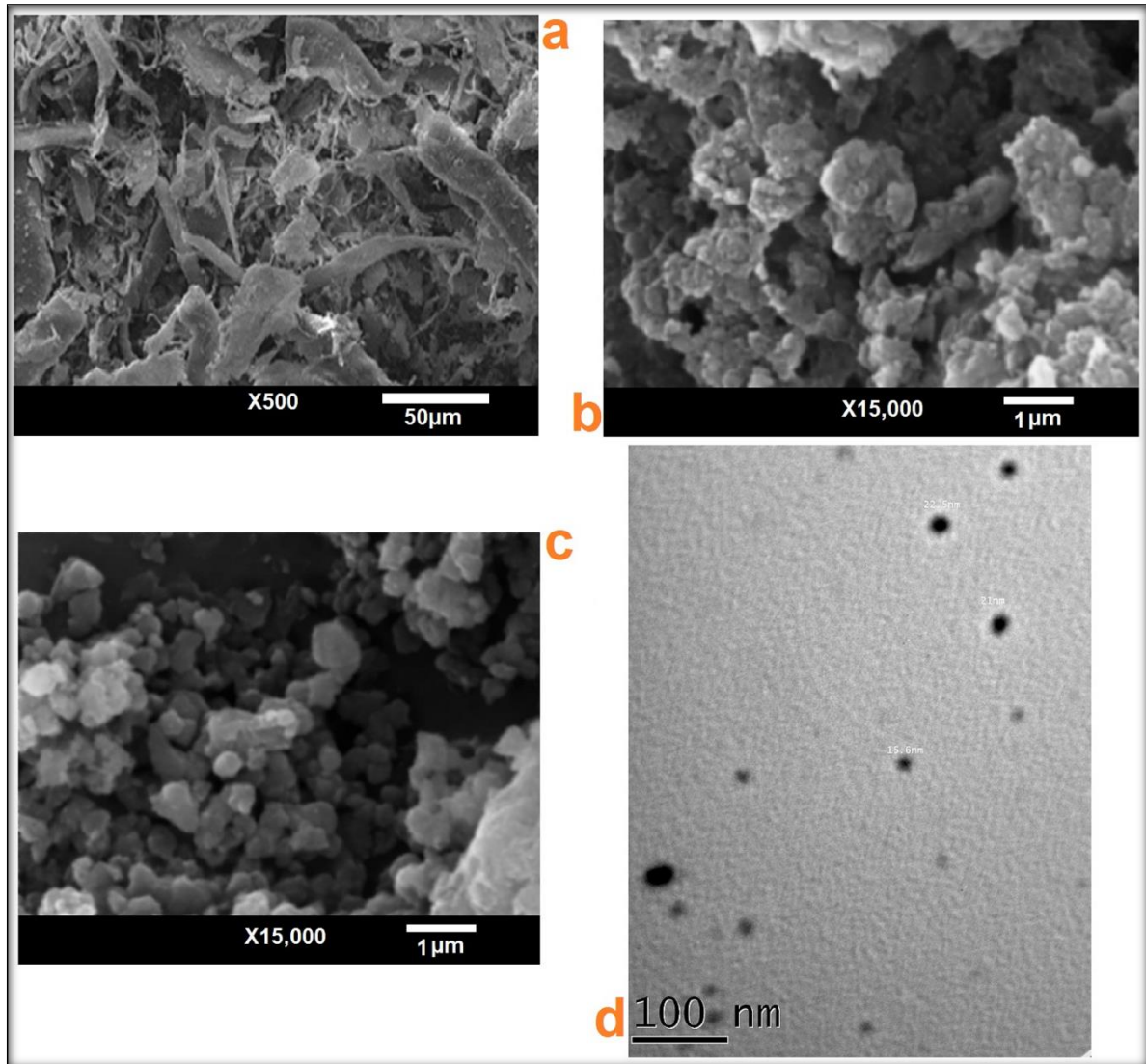
Where  $x_i$  and  $X_i$  are the coded and real values of variables respectively. The total experiments were found to be 46 experimental runs. A model was generated by the regression analysis of the response, and its efficiency was tested by ANOVA and F test [3]. Data analysis and optimization procedure were performed using the statistical software "Statistica" and the interaction effects of the variables could be described by the following quadratic Equation:

$$Y = \beta_0 + \sum \beta_i x_i + \sum \beta_{ii} x_i^2 + \sum \beta_{ij} x_i x_j \quad (2)$$

Where  $Y$  is the predicted response,  $\beta_0$  the intercept term,  $\beta_i$  the linear effect,  $\beta_{ii}$  is the square effect and  $\beta_{ij}$  is the interaction effect.

*Figures and Tables*

*Fig. 1 SEM image of (a) Waste Newspaper, (b) FCNCs before adsorption of Mn(VII), (c) FCNCs before adsorption of Mn(VII), and (d) TEM FCNCs Post-Adsorption of Mn(VII)*



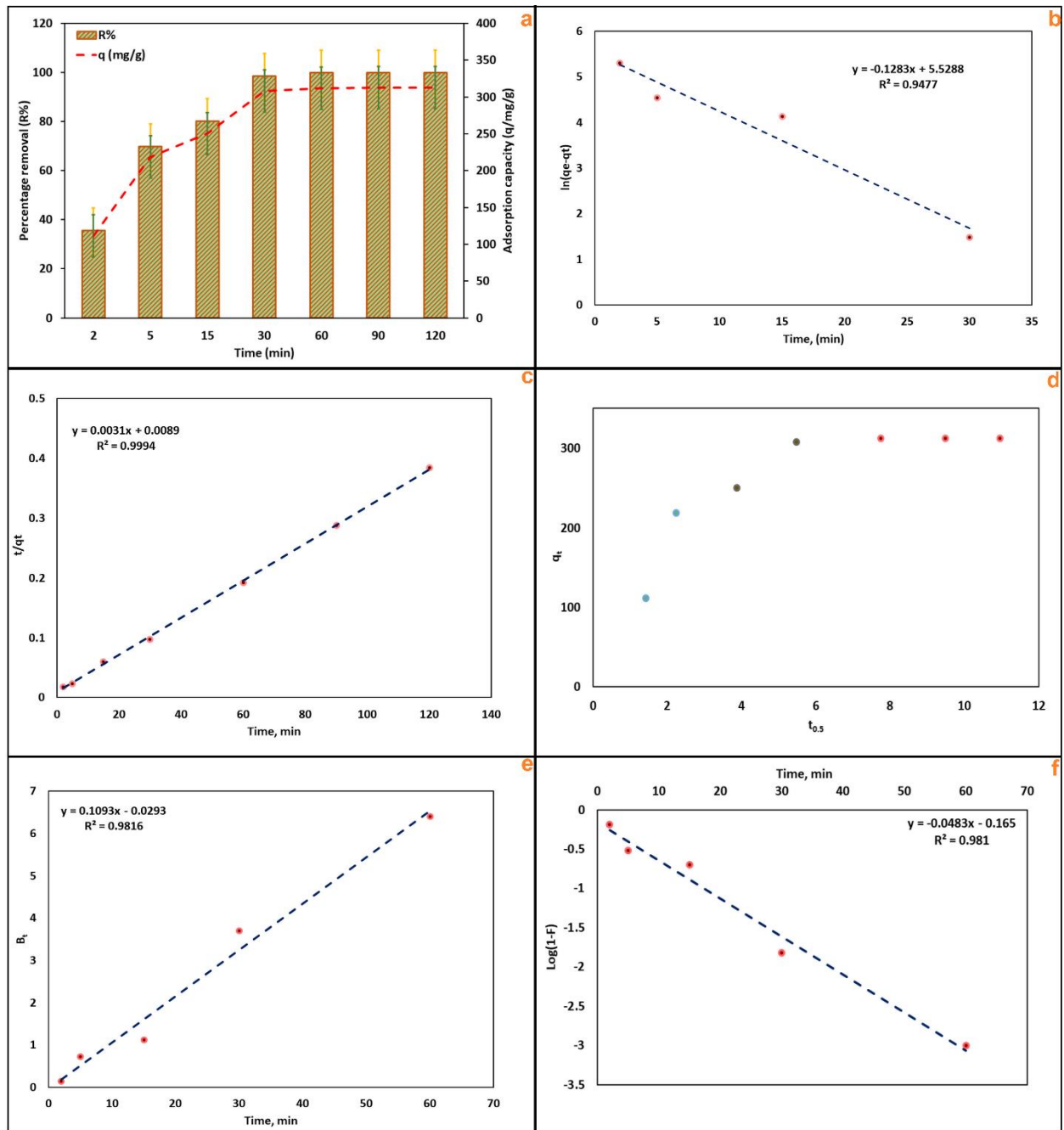


**Fig. 2** Adsorption kinetic modelling of (a) Effect of contact time, (b) The pseudo first order model, (c) the pseudo second order model, (d) intraparticle diffusion model, (e) and (f) Boyd model

*Table 1 Kinetic parameters of Mn(VII) adsorption by FCNCs*

<b>Kinetic model</b>	<b>Parameter</b>	<b>value</b>
<b>Pseudo-first-order</b>	$q_{e,cal}$ (mg/g)	312.18
	$q_{e,exp}$ (mg/g)	251.84
	$K_1$ ( $\text{min}^{-1}$ )	0.1283
	$R^2$	0.9477
<b>Pseudo-second-order</b>	$q_{e,cal}$ (mg/g)	312.18
	$q_{e,exp}$ (mg/g)	322.58
	$K_2$	0.00108
	(mg/g.min)	112.359
	$h$ (mol/g.min)	0.9994
<b>Intraparticle diffusion</b>	First step	
	$C_1$	159.58
	$K_{P1}$	17.188
	$R^2_1$	1
	Second step	
	$C_2$	111.5
	$K_{P2}$	35.842
	$R^2_2$	1
	Third step	
	$C_3$	311.46
	$K_{P3}$	0.0999
$R^2_3$	0.791	

*Table 2 Isotherm model parameters for adsorption of Mn(VII) by FCNCs*

<b>Langmuir</b>			<b>Freundlich</b>		
$q_{max}$ (mg/g)	$K_L$ (L/mg)	$R^2$	$k_f$ (mg/g)	$n$	$R^2$
384.615	0.530	0.989	2532.595	0.593	0.821



## CONCLUSIONS AND RECOMENDATIONS

Through this study, it has established the facile production of cellulose nanocrystals using old newspapers and then functionalized by amino group through reaction with anionic polymer (poly hydrex 6161) to produce FCNCs. The FCNCs adsorption affinity for removal of Mn (VII) ions has been investigated. Adsorption of Mn (VII) ions onto FCNCs was pH-dependant process with maximum removal efficiency at pH =2 and the equilibrium were reached within 60 min. Depending on the computational study, the Mn (VII) adsorption mechanism using FCNCs fulfills Freundlich and pseudo-second-order-kinetic models. The thermodynamic studies showed that the adsorption process was more favorable at higher temperatures. The regeneration capability of FCNCs was observed for the removal of Mn (VII) ions after six adsorption-desorption cycles. The result of the synthesized FCNCs, low cost, eco-friendly, technical feasibility, environmental benefits, and high adsorption capacity, it can be utilized as an efficient adsorbent for heavy metals removal from wastewater.

## ACKNOWLEDGMENT

The authors are thanks to Science and Technology Development Fund (STDF) for funding this project, no 46896 and the author would like to thank the Deanship of faculty of earth sciences for supporting this work.

## Citing References

1. Mohamed MA, Salleh WNW, Jaafar J, et al (2015) Physicochemical properties of “green” nanocrystalline cellulose isolated from recycled newspaper. *Rsc Adv* 5:29842–29849. <https://doi.org/10.1039/C4RA17020B>
2. Duchemin B (2017) Size, shape, orientation and crystallinity of cellulose I  $\beta$  by X-ray powder diffraction using a free spreadsheet program. *Cellulose* 24:2727–2741. <https://doi.org/10.1007/s10570-017-1318-6>
3. Sen S, Sarkar P (2019) Modelling of growth kinetics of isolated *Pseudomonas* sp. and optimisation of parameters for enhancement of xanthine oxidoreductase production by statistical design of experiments. *J Environ Sci Health A* 54:65–78. <https://doi.org/10.1080/10934529.2018.1516070>